Filamentous Phage Derived Biological Nanorods; Development of a Novel Display System

A thesis presented in partial fulfilment of the
requirements for the degree of

Master of Science
in
Microbiology

at Massey University, Manawatū, New Zealand.

Georgia Rose Davey

2018

Abstract

The Ff filamentous bacteriophage are filament-like bacterial viruses approximately 900 nm in length. The F-pilus-specific filamentous phage are resistant to heat, pH-extremes, and detergents in combination with their structural properties and amenability to DNA recombinant engineering has enabled their extensive use in modern biotechnology. However, the use of Ff-phage in vaccines and other such biological uses is controversial due to their ability to replicate in gut *Escherichia coli,* and the possibility of mobilisation and horizontal gene transfer of antibiotic resistance-encoding genes among the gut bacteria. As such, the novel system was established to create short, stable particles that cannot replicate, called NanoZap particles. However, this system has the disadvantage of often producing multiple-length particles, rather than the desired single-length particles; another disadvantage is that during packaging, one particle in a million packages the entire plasmid due to recombination that removes the terminator copy of the (+) ori, and given that these plasmids contain antibiotic resistance genes, this likely would spread antibiotic resistance throughout the surrounding environment. In this thesis several variations upon the original pNanoZap vector were created and tested to obtain monodisperse unit-length particles. The deletion of the complete multiple cloning site (MCS) that lied between the initiator and terminator of replication from the original pNanoZap vector achieved this aim. To eliminate rare antibiotic resistant particles that package the complete pNanoZap vector, the antibiotic resistance gene was removed from the pNanoZap 537 vector and replaced with an auxotrophic marker *nadC*; this vector was named pNanoZap 537N. It is yet to be seen if this new pNanoZap vector is capable of producing NanoZap particles.

For high-sensitivity diagnostics it is desirable to construct high-avidity particles, containing large number of detector molecules. To achieve this a double-display (detector displayed on phage which in turn is displayed on the surface of florescent *E. coli*) was designed and tested. When the *E. coli* expressing red fluorescent protein TinselPurple were infected with the bacteriophage, the chromogenic protein was lost , thereby showing that a different method of colouring *E. coli* will need to be used in order to construct the double-display particles.

Foreword and Acknowledgements

Firstly, I would like to thank my supervisor Dr. Jasna Rakonjac, for all her continuous help, support and critical evaluation throughout this project. Her encouragement and innovation are what enabled me to undertake this work. I would also like to thank my co-supervisor Dr. Dragana Gagic for all her valuable feedback and insights. I would also like to thank all my lab fellows from the Helipad team: Sofia Khanum, Marina Rajic, Stefanie Bagley, Stephanie Baird, Vuong Le, Raveen Weerasinghe, Fabian Rhem, Majela Gonzales, Catrina Olivera, Rayén Léon and Peter Gardner; for all of their support and for all the fun times. I would also like to thank all the staff at the Institute of Fundamental Sciences for all their help.

I would also like to extend a special thanks to my friends Angela Ryan, Matt Dobson, Daniel Bates, Zach Hucker, Kate Boyle and Eleanor Pepper, without whom I am not convinced I could have finished this project with my sanity intact. I have had a wonderful time with all of you, and I hope that we will all continue to make memories together in the future.

I would also like to thank the Company of the Raven, particularly my friends Dylan McLaughlin, Celina Embi, Sef Embi, Jonathan Parlevliet, and Johnathan Whye for all the camping, fighting and feasting. I would also like to thank honorary Raven Rachael Mildenhall. Each bruise I received from all of you was another lesson I needed to learn. Your presence in my life is a wonderful thing, and I will always treasure the times we have had together. Hopefully we will have many more of them.

I would also like to thank my family, in particular my grandmother Valerie Hicks, who always told me I could do great things, if I was only willing to try. My mother Rosie Davey-Hicks was always a valuable source of comfort, and my little brother Matthew always helpful with his quick sense of humour and grasp of role-playing games. Thank you also to my father Michael Davey for all the books and for looking after my dog, Max. A special mention to my Nana, Patricia Davey, who sadly passed away before she could see what I spent two and a half years of my life working on.

Abbreviations

2×YT	2 times strength Yeast Extract, Tryptone media
Amp	Ampicillin
BD	Becton, Dickinson and company
Cm	Chloramphenicol
CaCl	Calcium chloride
CsCl	Caesium chloride
DMSO	Dimethyl sulfoxide
DNA	Deoxyribose nucleic acid
E. coli	*Escherichia coli*
EDTA	Ethylene diamine tetra-acetic acid
EtOH	Ethanol
Ff	Filamentous
FLP	Site specific recombinase
FRT	FLP recombinase target
HCl	Hydrochloric acid
H_2O	Water
IPTG	Isopropyl β-D-1-thiogalactopyranoside
kbp	Kilo base pair
Kn	Kanamycin
$MgSO_4$	Magnesium sulfate
min	Minute(s)
MQ	Mili-Q H_2O
Na-Citrate	Sodium citrate
NaCl	Sodium chloride
NaOH	Sodium hydroxide
OD	Optical density
PBS	Phosphate-buffered saline
PEG	Polyethylene glycol
Phage	Bacteriophage
rpm	Revolutions per minute
SDS	Sodium dodecyl sulfate
sec	second(s)

SOC	Super Optimal Catabolite repression media
SN	Supernatant
ssDNA	single stranded DNA
TAE	Tris-acetate-EDTA
TBS	Tris-buffered saline
TE	Tris-EDTA
TEM	Transmission Electron Microscopy
VS	Vivaspin

List of Tables

List of Figures

Abstract

Foreword and Acknowledgments

Abbreviations

List of Tables

List of Figures

Table of Contents

Chapter I

Literature Review

1. Introduction

1.1. Filamentous Bacteriophage

The Ff filamentous bacteriophages (also called M13, f1 and fd) are filament-like bacterial viruses that use the F-pilus as their primary receptor to infect the enterobacterium *Escherichia coli* (Marvin *et al.*, 2014, Rakonjac *et al.*, 2011). The class of Ff filamentous bacteriophage belong to the genus *Inovirus*. The Ff filamentous bacteriophage are unlike conventional viruses in one major respect; the mode of replication. In a conventional temperate virus (such as lambda), the infection of a cell results in one of two outcomes; lysis or lysogeny (Rakonjac *et al.*, 2011). However, the Ff filamentous bacteriophages use neither of these, and are continuously assembled and released from the host cell through secretion (Model and Russel, 1988), thus allowing for huge titres of Ff bacteriophage to be produced and maintained.

Wild-type Ff bacteriophage particles are approximately 900 nm in length, and 5 nm wide (Rakonjac *et al.*, 2011, Specthrie *et al.*, 1992). Ff bacteriophages have simple morphology and a small ssDNA genome, comprised of 11 genes with 5 different proteins creating the virion. The major capsid protein, pVIII, which forms the shaft of the filament, is found in ~ 2700 copies in the wild-type Ff phages (Overman *et al.*, 1996); while (pIII + pVI) and (pIX + pVII) exist in five copies each at opposing ends of the filament (**Figure 1**) (Model and Russel, 1988, Rakonjac *et al.*, 2011, Sattar, 2013).

The major coat protein pVIII is an integral protein anchored to the inner membrane by a C-terminal hydrophobic transmembrane helix prior to the assembly of the virion. The N-terminal portion is found in the periplasm, while the C-terminal tail is found in the cytoplasm (Russel and Model, 1989). The structure of pVIII is conserved among the Ff filamentous bacteriophage, with the pVIII subunits arranged in a five-start helix with a 2-fold screw axis of about 32 Å, with five subunits in each “ring” of the virion tube, related by a 5-fold rotation

axis (Marvin *et al.*, 2006). The length of the mature Ff particle is dependent on the size of the encapsulated single stranded DNA (ssDNA), with the major coat protein pVIII existing in approximately 0.42 ± 0.01 subunit copies per nucleotide of genomic DNA (Newman *et al.*, 1977).

Therefore, insertion or deletion of DNA is a simple way to control the length of the virion; allowing the creation of bacteriophage only 50 nm in length, as compared to the standard length of approximately 900 nm (Rakonjac *et al.*, 2011).

The minor coat proteins (pVII, pXI, pIII and pVI) form the caps of the virion. Proteins pVII and pXI are incorporated into the virion at the beginning of virion assembly and are the first part of the virion to extrude from the host cell. Proteins pIII and pVI form the distal cap of the virion and are responsible for the release of the phage from the host cell; through termination of assembly and ensuring the structural stability of the virion model (Rakonjac *et al.*, 2011, Rakonjac and Model, 1998). pIII is also the protein responsible for interacting with the host cell during infection. It has been shown that there are five pIII subunits, through association with ZnS nanocrystals (Lee *et al.*, 2002, Rakonjac *et al.*, 2011). Since pVI and pIII are equimolar in the virion cap, it follows that there must also be five copies of pVI.

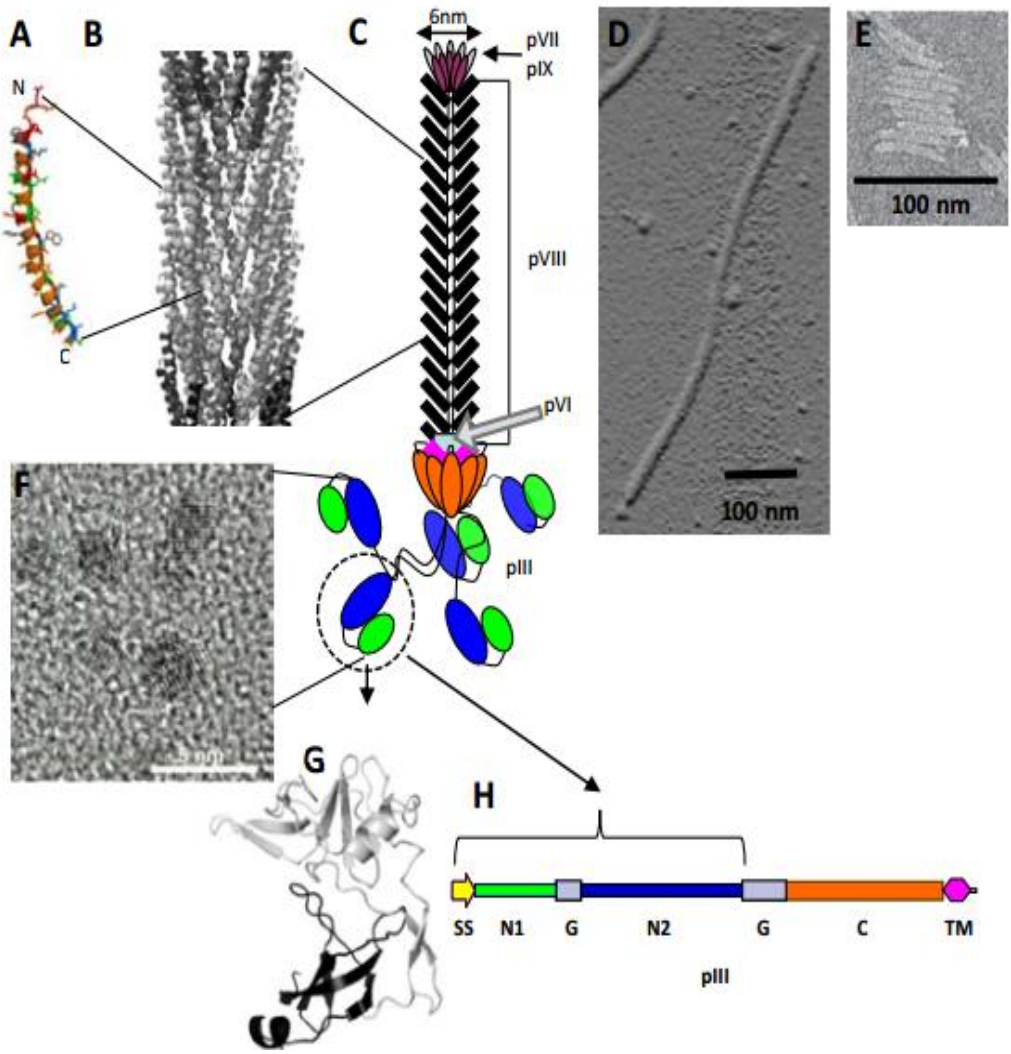

Figure 1: The Ff Virion.

A. Model of a pVIII monomer showing hydrophobic (green), and hydrophilic residues (orange), along with positively (blue), and negatively charged residues (red). The N and C termini of pVIII are indicated. **B.** Ribbon representation of the pVIII arrangement within the filamentous phage capsid. PVIII within the capsid forms a shingle-like array of helices. **C.** Schematic representation of the virion. **D.** Atomic force microscope image of Ff virion. **E.** Electron micrograph of microphage. **F.** High-resolution TEM lattice fringe images of five ZnS nanocrystals at the pIII-end of a single Ff virion. **G.** Ribbon representation of the N1 domain (dark grey) and the N2 domain (light grey) of pIII. **H.** Domain organization of pIII preprotein. SS (signal sequence), N1, N2, and C, are domains of pIII; G (glycine-rich linkers); TM (transmembrane helix). Figure and legend taken from (Rakonjac *et al.*, 2011) with permission.

1.1.1. Mechanism of Infection and Assembly

Ff bacteriophage can only infect *Escherichia coli* cells which express an F-pilus, which is the structure otherwise responsible for conjugation. In the initial stage of infection, pIII interacts with the primary receptor (the tip of the F conjugative pilus) through the N2 domain and pilus retraction (a process that occurs independently of phage infection) brings pIII across the outer membrane and into the periplasm (Click and Webster, 1998) where the N1 pIII domain interacts with the secondary receptor, periplasmic protein TolA, of the TolQRA complex (**Figure 4**). This results in the encapsulated ssDNA being released into the cell, while the major protein pVIII is integrated into the host inner membrane as the DNA enters the cytoplasm (Rakonjac *et al.*, 2011). Knockout studies have shown that the absence of any of the TolQRA complex genes, *tolQ*, *-R* or *–A,* inhibits bacteriophage infection and pVIII incorporation (Click and Webster, 1998).

Following the entry of the circular ssDNA into the cell, the second strand (also known as the minus (-) strand) of the phage genome is synthesised, using the cell's own RNA polymerase to form a primer at the (-) origin of replication, and DNA polymerase III to synthesise the remainder of the second strand (Higashitani *et al.*, 1997). The double stranded circular form is known as the replicative form, and it is this which serves as a template for synthesis of phage proteins and replication of positive (+) strands. Replication of (+) strand is initiated by phage protein pII, which binds to the (+) strand *ori* on the replicative form. pII causes a single-stranded nick in the (+) strand and forms a covalent bond to the 5' phosphate; the 3' end then acts as a primer, promoting rolling-circle replication of the (+) strand. As synthesis of the new (+) strand occurs, the old strand is displaced, until the positive *ori* is reached again – at this point, pII cleaves the dissociated single-strand from the replicative form, re-ligates the 5' and 3' ends of the cleaved strand, and dissociates from the molecule, leaving a circular ssDNA (+) strand, as well as the original double-stranded replicative form (Horiuchi, 1997).

The (-) and (+) strand origins are found in close proximity, along with a sequence known as the packaging signal, within a 400-nucleotide intergenic sequence on the phage genome. This region is known as the f1 origin of replication (Russel and Model, 1989). In the ssDNA (+) strand form, five hairpin loops are formed in this region; one corresponding to the packaging signal, and two each corresponding to the (-) and (+) strand origins (**Figure 2A**).

Interestingly, it has been found that the (+) origin can be divided into two regions, based on respective functionalities: the downstream region (**Region II in Figure 2A**) is involved in termination of (+) strand synthesis (Specthrie *et al.*, 1992). In fact, introduction of a (+) strand origin containing a 29-nucleotide deletion in Region II downstream of a complete (+) origin can result in synthesis of circular ssDNA that is much smaller than the length of the entire plasmid, comprising only the nucleotides between those two origins.

The newly synthesized circular small ssDNA molecule is coated with pV, leaving only the packaging signal of the genome exposed. The packaging signal must interact with the inner membrane component of the phage assembly complex which is composed of pI/pXI. The outer membrane component is pIV. As the DNA crosses the inner membrane; pV dissociates and is replaced by pVIII. When DNA is completely coated with pVIII, the minor capsid proteins pVI and pIII are added to the virion cap and the phage is released. If either of these minor capsid proteins are absent, the bacteriophages remain tethered to the membrane (Rakonjac *et al.*, 2011) creating what are called "hairy *E. coli*" (**Figure 3**).

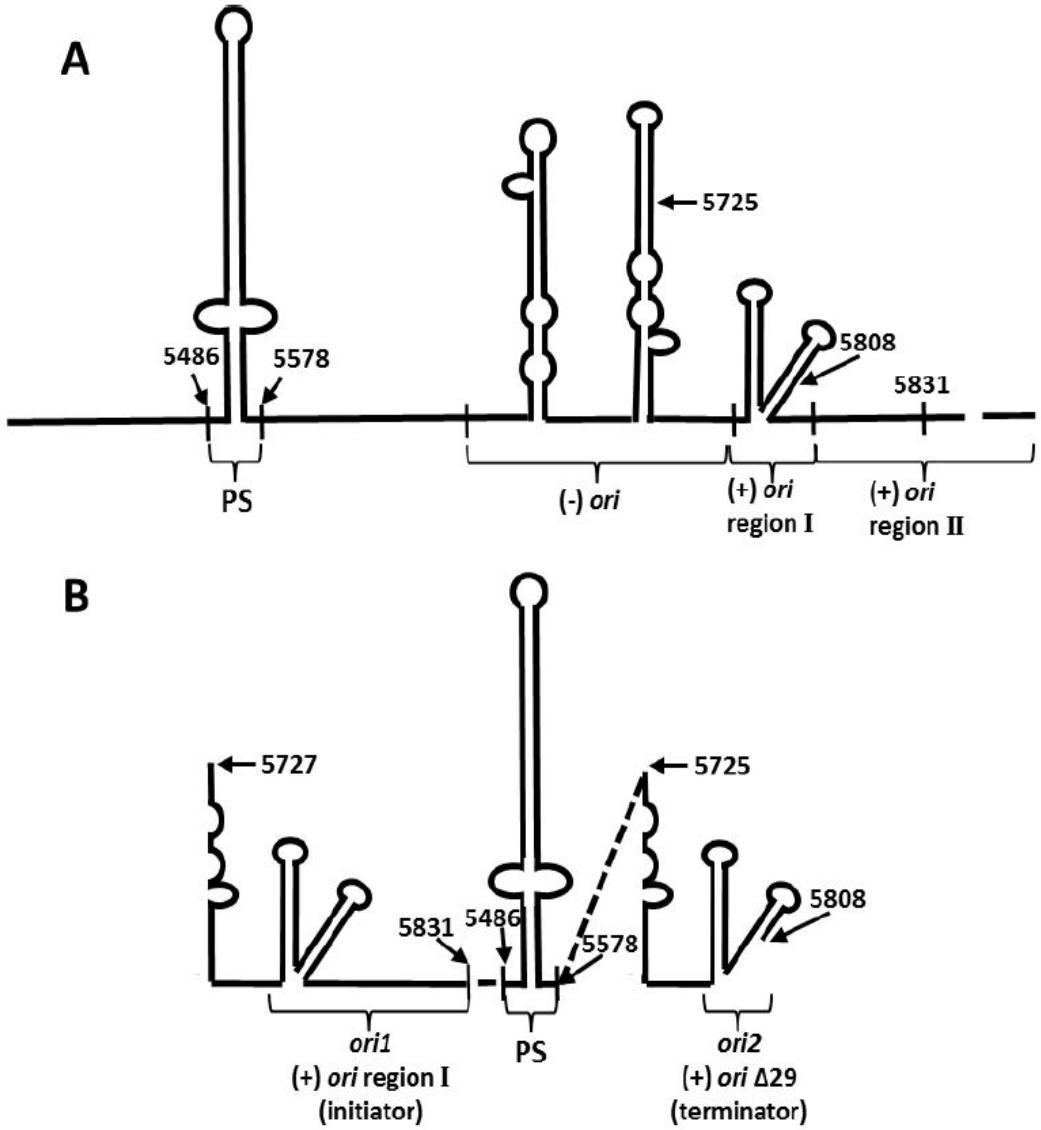

Figure 2: Structure of f1 *ori*

(**A**) Structure of f1 *ori* showing hairpin loops as found in ssDNA (+) strand form. PS is the packaging signal, (-) *ori* is the (-) strand origin, and (+) origin is the (+) strand origin of synthesis. Region I of (+) *ori* acts as a terminator of synthesis, while region II acts as the initiator. (**B**) Summary of the system used by (Specthrie *et al.*, 1992) to produce 50-nm particles. *Ori1* is a complete (+) origin, which acts as the initiator of (+) strand synthesis. *Ori2* contains a 29-nucleotide deletion in region II, preventing it from acting as an initiator but allows it to act as a terminator. The overall effect of placing the 'terminating' *ori2* downstream of the 'initiating' *ori1* is that only the sequence between the two *ori*'s is synthesized as circular ssDNA; the inclusion of a packaging signal between these origins allows the ssDNA to be assembled into particles. Figure adapted and legend taken with permission from (Bisset and Rakonjac, unpublished).

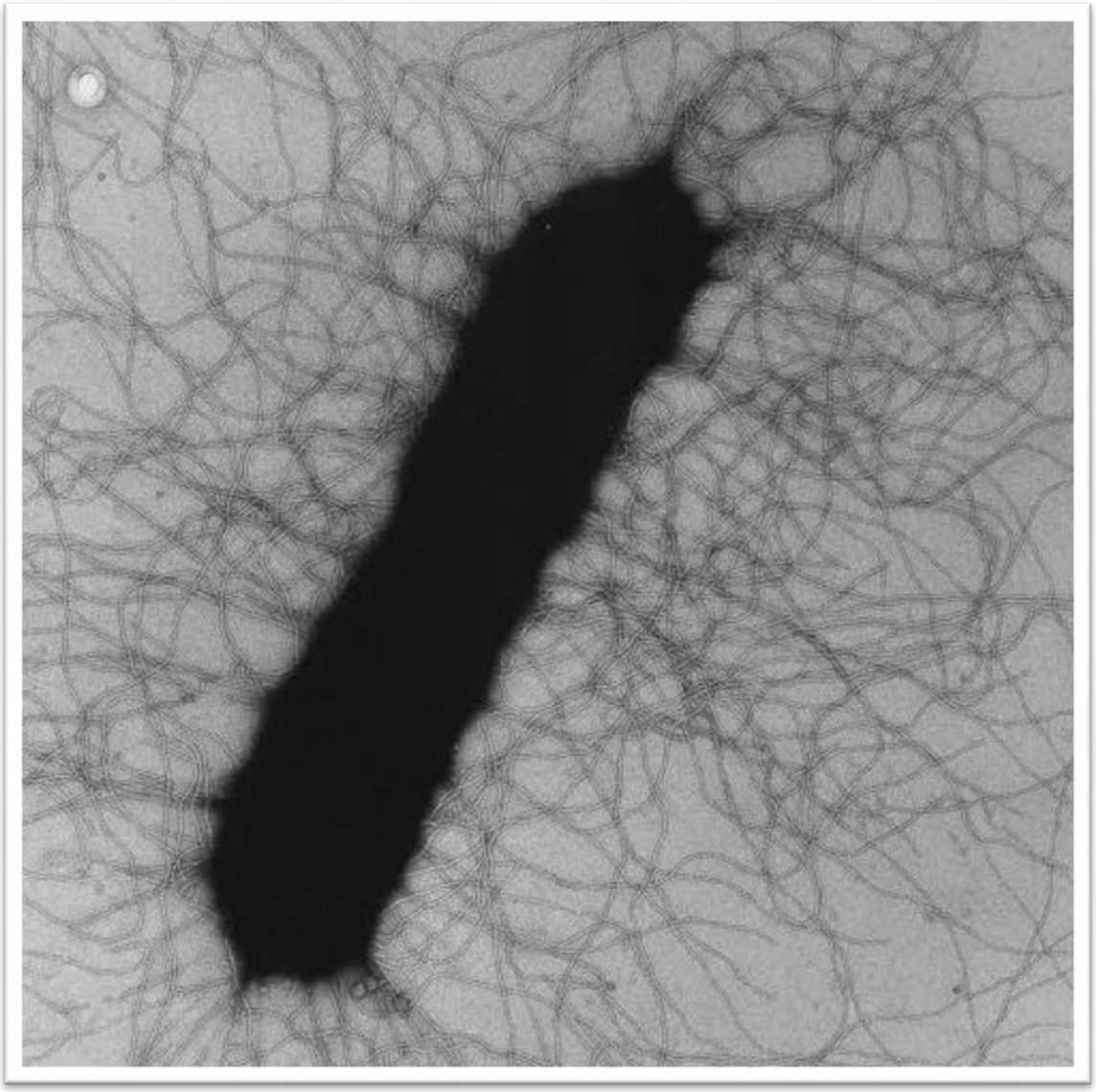

Figure 3: TEM *E. coli* infected with *gIII* deleted bacteriophage f1d3.

E. coli laboratory strain K2245 was infected with *gIII* deleted f1 bacteriophage. As this *E. coli* strain does not complement *gIII* deficiency, the filaments cannot dissociate from the membrane. Figure taken with permission from (Rakonjac and Model, 1998).

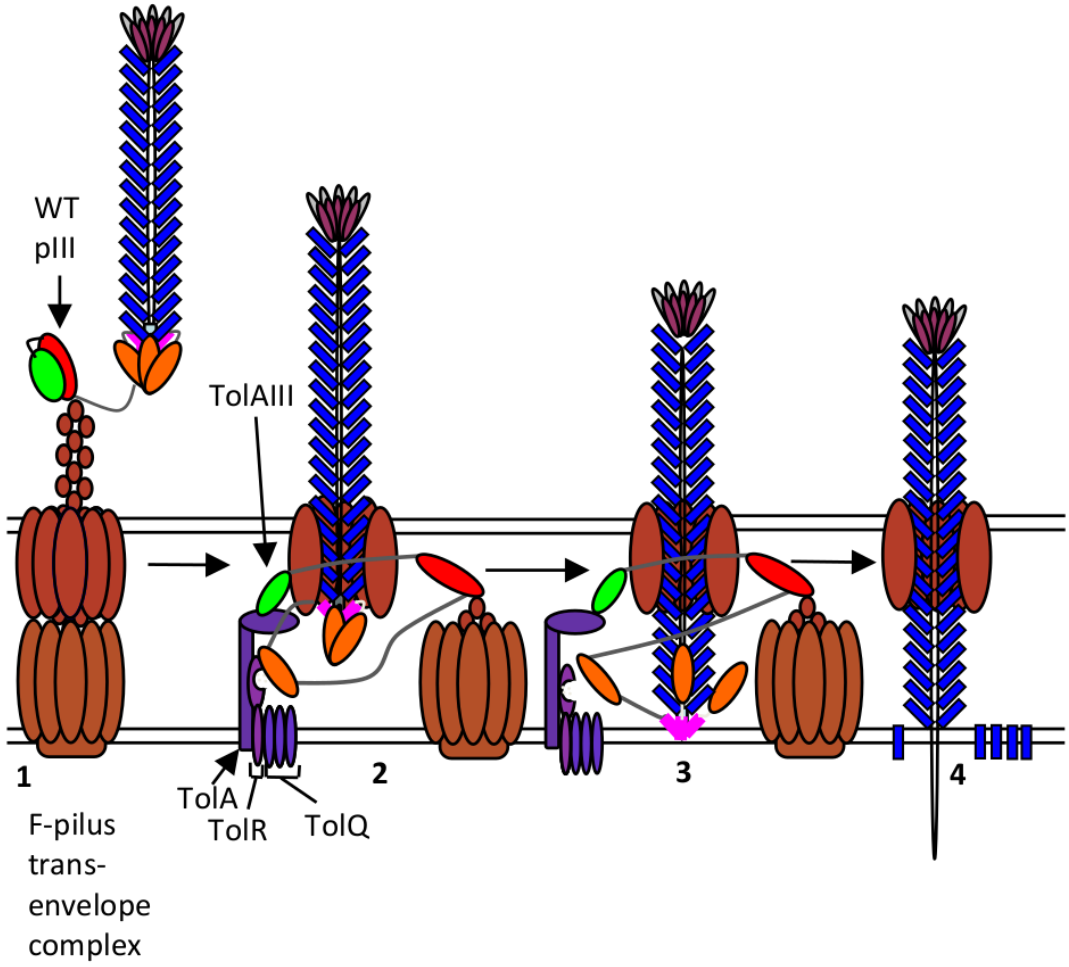

Figure 4: Infection process by filamentous phage

1) Binding of N2 domain (red oval) to the tip of the F-pilus (brown circles) and pilus retraction. **2**) Binding of N1 domain (bright-green oval) to TolA III domain (purple oval).
3) "Opening" of the C-domain and insertion of the C-terminal hydrophobic helix into the inner membrane. **4**) Entry of phage DNA into the cytoplasm and integration of the major coat protein pVIII into the inner membrane. Steps 1 and 4 are based on published findings, whereas steps 2 and 3 are speculative. Symbols: pIII N1 domain, red oval; pIII N2 domain, bright-green oval; pIII C domain, orange oval; pIII C-terminal hydrophobic helix (membrane anchor), pink rectangle; pIII glycine linkers, grey lines; major coat protein pVIII, dark blue rectangles; pVII, grey ovals, pIX, pink ovals; TolA and TolRQ, purple shapes; F-pilus, and the trans-envelope pilus assembly/retraction system, brown. The phage contains 5 copies of pIII, but for simplicity only one full-length pIII is shown. Figure and legend taken with permission from (Rakonjac *et al.*, 2011).

Following replication, the circular ssDNA (+) strand is coated in pV (a phage-encoded single-stranded DNA binding protein), causing the DNA to arrange in a rod-like structure. The only exposed segment of the DNA is a 45 base pair hairpin loop formed by the packaging signal. The exposed packaging signal then directs the genome to the inner membrane, where it interacts with the minor coat protein pXI and the complex formed by pI and pXI (which is integrated in the inner membrane) (Russel and Model, 1989). The two minor coat proteins, pVII and pXI, are added to the end of the assembling particle first. As the phage passes through the pI/pXI complex pV copies dissociate and are replaced by major coat protein pVIII. A large outer membrane channel encoded by phage gene pIV (*gIV*) provides the exit pore for the phage. This assembly-secretion process continues until the end of the ssDNA is reached; at this point, minor coat proteins pIII and pVI are added to the end of the particle, and the mature virion is released (Russel and Model, 1989). It has been noted that if the capping of phage ends with pIII and pVI is not efficient or these proteins are not available, rather than terminating growth the particles continue to elongate, packaging two or more ssDNA genomes sequentially (Rakonjac and Model, 1998).

1.2. Modifications of Ff Bacteriophage

Attaching functional molecules to the surface of filamentous bacteriophages is most commonly achieved by genetic or chemical modification, although enzymatic and ionic-interaction modes of attachment have also been reported. All listed methods are used in combination to obtain multifunctional particles required for vaccine and diagnostic applications.

1.2.1. Genetic Modifications

Ff bacteriophages are suitable modification templates not only because of their high symmetry, but also because they possess exceptional stability to a broad range of pH and temperature (Branston *et al.*, 2013). The major (pVIII) and minor (pIII, pIX and pVII) capsid proteins are oriented so that the N terminus is exposed on the surface of the particle and the C terminus interacts with the DNA inside the capsid (Hemminga *et al.*, 2010). Phage minor and major capsid proteins pIII and pVIII are common targets for genetic manipulation. The nascently translated pIII and pVIII each have an N terminal signal sequence that is essential

for targeting to the inner membrane. The signal sequence is cleaved by signal peptidase upon translocation of their N-termini across the inner membrane. This converts pIII and pVIII into "mature" proteins. Both proteins contain additional targeting motif at the C-terminus, a hydrophobic α-helix or "stop transfer" that anchors the mature protein in the inner membrane. As a result, the N terminus of the mature peptide is exposed in the periplasm, while the membrane-anchoring leaves a few positively charged residues at the C terminus exposed to the cytoplasm. These positively charged residues interact with negatively charged phosphates of DNA during virion assembly. For a protein or peptide to be displayed on the surface of the Ff-phage, its coding sequence needs to be inserted, in frame, between the signal sequence and the mature portion of the pIII (Rakonjac *et al.*, 2011).

All virion proteins are integral membrane proteins prior to assembly into the virion. Peptides or proteins fused to the N-termini of pIII or pVIII, pVII and pIX fold in the oxidative environment of bacterial periplasm, where sulfhydryl groups of cysteines are oxidised to form S-S bridges. Ff is therefore more suitable for folding and display of secreted or cell-surface proteins, such as antibody fragments or other proteins that fold in the oxidative cellular compartments in eukarya, bacteria and archaea. Proteins which are normally expressed and fold within the cytoplasm are usually successfully displayed unless they contain multiple cysteine residues or require special cytoplasmic chaperones for folding. For cysteine containing cytoplasmic proteins, growth under strongly reducing conditions or using host mutants that are deficient in oxidative functions in the periplasm can allow folding of proteins with domains containing obligatory reduced cysteine residues (Rebar and Pabo, 1994, Velappan *et al.*, 2010).

Genetic engineering of bacteriophages allows the peptide to be displayed accurately, but the method has its limitations. Two "standard" classes of vectors are available for phage display: phagemid and phage. A phagemid is a plasmid that contains the Ff origin of replication and packaging signal, as well as a "display" cloning cassette for constructing fusions with Ff proteins. Depending on the phagemid design, it can express fusions with any of the five Ff phage capsid proteins. Phagemids are used in conjunction with helper phages, which in most arrangements encode a wild-type copy of each virion protein. As both the fusion and the wild-type protein are produced in the helper-infected *E. coli* cells, the virions are mosaic, minimising interference of large fused domains with the assembly of the virions. However, in this arrangement fusions are competing with wild-type proteins and are often incorporated

into the virion and displayed at relatively low efficacy. In a phage vector, the bacteriophage genome is modified directly, and thus every copy of the relevant capsid protein in the phage is recombinant (Hess *et al.*, 2012).

As discussed, the inserted protein should not interfere with the virus assembly and must be correctly targeted to assemble into the particle with other virion proteins, to be displayed on the phage surface. However, even if the fusion product is incorporated into the virion, this does not guarantee that the recombinant protein or peptide will fold into a functional protein. If the fused protein does not fold properly in the periplasm, it is degraded by periplasmic proteases that normally degrade misfolded proteins (Forrer *et al.*, 1999). In the case of phage vectors where all copies of a given virion are fusions, interference with virion assembly or infectivity typically results in selection of internal in-frame deletions that provide competitive advantage over the original construct, but also reduce the size of the insert and typically eliminate functions of interest (Merzlyak and Lee, 2009).

1.2.2. Chemical Modifications

Chemical modification strategies are required to help expand the variety of displayed functions by attaching non-peptide organic molecules or displaying proteins that cannot fold on the surface of phage, such as green fluorescent proteins and their derivatives (Bernard and Francis, 2014).

There are three ways through which chemicals can be attached to intact filamentous phage: covalent attachment (Bar *et al.*, 2008), ionic attachment (Ngweniform *et al.*, 2009) or enzymatic attachment (Hess *et al.*, 2012). Covalent modification relies on the non-specific modification of the free amine groups of the phage capsid proteins. In addition to modification of free amines (in the N-terminal residue or lysine side-chain), other groups can be modified: carboxyl groups and tyrosine. More specific modification of only N-terminal amines of the major coat protein was achieved using transamination/oxime formation technique (Carrico *et al.*, 2012). These methods fit the general requirements for modifying biological molecules; relatively mild reaction conditions (temperature and pH tolerated by the virion), and in particular in aqueous solution. Ff phage can tolerate a wide range of pH (3 ~ 11) and temperature (below 80ºC) (Branston *et al.*, 2013), but are sensitive to organic

solvents. Interestingly, Ff containing mutations in pVIII that increase resistance to organic solvents have been reported (Petrenko *et al.*, 1996).

Modification of amines in Ff using *N*-hydroxysuccinimide (NHS) ester chemistry is a reliable strategy for modifying the virion capsid proteins, resulting in hundreds of attached functional groups along the filament shaft. However, this also leads to unwanted modification of the lysine residues on proteins that are displayed on the particle as pIII fusions using recombinant DNA technology, potentially inactivating lysine side-chain amines required for interactions (Hermanson, 2013). Gauging the extent of modification can avoid modification of the pIII fusions at the filament terminus, while providing sufficient number of copies along the shaft. One typical modification using this method is attachment of fluorescent dyes that allow tracking of phage displaying an antibody that recognises a target of interest at the pIII site (Li *et al.*, 2010).

Diazonium salts are known to react with tyrosine, lysine and histidine residues. In Li *et al.* (2010) the diazonium salts were used to modify tyrosine residues in pVIII (Tyr 21, Tyr 24); the lysine and histidine residues in pVIII remained unchanged. Like amine modification, the lack of discrimination between the desired tyrosine's and those in the displayed structure can result in undesired modifications of displayed recombinant antibodies containing tyrosines' involved in the antigen binding (Bernard and Francis, 2014).

Carbodiimide compounds, such as 1-ethyl-3-(3-dimethylaminopropyl) carbodiimide hydrochloride (EDC) are used to modify carboxylic acid containing residues: aspartate and glutamate residues. EDC coupling can be used effectively to target the carboxylic acid moieties on the phage scaffold; however, EDC coupling is not site-specific, it will target any carboxyl groups of the recombinant proteins (e.g. antibodies) and potentially modify the active sites. Besides gauging the reaction to limit modification of pIII and displayed fusions, another way to prevent this is to remove the negatively charged amino acids from non-target proteins; however, this could result in a non-functional protein (Bernard and Francis, 2014, Li *et al.*, 2010).

1.2.3. Alternate Modifications

In contrast to modification strategies described above, a transamination/oxime formation technique modifies N-terminal alanine's' if there is a proximal lysine residue. This approach is suitable for Ff modification, as the pVIII has an alanine (position 1) and a lysine (position 8) at the N-terminus (Carrico *et al.*, 2012). The authors achieved a high modification level of every second pVIII, while the binding capabilities of the displayed fusion peptides on pIII were preserved (Bernard and Francis, 2014).

An alternative to covalently attaching molecules to Ff is through enzymes, where specific attachment motifs are displayed on pIII or pVIII using recombinant DNA technology in a way that they can then be enzymatically modified. The enzymes used in this approach, for instance sortases, specifically modify short motifs displayed on pIII and pVIII (Hess *et al.*, 2012).

Another approach to functionalising phage is through ionic-interaction, where the overall charge of the particle is changed. Phages engineered to be negatively charged through modification of pVIII were combined with positively charged liposomes carrying a protein and/or drug of interest, resulting in an association (Ngweniform *et al.*, 2009). Peptides designed to target this phage-liposome complex to specific cells or tissues were displayed on pIII, triggering delivery of the contents of the liposome (Bar *et al.*, 2008).

1.3. Phage Display

pVIII is commonly used for displaying large number of copies of short peptides per virion. However, the display on each pVIII copy has severe size limitations. Peptides fused to pVIII can have up to 10 amino acids; longer peptides interfere with assembly of the Ff filament. Display of longer peptides and even protein domains is possible using phagemids, in combination with the wild-type pVIII expressed from the helper phage. In this case the desired fusion product makes up less than 25% of the total pVIII molecules in a mosaic virion (Hess *et al.*, 2012). This mosaic display nevertheless results in very high copy number of peptides per virion (~650); given that there are ~ 2700 copies of pVIII per virion (Overman *et al.*, 1996).

Large peptides and proteins have been genetically fused to all four minor capsid proteins (pIII, pVI, pVII & pIX) using a phagemid vector and mosaic display. Of those, pIII can accommodate the largest protein inserts and has been extensively used in the phage and phagemid system for mosaic and uniform display. Fusions to pIII do not interfere with virion assembly, however they can interfere with infection, which is mediated by the N-terminal two-thirds of the protein (Gao *et al.*, 1999).

Bacteriophages have been used as nanoparticles due to their highly symmetrical structure. Ff bacteriophage's highly symmetrical shaft has been used as template for assembly of inorganic nanocrystals along the length of the filament for nanotechnology applications, whereas the filament ends were used for diagnostic applications (Bardhan *et al.*, 2014, Ghosh *et al.*, 2012, Sattar, 2013, Schmelcher and Loessner, 2014, Smartt and Ripp, 2011, Whaley *et al.*, 2000). Genetic modification of the capsid proteins is widely used to functionalise the phage; however, chemical strategies have been used to covalently attach non-protein organic molecules, widening the range of applications (Bernard and Francis, 2014, Hemminga *et al.*, 2010).

pIII and pIX have been functionalised with materials ranging from small molecules to large correctly folded proteins (Hess *et al.*, 2012). There are two variants of pIII display: fusing foreign proteins to the N-terminus of the full-length mature protein, or to a truncated protein (C-domain). The C-domain of pIII is required for assembly into the virion and can be used as long as there is a signal sequence upstream of the inserted sequence. Given that the N-terminal portion of pIII is required for infectivity of the virus particles, any N-terminal truncation of the pIII requires mosaic display in combination with a wild-type pIII if infection is desired. If non-infectious particles are sufficient for an application, a helper phage containing *gIII* deletion can be used to produce non-infectious particles displaying five copies of fusion to the C-domain of pIII. As with pVIII, the foreign insert needs to be in frame with the upstream signal sequence and the downstream mature (or truncated) pIII (Rakonjac *et al.*, 2011).

The roots of using Ff as a display particle lie in phage display technology, first published by Smith (1985). This technology exploits the physical connection between the protein displayed on the surface and coding sequence packaged into the virion, allowing screening of large libraries of peptide or protein variants (up to 10^{13}) (Loset and Sandlie, 2012) for affinity to

specific targets. Two “standard” classes of vectors are available for phage display: phagemid and phage. Phagemids are used in conjunction with helper phages, which in most arrangements encode a wild-type copy of each virion protein (Hess *et al.*, 2012).

1.4. Phage Display Technology

Ff bacteriophage are central to phage display, a combinatorial technology in which libraries of peptides, antibodies, or proteins are displayed on the virion surface, whilst the corresponding coding sequences are encapsulated inside the virion. This physical link between the displayed protein and its coding sequence allows for affinity screening and enrichment of rare variants that bind to a specific ligand, from vast libraries of variants.

Physical link between the protein and its encoding sequence is achieved by construction of the virion gene fusions with coding sequences of peptides, which are packaged into the virion that display the fusion (chimeric) protein on the surface of the virion. Most commonly used fusions are to the minor virion protein pIII, followed by the major coat protein pVIII. Minor virion proteins pVII, pIX are used less frequently, with the least frequently used minor virion protein pVI (Salmond and Fineran, 2015, Wu *et al.*, 2016).

Two types of vectors are used in phage display, phage and phagemid vectors. While display in a phage vector system is simple; involving a single episome, it is prone to selection against the recombinant clones due to impairment of phage infection and/or assembly (Salmond and Fineran, 2015, Wu *et al.*, 2016). To alleviate the constant selective pressure for clones that replicate most efficiently, phagemid display vectors are used, in conjunction with helper phage. Phagemid vectors are plasmid vectors that contain a plasmid and an Ff origin of replication; phage display phagemid vectors also carry a display cassette, a specific virion-protein-encoding gene including a cloning site for inserts, to allow construction of virion protein fusions (Salmond and Fineran, 2015, Wu *et al.*, 2016) Library construction in a phagemid phage display vector does not involve phage and henceforth avoids the selective pressure for the most efficiently replicating clones.

In order to display a peptide-virion-protein fusion encoded by recombinant phagemids, the library pool of recombinant clones is infected with a helper Ff phage that is specially

constructed to maximise phagemid replication from the Ff origin and packaging into Ff-like phagemid particles (PPs). These particles contain phagemid ssDNA and display the protein fusion encoded by the insert.

1.5. Functionalised Bacteriophage

Besides their use in phage display, Ff phage displaying functionalities of interest are used as nanoparticles in a variety of applications. In contrast to chemically synthesised nanoparticles they self-replicate, providing constant and limitless source of the nanoparticles. In addition, they are manufactured in aqueous solution, decreasing the organic waste. Ff phage are resistant to heat (up to 80 °C) and to a wide range of pH. They have a long shelf life, thus meaning a lesser turn-over and therefore even lower long-term cost; they are low-cost to engineer using recombinant DNA technology. Combined with display that allows selection of peptides and antibodies of high-affinity to an analyte of interest, phage displaying a specific detector is already identified and attached to the detector particle in the process of library construction and screening (Rakonjac *et al.*, 2011).

Diagnostics application of Ff nanofilaments take advantage of a high length-to-diameter ratio. Signal from particles displaying analyte-binding proteins at one end (e.g. as fusion to minor virion protein pIII)) can be highly amplified due to the high-copy-number signal coming from pVIII along the length of the phage (Schmelcher and Loessner, 2014). The signal is often amplified by labelling the major coat protein pVIII through direct or indirect attachment of enzymes, fluorescent dyes, paramagnetic metal nanocrystals, nanogold or other signal-generating functionalities along the shaft of the filamentous virion. The large number of pVIII copies help amplify the signal using enzyme-linked, fluorescent dye-based or ELISA or dip-stick assays (Bradbury and Marks, 2004, Sattar *et al.*, 2015, Schmelcher and Loessner, 2014, Smartt and Ripp, 2011).

Ff bacteriophage displaying multiple functionalities are used in a wide variety of other applications, including: the templates for assembly of inorganic structures; diagnostics using optical properties of filaments; tissue templating; imaging; and drug targeting (Bar *et al.*, 2008, Chung *et al.*, 2011, Dang *et al.*, 2013, Lee *et al.*, 2009, Oh *et al.*, 2014, Sattar *et al.*, 2015).

1.6. Dipstick Assays

A simple lateral flow assay for home- or point-of-care use is a dipstick assay, such as a pregnancy test. Dip-stick a strip of nitrocellulose backed with plastic support and encased usually within a plastic case and is impregnated with reagents for identification of an analyte (e.g. a hormone, metabolite, toxin, pollutant etc.) in the fluid being tested (e.g. urine, blood or other fluids, environmental samples). The capturing molecules are printed as lines across the strip, whereas the detector particles are deposited in an absorbent cushion at the bottom of the strip. These detector particles become solubilised as the stick is dipped into the assayed fluid. A characteristic of a dipstick assay is the presence of a test, and a control line. The test line detects the analyte-bound detector particles, and control line is designed to capture the detector particles even if the fluid being tested does not contain the analyte that is being tested for. The control line allows trust in the result of the dipstick assay, as the positive control result shows that the nitrocellulose has been processed correctly, the correct reagents have been applied and provides a benchmark for how dark a positive result on the test line should generally be (Buhrer *et al.*, 1998). The test line usually consists of a capturing molecule that is paired to an analyte; detector particle interacts with a non-overlapping epitope on the analyte. Dip-sticks are used for qualitative and semi-quantitative assays, and their sensitivity depends on the application and the method of detection. Detector particles are usually chemically synthetises functionalised gold or blue beads displaying chemically attached detector molecules. Use of biological nanoparticles, including the Ff phage or Ff-derived nanorods has been reported {Sattar, 2015 #1}.

1.7. Short Ff-derived Nanorods in Dipstick Assays

One drawback of filamentous phage use in diagnostic applications that involve lateral diffusion was the extreme length-to-diameter ratio, which does increase the signal, but results in drag, which in turn leads to unclean-looking dip-stick bands and high background signal (S. Sattar et al., unpublished). This was overcome by production of extremely short (50 nm) Ff-derived particles, named Ff-nano (Sattar *et al.* 2015).

Ff-nano were functionalised to display the FnB domain as a “detector molecule” for use in a dip-stick setup. The control line of the simple dipstick assay was then printed with anti-pVIII

antibody – ensuring that any particles that were not captured by the test line would then bind to the control line, as pVIII is the most prevalent (major) coat protein in Ff bacteriophage. The test line of this dipstick assay was printed with collagen, which is known to bind fibronectin at a different epitope from that of FnB protein, with high affinity (Balian *et al.*, 1979, Engvall, 1978, Hayman and Ruoslahti, 1979, Ruoslahti *et al.*, 1978)

The short nanorods were obtained using a method of controlling the length of phage particles does not involve replicating an entire episome for packaging, as in phagemid vectors. Rather, just a small region of a plasmid is amplified. This was first carried out by Specthrie *et al.* (1992), who demonstrated that if a (+) *ori* containing a specific deletion (*Δ29*) that removes its ability to initiate replication was placed downstream of an unmodified (+) *ori*, with a packaging signal in between the two, only the span of DNA between the two origins would be amplified (Dotto *et al.*, 1982). Incorporation of the packaging signal between these two origins results in extremely small (~221 nucleotides) ssDNA circles being synthesized and packaged, which translates to Ff particles approximately 50 nm in length (Specthrie *et al.*, 1992). Because the remaining portion of the plasmid is not packaged in this process, the ssDNA within the phage particles does not contain any coding sequences, and so is unable to replicate autonomously in any cells they infect or transfer any unwanted genes, such as those conferring antibiotic resistance.

The drawback of the outlined system is that the particle production is poor due to the lack of (-) origin in the replication cassette. Further shortcoming of the published system is the use of helper phage which could not be completely eliminated form purified short particle samples. Utilizing helper plasmids over helper phage in production of short particles appears to be the natural next step in developing short, tuneable-length phage-derived particles for nanotechnology purposes.

1.8. Ff-derived 75-110-nm Particles

To improve production of short particles, the replication unit was changed to introduce a ‘zap’-style Ff-dependent replicon that involves a segment of ssDNA being excised via Ff pII-mediated rolling circle replication from a larger plasmid during phage infection (Short *et al.*, 1988). This plasmid, similarly to Sattar *et al.* (2015) and Specthrie *et al.* (1992) contains duplicated f1 (+) origin of replication, where the upstream (+) *ori* is ‘complete’, capable of

initiating synthesis of ssDNA in the presence of phage protein pII, followed by the f1 intergenic sequence containing (-) *ori*, packaging signal and a truncated (+) *ori* that contains a 29 nucleotide deletion, causing it to act as a terminator of ssDNA synthesis (Specthrie *et al.*, 1992) (see **Figure 3**). The overall effect means that, in the presence of the phage replication protein pII, only the regions between the two (+) origins are synthesized into circular ssDNA copies which can now replicate independently of the plasmid (in the presence of pII) using both (-) and the restored (+) origin and packaged due to the presence of a packaging signal (see **Figure 5**). When compared to previously published Ff-nano, which lacks the (-) *ori* (Sattar *et al.*, 2015), NanoZap was found to produce particles at around a 4-fold greater rate. As both pNanoZap and the plasmid used to produce Ff-nano contain the same plasmid *ori* (MB1), the presence of the (-) *ori* on the excised NanoZap replicons would appear to be the major cause of this increased production efficiency.

The phagemid and Ff-nano systems required the subsequent infection of helper phage to initiate particle assembly. As the helper phage also encapsulate their own genome, with their own f1 *ori*, this results in the production of the "full-length" helper phage in addition to short particles, requiring additional purification steps to separate full- and short-length particles, a process that may prove difficult if the sizes are not greatly different (Sattar *et al.*, 2015) (**Figure 6A**). One method designed to avoid this issue is to convert the genome of the helper phage into a plasmid, by replacing the f1 *ori* with a plasmid *ori* (Chasteen *et al.*, 2006). By transforming cells with both the helper plasmid and a phagemid, only one size of circular ssDNA will be synthesized and therefore single-length phage particles will be assembled (**Figure 6B**).

However, it was observed that the particles produced from the NanoZap system, were multiple-length (**Figure 7**) (Bisset and Rakonjac, unpublished), rather than the desired single-length particles, likely due to two or three ssDNA copies being sequentially packaged. These multiple-length NanoZap particles were seen when in use with the pRNano3 helper plasmid (**Figure 7**) (Section 1.6). Multiple-length particles are not desirable for diagnostic assays that involve diffusion, such as dip-stick assay that requires particles of uniform size. Furthermore, the purpose of the system was production of short particles, hence longer than unit-length particles are not desirable.

Another problem with the system shown in preliminary work is emergence of around one in a million particles containing the complete plasmid (Rakonjac, unpublished), due to a low-frequency recombination between the two (+) origins in the pNanoZap replication templates. These particles easily transduce antibiotic resistance to sensitive *E. coli* and thereby could contribute to the spread of antibiotic resistance in biomedical applications.

1.9. Helper Plasmid pRNano3

To assemble phage particles in the absence of helper phage, conversion of the helper phage genome into a plasmid was expected to provide the full complement of genes required for particle assembly while removing the side-product of additional helper phage (Marzari *et al.*, 1997). To achieve this, Bisset and Rakonjac (unpublished) modified the helper phage RNano3, through the removal of the f1 origin of replication from the helper phage genome; this was replaced with a plasmid *ori* and antibiotic resistance marker, effectively converting the helper phage into a plasmid expressing all phage proteins. A low copy-number plasmid *ori* p15a was chosen, along with the Kn resistance marker, from helper plasmid VCSM13 (Stratagene). This new helper plasmid was termed pRNano3 **(Figure 8)** (Bisset and Rakonjac, unpublished).

The Ff-derived helper plasmids slow down the growth of *E. coli* and often result in non-functional mutants due to the toxicity of the major coat protein, pVIII (Marzari *et al.*, 1997); Gagic and Rakonjac, unpublished). The major coat protein is produced in a large number of copies in the cell and contains the SecYEG-targeting signal sequence and membrane anchor (Stiegler *et al.*, 2011). The massive expression of pVIII in the absence of phage assembly (e.g. in mutants that lack assembly machinery) results in mitochondrial-cristae-like folding of inner membrane and cell death (Schwartz and Zinder, 1968). To overcome this problem, the helper plasmid pRNano3 was engineered to contain an *amber* stop codon at the codon 25 of gene VIII (*gVIII*), resulting in premature termination of translation that eliminates the membrane anchor; these properties resulted in relief of the cellular toxicity during construction and amplification steps in the low-efficiency suppression strain TG-1 and non-suppressor K2245.

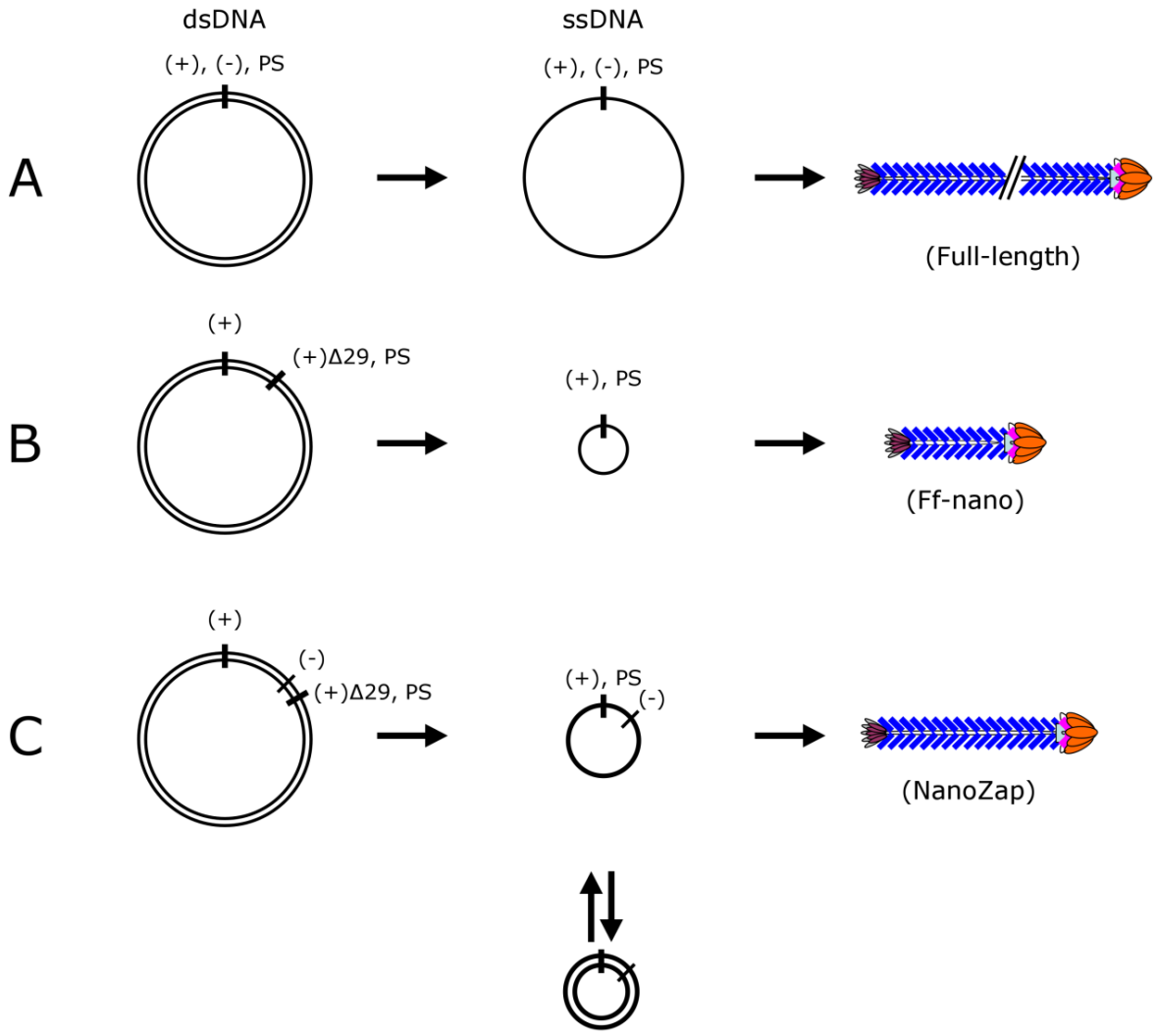

Figure 5: Principle behind NanoZap

(**A**) Double-stranded RF form of Ff genome contains a (+) *ori* which is used to produce a circular, ssDNA copy of the same length. (**B**) Scheme of particle-producing plasmid used to generate Ff-nano (Sattar *et al.*, 2015). Plasmid contains a complete (+) *ori* followed by (+) *ori* with 29 nucleotide deletion (Δ29) and packaging signal (PS), resulting in short (221 nucleotide) ssDNA being synthesized packaged into short Ff-nano particles. (**C**) A (+) origin of replication followed by a truncated f1 intergenic sequence containing (-) *ori*, packaging signal (PS) and (+) Δ29 *ori* results in circular ssDNA that promotes synthesis of (-) DNA strand. Due to additional DNA attributed to the (-) *ori*, ssDNA produced by pNanoZap is longer than that of Ff-Nano, consequently leading to longer particles. Advantage of the NanoZap over Ff-nano system is that given the (+) strand is replicated not only from pNanoZap, but also from the 736 base pair dsDNA circle, it leads to higher copy-number of templates per cell, and consequently higher number of assembled particles per cell (Sattar *et al.*, 2015). Figure and legend taken with permission from (Bisset and Rakonjac, unpublished).

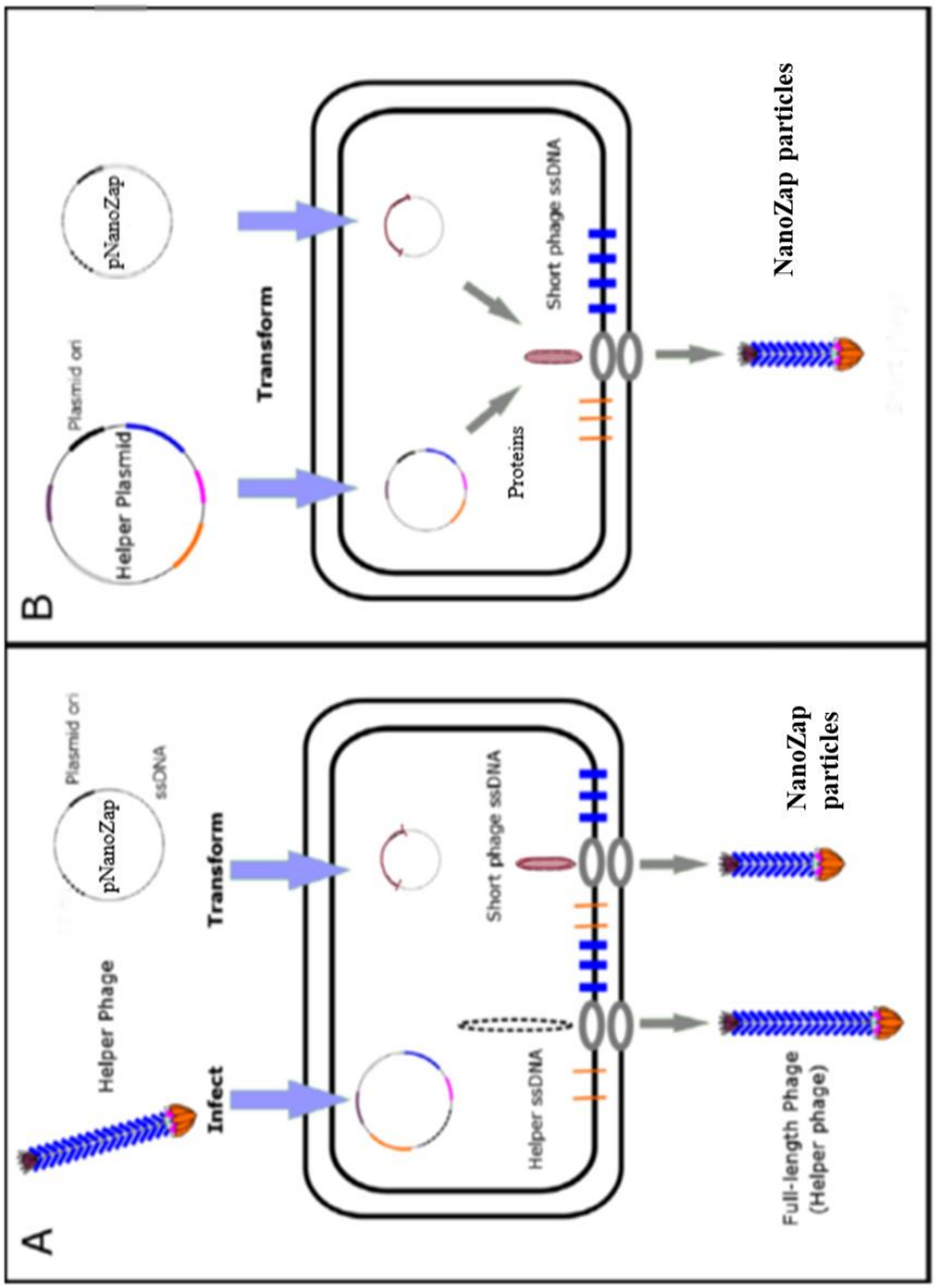

Figure 6: Comparison of helper phage - and helper plasmid-assisted production systems

(**A**) Conventional phagemid-based methods of producing short phage relies on subsequent infection of phagemid-carrying cells by 'helper phage', which provides a source of phage proteins. Only on the presence of Ff proteins can circular ssDNA copies of the phagemid be produced through activation of f1 *ori*. However, presence of helper phage genome results in co-production of full-length phage along with short phagemid-derived particles. (**B**) Subsequent removal of f1 *ori* from helper phage genome and replacement with plasmid *ori* results in a helper plasmid. The helper plasmid provides the cell with all the proteins normally supplied by the helper phage, but the absence of f1 *ori* prevents packaging into full-length phage particles; only one size of particle is assembled, using pNanoZap-derived ssDNA. Figure adapted from (Bisset and Rakonjac, unpublished).

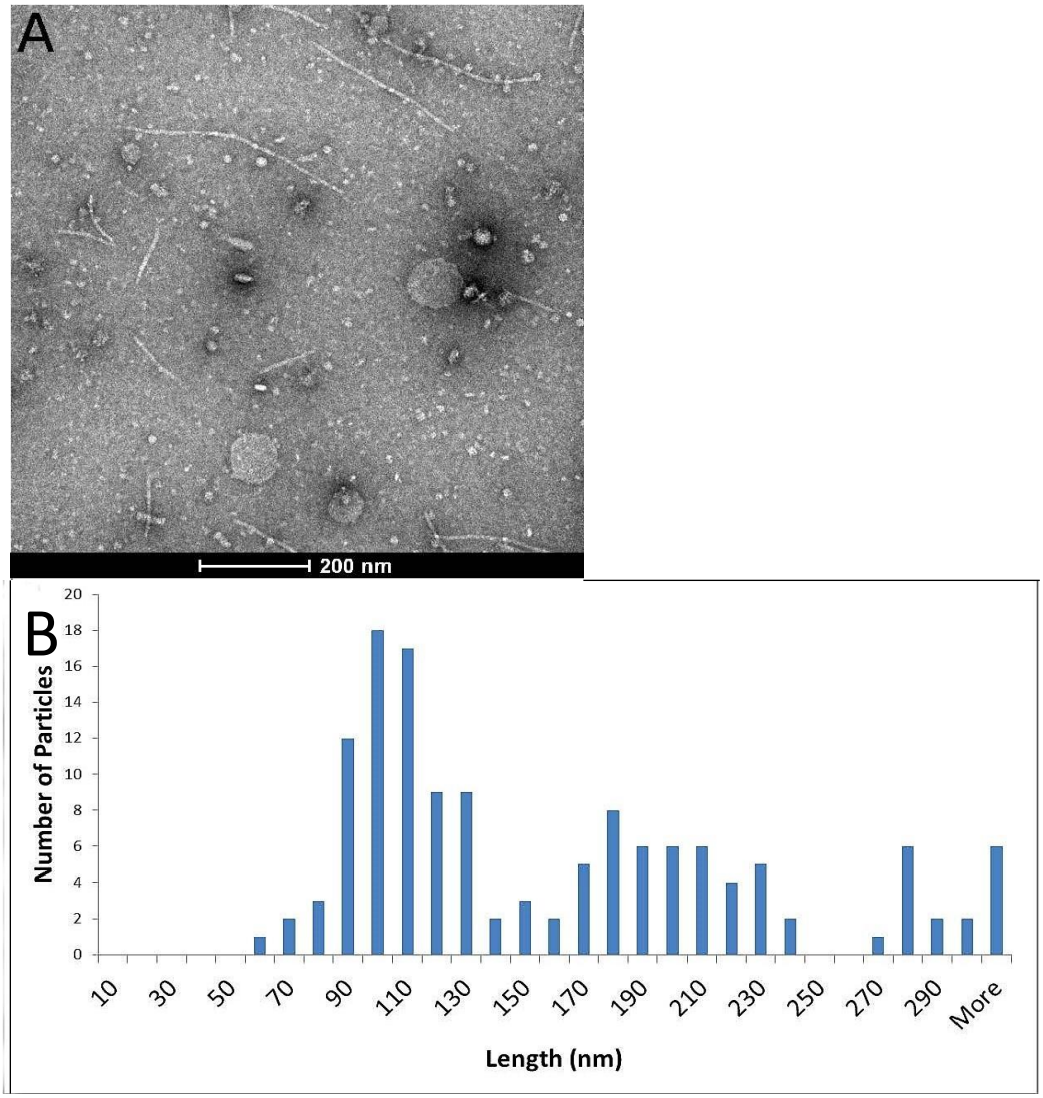

Figure 7: TEM of NanoZap particles

TEM of the NanoZap produced by helper plasmids pRnano3 (**A**). In the image, a variety of different lengths can be seen due to nanorods aligned in different positions along the surface, not all completely flat. Additionally, long particles due to two or more genomes being packaged in a single phage particle can be seen. Scale bars represent 200 nm. Size distributions of nanorods produced by the helper plasmid pRnano3 (**B**) are presented as histograms. Histograms were generated by measuring the length of 200 particles in each sample using the ImageJ measurement function. Figure and legend taken with permission from Bisset and Rakonjac (unpublished).

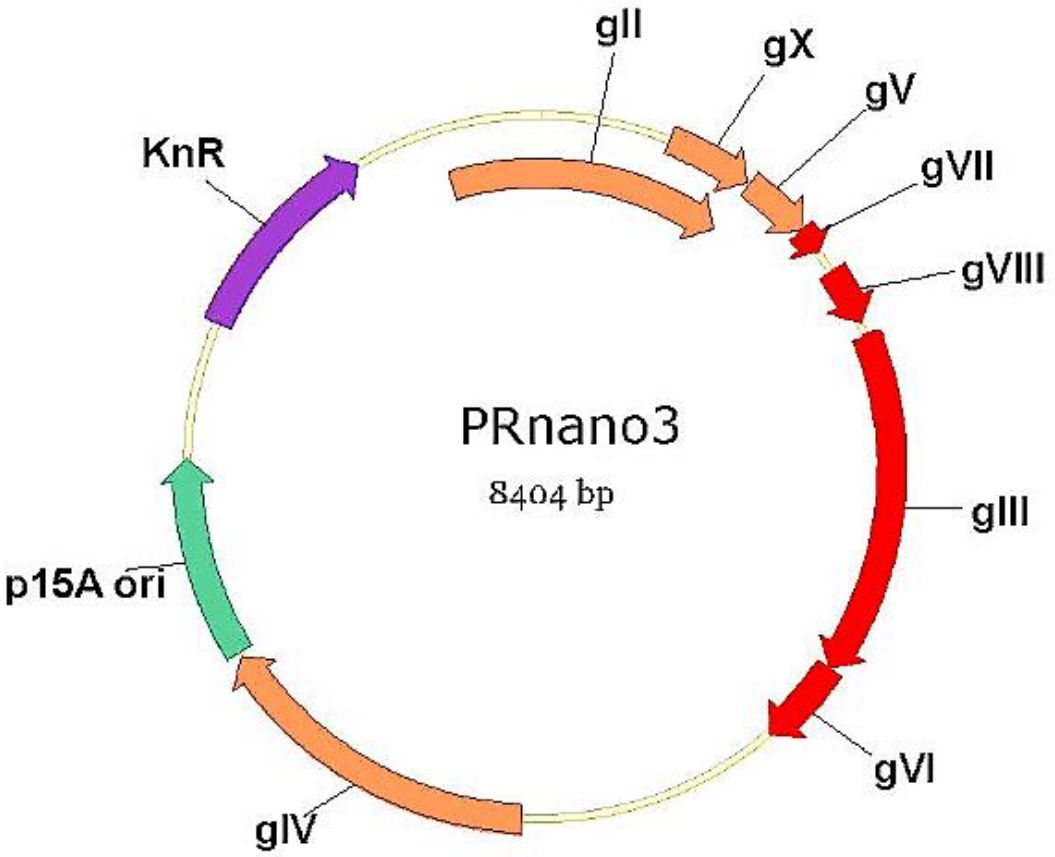

Figure 8: pRNano3 Helper Plasmid Map.

pRNano3 is derived from genome of helper phage RNano3. It contains all Ff genes encoding proteins required for phage particle assembly. Plasmid *ori* is shown in green, kanamycin resistance marker purple, genes encoding virion coat proteins red, and genes encoding replication and assembly proteins, orange. Figure and legend taken with permission from (Bisset and Rakonjac, unpublished).

1.10. Research Goals

There are three parts of my research project, and as such, each has its own goal.

The major aim of part one of this project is to construct and investigate the double-display *E. coli*-filamentous bacteriophage particles for use in diagnostic assays. This was planned to be achieved through three main objectives: to functionalise *E. coli*-displayed filamentous phage with detector molecules for specific analytes; to show that the double-display system (detector displayed on phage which in turn is displayed on the surface of fluorescent *E. coli*) can be used in dipstick assays and to measure the sensitivity using a model detector-analyte pair (e.g. fibronectin-binding protein and fibronectin); and finally, to develop assays for detection of food contaminants (e.g. botulinum toxin) using the double-display system.

The major aim of part two of this research project was to create a reliable method of creating NanoZap particles of a single-unit length. This was achieved through one objective: overexpress minor proteins pVII and pIX and thereby increase the rate of particle assembly initiation and particle production, as well as decrease the proportion of multiple-length particles.

The major aim of part three of this project was to create a new NanoZap particle template plasmid, where the antibiotic marker is replaced by an auxotrophic marker, to avoid the low – frequency packaging of antibiotic resistant gene into the particle, and thereby avoid horizontal transfer of antibiotic resistance among *E. coli* in the human GIT or outside of the laboratory containment.

Chapter II

2. Materials and Methods

2.1. Materials and Growth Conditions

2.1.1. Bacterial Strains and Growth Conditions

All *E. coli* strains, plasmids, bacteriophage, oligonucleotides and antibodies used in this study are listed in Tables 1 - 5 respectively. Cells were cultured in Difco^{TM} 2×YT liquid medium (Becton-Dickinson, BD) at 37^{o}C with continuous shaking (200 rpm) or were grown on solid 2×YT media plates lacking antibiotics (1% Bacto-agar, BD) at 37^{o}C, unless otherwise stated. Antibiotic was supplemented when required at the following concentration: ampicillin (Amp) at 100 µg/mL; kanamycin (Kn) at 50 µg/mL; chloramphenicol (Cm) at 25 µg/mL. The antibiotics used were purchased from Sigma Aldrich.

2.1.2. Plasmids, Helper Plasmids and Bacteriophage

Several different plasmids and helper plasmids were used during the experiments. The plasmids and helper plasmids are outlined in Table 2. Bacteriophage used are outlined in Table 3.

2.1.3. Oligonucleotides and Restriction Enzymes

The oligonucleotides used are shown in Table 4. The restriction enzymes used were all used at a concentration of 0.4 U/µL, unless otherwise stated.

2.1.4. Antibodies

The antibodies used are shown in Table 5. Rabbit polyclonal anti-Fd (f1) phage antibodies were used, along with rabbit polyclonal anti-f1 antibodies, along with an anti-mouse IgG antibody used as a non-specific antibody.

Table 1: *E. coli* strains

Strain	Genotype	Reference
JW0105	*Δ(araD-araB)567, ΔlacZ4787(::rrnB-3), λ-, rph-1, Δ(rhaD-rhaB)568, hsdR514 ΔnadC727::kan*	(Baba *et al.*, 2006)
JW0157	*F-, Δ(araD-araB)567, ΔdegP775::kan, ΔlacZ4787(::rrnB-3), λ-, rph-1, Δ(rhaD-rhaB)568, hsdR514*	(Baba *et al.*, 2006)
K91	*HfrC, λ-, S26 RIE, fadL701 phoM510 mcrB rrnB ton A22, gar B10, ompF, relAl, pit 10, spoT1, T2R*	The Rockefeller University collection
K561	*HfrC, S26 RIE, fadL701 phoM510 mcrB rrnB ton A22, gar B10, ompF, relAl, pit 10, spoT1, T2R, lacI^q*	The Rockefeller University collection
K1030	K91, *supD, zed508::Tn10*	The Rockefeller University collection
K1466	*MC1061 redC tet^R (P1cl100Cm^R dam?1 rev6)*	The Rockefeller University collection
K1976	TG-1 carries pJARA112	The Rockefeller University collection
K2091	*K561 supD, zed508::Tn10*	The Rockefeller University collection
K2245	*Δ(araD-araB)567, ΔlacZ4787(::rrnB-3), λ-, ΔrecO737, rph-1, Δ(rhaD-rhaB)568, hsdR514; F'[::Tn10 proAB+ lacIq Δ(lacZ)M15]*	(Baba *et al.*, 2006)

K2379	*Δ(araD-araB)567, ΔlacZ4787(::rrnB-3), λ-, ΔrecO737, rph-1, Δ(rhaD-rhaB)568, hsdR514; F'[::Tn10 proAB+ lacIq Δ(lacZ)M15]/pTinselPurple*	This study
K2441	*K1030, ΔdegP775*	This study
K2442	*K2091, ΔdegP775*	This study
K2448	*K1030, ΔmetE774*	This study
K2449	*K2091, ΔmetE774*	This study
K2484	*K2448 ΔnadC727::kan*	This study
K2485	*K2449 ΔnadC727::kan*	This study
K2486	*K2484 ΔnadC727*	This study
K2487	*K2485 ΔnadC727*	This study
K2515	*JW0105 Δkan*	This study
TG1	*K-12 supE44* Δ*(hsdM-mcrB)5* (rk^- mk^- $McrB^-$) *thi* Δ*(lac-proAB)* F' [*traΔ36 lacI*^{q} Δ*(lacZ)M15 proAB*]	(Sambrook and Russell, 2001)
Top 10	*F- mcrA Δ(mrr-hsdRMS-mcrBC) φ80lacZΔM15 ΔlacX74 deoR recA1 araD139 Δ(araA-)*	Invitrogen, USA

Table 2: Plasmids

Name	Protein Expressed or Function	Expression Promoter	Resistance	Origin of Replication	Reference
pCP20	FLP recombinase	λ	Amp	Rep101^{ts}	(Cherepanov and Wackernagel, 1995)
pCR-Blunt	Vector	*lac*	Kn	pUC	Invitrogen, USA
pFLP2	FLP recombinase	λ	Amp		(Hoang *et al.*, 1998)
pJARA112	pIII	psp	Amp	pMB1	(Rakonjac *et al.*, 1997)
pRNano3	Helper plasmid		Kn	pA15	(Sattar *et al.*, 2015)
pNanoZap 537	Template for the NanoZap Particle production		Amp	pUC; f1 NanoZap	Rakonjac Lab, unpublished
pNanoZap 537N	Template for the NanoZap Particle production, with an auxotrophic marker		N/A	pUC; f1 NanoZap	Rakonjac Lab, unpublished

pNanoZap 719	Template for the NanoZap Particle production		Amp	pUC; f1 NanoZap	Rakonjac Lab, unpublished
pNanoZap SNgII	pVII and pIX / Template for the NanoZap Particle production	*gII*	Amp	pUC; f1 NanoZap	Rakonjac Lab, unpublished
pNanoZap SN*lac*	pVII and pIX / Template for the NanoZap Particles	*lac*	Amp	pUC; f1 NanoZap	Rakonjac Lab, unpublished
pTinselPurple (commercial name pCBP 38-444)	Tinsel Purple (derived from GFP)	T5	Amp	pUC	DNA 2.0/ATUM

Table 3: Bacteriophage

Name	Details	Reference
f1	Wild-type	(Sambrook and Russell, 2001)
f1d3	*gIII* deleted	(Rakonjac and Model, 1998)

Table 4: Oligonucleotides

Name	Sequence	Notes
GD01	GTG GCA TTA CGT ACT GTC AGA CCA AGT TTA CTC A	SnaB1 and BamH1 cut sites
GD02	CGC GGA TCC TGT ATT TAG AAA AAT AAA CAA ATA GG	SnaB1 and BamH1 cut sites
GD03	CGC GGA TCC TAT ATG TGG TGC TAA TAC CCG GT	SnaB1 and BamH1 cut sites
GD04	GTG GCA TTA CGT ATT AGC GAA AAC GCA TTG AAA GGT	SnaB1 and BamH1 cut sites

Table 5: Antibodies

Name	Details	Reference
Antibody 1	Anti-fd (f1) phage; Rabbit polyclonal Ab	Sigma Aldrich
Antibody 2	Anti-fd (f1), biotin conjugate. Rabbit Polyclonal Ab	Sigma Aldrich
Antibody 3	Anti-f1. Rabbit Polyclonal Ab, 1993	Rockefeller University Collection
Antibody 4	Anti-f1. Rabbit Polyclonal Ab, 1994	Rockefeller University Collection
Antibody 5	Anti-Mouse IgG A5781. Used as a non-specific antibody.	Sigma Aldrich

2.1.5. Solutions and Buffers

All solutions and buffers were used at the following concentrations (unless otherwise stated in the text): calcium chloride was used at a final concentration of 100 mM and stored at 4^{o}C when not in use; PBS was used at a concentration of 1x (137 mM NaCl, 2.7 mM KCl, 10 mM Na_2HPO_4, 1.8 mM KH_2PO_4, pH 7.4), and stored at 25^{o}C when not in use; glycerol was used at a concentration of 10% and stored at 4^{o}C when not in use. Blocking buffer was used at a final concentration of 5% skim milk + 1 x PBS and stored at 4^{o}C when not in use. Glucose was used at a concentration of 1 mM and stored at 4^{o}C when not in use. Ligation buffer was used at a 1 x concentration (50 mM Tris-HCl, 10 mM $MgCl_2$, 1 mM ATP, 10 mM DTT, pH 7.5) and stored at -20^{o}C when not in use.

M9 salts was used at a final concentration of 1 × (15 g/L KH_2PO_4, 64 g/L Na_2HPO_4, 2.5 g/L NaCl, 5 g/L NH_4Cl, pH 7.2), and was stored at 20^{o}C when not in use, as were 1 × TBS (150 mM NaCl, 50 mM Tris-Cl, pH 7.6) and 1 × TAE (40 mM Tris, 2 mM EDTA, 20 mM Acetic Acid, pH 9.0). 1 × TAE (40 mM Tris, 2 mM EDTA, 20 mM Acetic Acid, pH 9.0) had its pH adjusted to pH 8.3 using 1 M HCl when running 0.8% agarose gels containing DNA samples.

The liquid media 2×YT was used at a concentration of 1 × (16 g/L Tryptone, 10 g/L Yeast Extract, 5.0 g/L NaCl, pH 7.4 – 7.6), and stored at 20^{o}C when not in use. 2xYT is a standard microbial growth medium used for the cultivation of *E. coli* and M13 bacteriophage. This nutrient-rich microbial broth contains peptides, amino acids, and water-soluble vitamins in a low-salt formulation. When required as a solid media, 2×YT was used at a concentration of 1 × (16 g/L Tryptone, 10 g/L Yeast Extract, 5.0 g/L NaCl, 1 – 2% Agar, pH 7.4 – 7.6), and stored at 4^{o}C when not in use. Agar (BD Difco) is a solidifying agent and has been purified so that extraneous matter and salts have been reduced to a minimum.

Minimal media (M9 Glu Cas) was used at a concentration of 1 × (200 g/L M9 Salts, 2 g/L $MgSO_4$, 22 g/L Glucose, 0.1 g/L $CaCl_2$, 2 g/L Casamino Acids (Sigma Aldrich), pH 7.1). Minimal media is not a standard growth medium, as it lacks several key nutrients for normal cell growth, such as nicotinic acid (NA) (Sigma Aldrich). Casamino acids is a mixture of amino acids and some very small peptides obtained from acid hydrolysis of casein; typically used in microbial growth media. It has all the essential amino acids except tryptophan, which is destroyed when digested with hydrochloric acid. When required as a solid media, minimal media (MM) was used at a concentration of 1 × (200 g/L M9 Salts, 2 g/L $MgSO_4$, 22 g/L Glucose, 0.1 g/L $CaCl_2$, 2 g/L Casamino Acids (Sigma Aldrich), 1.5 g/L Agar, pH 7.1) and stored at 4^{o}C when not in use. Agar (BD Difco) is a solidifying agent and has been purified s that extraneous matter and salts have been reduced to a minimum. Nicotinic acid (NA) was supplied into the minimal media as required at a concentration of 10 µg/mL.

2.1.6. Chemicals and Reagents

Other chemicals used were supplemented at the following concentrations, unless otherwise stated: isopropyl β-D-1-thiogalactopyranoside (IPTG) at 0.1 mM; X-gal at 80 µg/mL. IPTG was purchased from GoldBio (USA), while X-gal was purchased from AppliChem. When not in use, IPTG and X-gal were kept in the dark at -20^{o}C. Caesium chloride was made up to the exact concentrations as stated in the text when required. Ethidium bromide was used at a concentration of 1 µg/mL for staining gels.

2.2. Methods

2.2.1. Transformation

Transformation of chemically competent cells by heat-shock method was carried out using the method outlined in Sambrook and Russell (2001). To prepare bacterial cells for chemical transformation, an exponentially growing cell culture of K2245 was set; left at 200 rpm and at 37^{o}C. At OD_{600} = 0.2 cells were harvested and made chemically competent through re-suspension in the ice-cold solution composed of $CaCl_2$ (0.1 M) and glycerol (10%). The cells are then transformed with the relevant plasmid (pTinselPurple (DNA 2.0)) through the heat shock transformation method; and plated onto plates containing the relevant antibiotic and any chemicals required to induce protein expression (final dilutions of 10^{-2}, 10^{-4}, 10^{-5}, 10^{-6}). In the case of K2245 cells transformed with pTinselPurple plasmid (K2379), various concentrations of IPTG were added to the plates.

Transformation by electroporation was carried out using a method outlined in (Sambrook and Russell, 2001). Cells for electrical transformation (for example K1030, K2441 (Table 1)) were prepared through setting an exponentially growing cell culture; at 37^{o}C with aeration by rotatory agitation at 200 rpm. At OD_{600} = 0.6 cells were harvested by centrifugation (10 min, 4000 × g) and made electrically competent through re-suspension in glycerol. The cells were then transformed with the relevant plasmid (for example pRNano3, pNanoZap 719 (Table 2)) through applying an electrical shock. The cells were recovered in the SOC medium (2% Tryptone, 0.5% Yeast Extract, 10 mM NaCl, 2.5 mM KCl, 10 mM $MgCl_2$, 20 mM Glucose, pH 7); and plated onto the corresponding antibiotic plates (undiluted or diluted as required).

Plasmid-based production of phage or derived particles requires the transformation of two plasmids into a cell. K1030 transformed with the helper plasmid pRNano3 **(Figure 8)** were further transformed with one of the pNanoZap plasmids that contain modified f1 origins of replication (see results for details). After the second transformation, the pool of transformed cells was not plated but rather diluted into the 2xYT containing the requisite antibiotics (Kn for pRNano3 and Amp for transformation with pNanoZap plasmids). The volume of double-transformed cultures depended on the experiment and was between 10 mL and 1 L. Cultures were incubated with aeration (shaking at 200 rpm) at 37ºC overnight for particle production, unless otherwise specified.

2.2.2. Preparation and Titration of Bacteriophage Stocks

Strain K1976 containing pIII-expressing complementing plasmid was cultured overnight in 2×YT liquid media + Amp. Soft agar (0.5%) was prepared and kept at 50ºC, then mixed with the K1976 cells before the mixture was poured over 2×YT Amp media plates, creating a thin layer. To determine bacteriophage titre, pre-existing stocks of f1 wild-type bacteriophage and f1d3 bacteriophage (Table 3) were serially diluted (10^{-2}, 10^{-4}, 10^{-5}, 10^{-6}, 10^{-8}, and 10^{-10}). The bacteriophage dilutions (5 µL drops) were then dispensed onto the soft agar and incubated overnight at 37 ºC. Counting single plaques in the areas covered by drops of specific dilutions allowed calculation of stock titres.

Strain K1976 (expressing *gIII* under the phage-induced promoter, psp) and TG1 (Table 1) were used to prepare and titre stocks of f1d3 (containing deletion of *gIII*) and wild type f1 (Table 3), respectively. One plaque was selected from each titration experiment described above and re-suspended in liquid media. The suspension was filtered to remove bacterial cells. The bacteriophage titration experiment was then performed to determine the titre of the phage in extracted plaque. About 10^6 - 10^7 bacteriophage were used to prepare a plate stock. Both bacteria

and bacteriophages were added to soft agar and poured over media plates and incubated overnight at 37°C. Pre-warmed liquid media (37°C) was added to the media plates and left on a shaker at room temperature for one hour. Liquid media was then collected, and bacterial cells were sedimented by centrifugation (4000 × g, 15 min). Supernatant was filtered through a 0.45 µm filter to remove remaining bacterial cells. The bacteriophage stocks were stored at 4°C and their titre was determined as described above.

2.2.3. Preparing Bacteriophage-Decorated *E. coli*

K2379 was cultured overnight in 2×YT Amp liquid media. Two 100-fold dilutions were made into liquid media with ampicillin and left to shake at 37°C. When OD_{600} = 0.2 was reached, one of the cultures was inoculated with 50-fold of stock f1d3 bacteriophage and incubated at 37°C for half an hour. IPTG was then added to both tubes to induce the Tinsel purple protein expression and left to shake at 37°C overnight. The colour of the cells was observed.

Cultures were then centrifuged (4°C, 700 × g, 30 mins). Supernatant was discarded, and pellet re-suspended in a volume of 1 × PBS at a density of OD_{600} = 10 per mL. K91 overnight culture (OD_{600} = 0.2) was also infected with f1d3 and plated on agar containing X-gal and IPTG, allowing the hydrolysis of X-gal by host cells and colouring the K91 cells blue.

K91 (Table 1) was cultured overnight in 2×YT. Two 100-fold dilutions were made into liquid media with ampicillin and incubated at 37°C with aeration by rotatory agitation at 200 rpm. When OD_{600} = 0.2 was reached, one of the cultures was inoculated with stock f1d3 bacteriophage at multiplicity of infection (m.o.i.) of 50 and incubated at 37°C without agitation for half an hour. The cultures were then diluted (final dilutions of 10^2, 10^4, 10^5, 10^6-fold) and plated onto 2×YT media

plates containing IPTG and X-gal incubated at 37^{o}C. Blue colonies were then taken from the agar plates and re-suspended in PBS. The cells from suspension were collected by centrifugation to determine whether they retained the coloured molecule (5,5'-dibromo-4,4'-dichloro-indigo).

2.2.4. Visibility Assay/Dot Blot

Nitrocellulose membrane was cut into strips and labelled as positive (+) for f1d3-infected cells or negative (-) for uninfected cells. It was also labelled vertically from 1 to 5, with 1-4 corresponding to four different antibodies specific for Ff phage and 5 a non-specific antibody (Table 5). The nitrocellulose membrane was then placed in Milli-Q water and then 1 × PBS to wet it thoroughly, followed by draining of liquid and brief drying. A drop (1 µL) of each antibody was placed onto the nitrocellulose membrane and left to dry for half an hour. The membrane was then blocked in blocking buffer (5% skim milk powder in 1 × PBS) overnight at 4^{o}C, followed by washing 4 × 5 mins in PBS at room temperature. The membranes were then taken straight from the PBS wash and were each placed into a solution of the coloured f1d3-infected and non-infected cells and left to rotate for an hour. Membranes were then visually inspected to determine whether the spots of antibodies were coloured by binding of colour-tagged cells.

2.2.5. Generalised Transduction

2.2.5.1. Induction of the P1 Phage from a Lysogen

The P1 lysogen host K1466 (containing a temperature-inducible Cm^{R} phage P1 genome) was streaked from a frozen stock onto a 2×YT + Cm plate and incubated at 30^{o}C for 24 hours. An overnight culture was seeded with a colony from the plate in 2×YT liquid media + Cm and incubated at 30^{o}C. The next day, the overnight culture was diluted 100x into 15 mL of fresh 2×YT liquid media + Cm in a sterile flask and

incubated at 30 - 32ºC with aeration by rotatory agitation at 200 rpm until the OD_{600} = 0.4. An equal volume of 2×YT + Cm + 10 mM $CaCl_2$ (pre-mixed and pre-warmed at 50ºC) was added and then the mixture was transferred to a 42ºC water-bath-shaker incubated with aeration by rotatory agitation at 200 rpm for 15 min. Water bath temperature was then reduced to 39ºC and vigorous shaking was continued until a visible lysis occurred (4 - 6 hours). A few drops of chloroform were added and then the mixture was shaken vigorously to kill the remaining cells. The mixture was then transferred into a 50 mL centrifuge tube and spun for 15 mins at 8000 × g to remove debris. Stock was then titrated on a strain that will be infected in the subsequent step (infection of a "donor" strain), to ensure that the titre was sufficiently high.

2.2.5.2. Preparation of Donor Stocks

The donor stock strain (e.g. JW0157) was grown overnight in 2×YT + Kn at 39ºC. Flasks and 2×YT + 10 mM $CaCl_2$ were prewarmed in a water bath to 39ºC. The overnight culture was taken straight from the dry incubator and put into the pre-warmed water bath. 50 µL of overnight culture was pipetted into a pre-warmed empty flask, along with 100 µL of pre-warmed 2×YT + 10 mM $CaCl_2$ and approx. $10^7 – 10^8$ of the P1 bacteriophage stock. The mixture was incubated for 5 min without shaking. 10 mL of the 2×YT + 10 mM $CaCl_2$ was added and the shaker was turned on to 160 – 200 rpm and culture was incubated for 2 to 6 hours to allow lysis of the culture by induced P1 phage. Several drops of chloroform were added to lyse remaining cells and then the mixture was transferred to a 50 mL centrifuge tube and debris was pelleted by centrifugation (4000 × g, 10 min, 4ºC). The supernatant was then filtered through a 0.45 µm filter, and titred on the recipient strains on 2×YT agarose + 10 mM $CaCl_2$.

2.2.5.3. P1 Transduction

A fresh overnight culture of the recipient stocks (e.g. K1030, K2901) was grown in 2 mL of 2×YT. 1 mL of overnight culture was pipetted into a microcentrifuge tube and pelleted by spinning at 16,000 × g for 3 min at room temperature. Pellet was then re-suspended in an equal volume of sterile 10 mM $MgSO_4$, spun centrifuged again and then re-suspended in the equal volume of 10 mM $MgSO_4$. 2-20 µL of the P1 lysate that was prepared on the donor strain was added to the cells, along with 100 µL of 10 mM $MgSO_4$, and incubated at 39^oC for 10 min. After this brief incubation (allowing phage infection) 1 mL of pre-warmed 2×YT + 10 mM Na-citrate was added, and cells were incubated for 1 hour with vigorous shaking. Cells were then transferred into a microfuge tube and pelleted by centrifugation at 8000 × g for 2 min at room temperature, before being resuspended in an equal volume of 10 mM $MgSO_4$, centrifuged again and then re-suspended.

Transductants were then plated onto: 2×YT + 10 mM Na-citrate plates, which also contained the antibiotic that was transduced into the host (e.g. Kn) and incubated at 39^oC; 2×YT + 10 mM Na-citrate + Cm plates to check for lysogens; and finally, 2×YT + the antibiotic that was transduced into the host cells (e.g. Kn) to get single colonies.

2.2.6. FRT – FLP Recombination

After P1 transduction from the Keio knock-out strains (Baba *et al.*, 2006), a new antibiotic resistance (Kn^R) marker had been added into the host cell genome (K1030) along with the gene deletion that was desired. However, this antibiotic resistance marker must be removed from the cells in order to be able to use them as hosts for Kn^R plasmids. Given that the Kn^R marker in the Keio collection strain is designed with flanking FRT sites that are the substrate of the yeast site-specific recombinase FLP, a transient transformation with a FLP-expressing plasmid was used

to remove the marker. This was achieved through making the transduced cells electrocompetent, and transforming them with the pFLP2 plasmid, which expresses FLP recombinase for site specific excision of the sequence between the FLP recognition target (FRT) sites, an ampicillin resistance cassette (Amp^R) and a *sacB* counter selection marker to remove the pFLP2 plasmid after the Kn^R marker had been removed.

After transformation with pFLP2, transformants were plated onto agar containing ampicillin. 10 colonies were screened for loss of Kn^R marker by passaging onto plates that contained both kanamycin and ampicillin; colonies that did not grow upon passaging to these plates were sensitive to Kn and have therefore lost the Kn^R marker. The next step was to remove the pFLP2 plasmid. This was achieved by taking the advantage of the *sacB* gene, which is dominant lethal on sucrose-containing medium. A bacterial suspension was made in 2×YT and at OD_{600} = 0.1, 10-fold dilutions were made and plated onto agar plates containing 10% sucrose. These plates were then incubated at 25^{o}C until colonies grew. These colonies were the clones that had lost the helper plasmid pFLP2. To prove loss of the pFLP2 plasmid, colonies were grown overnight and then plated onto 2×YT and 2×YT + Amp. The cultures derived from colonies that had lost the pFLP2 plasmid were confirmed if they did not give any colonies when spread on Amp plates. These cells were then stocked at -80^{o}C under a new strain name.

2.2.7. Nanoparticle Production

Host cells were made electrocompetent and transformed with helper plasmid to produce the f1-like phage particles pRNano3. Cells carrying pRNano3 were selected for using Kn^R. These transformed cells were made competent again and transformed with one of the pNanoZap plasmids that serve as templates for the nanoparticle production (Amp selection). After transformation with a pNanoZap 10 mL of liquid media containing ampicillin and kanamycin was mixed with the transformation

mixture and incubated for 1 hour at 37ºC. The 5 ml of inoculated liquid media was then added into a 2 L flask containing 500 ml of sterile pre-warmed liquid media (2xYT containing Amp and Kn) and incubated overnight at 37ºC with aeration.

The cells from the overnight culture were pelleted by centrifugation (8000 × g at 4ºC). The supernatant was collected, and the f1-derived particles were precipitated using PEG. Briefly, the supernatant was poured into sterile centrifuge bottles and the PEG8000 powder was added up to 15%. After the PEG dissolved, NaCl powder was added to 0.5 M, dissolved, and the suspension was incubated on ice for 2 hours. Mixture was then pelleted by centrifugation at 8000 x g for 30 minutes at 4ºC. Supernatant was decanted and the "empty" centrifuge bottles were centrifuged again under the same conditions for 5 minutes to collapse the phage particle pellet to the bottom of the bottle. This is required because the filamentous phage PEG pellet precipitates during centrifugation as a sticky film along the wall of the bottle.

Pellet was then re-suspended in 5 ml of 1 × TBS (pH 7.6) and re-spun at 8000 × g for 30 minutes at 4ºC to remove the remaining insoluble debris. 1 × DNAse and RNAse were then added to the supernatant and left to incubate at room temperature for 1 hour. The DNAse and RNAse were then inactivated through the addition of EDTA at 0.5 M. Particles were re-purified by PEG precipitation. PEG800 powder was then added to 15% and dissolved, followed by adding NaCl to 0.5 M and dissolving. The solution was stored in the cold room (4ºC) overnight.

After incubation overnight, the phage-derived particles were precipitated by centrifugation 8000 x g for 30 minutes at 4ºC. Supernatant was discarded, and the pellet was then re-suspended in 0.5 mL 1 × TBS (pH 7.6) and centrifuged again at 4000 × g for 10 minutes at room temperature to remove the insoluble debris. The supernatant was then purified through by caesium chloride gradient centrifugation, followed by dialysis, and the nanoparticles were then concentrated using the Vivaspin

filtration system. The nanoparticles were then quantified by densitometry of their DNA content using disassembled phage agarose gel electrophoresis.

2.2.8. Purification of Bacteriophage Nanoparticles

2.2.8.1. Caesium Chloride

Caesium chloride (CsCl) gradient centrifugation was carried out on NanoZap particles to further purify the samples and remove any residual DNA/RNA. Between 0.15 and 0.3 mL of the PEG-precipitated NanoZap particles were suspended in CsCl solutions (0.375 g/mL). The final suspension has CsCl density of 1.29 g/mL. After centrifugation at 100,000 × g for 19 hours which resulted in formation of CsCl gradient. The contents of the centrifuge tube were then fractionated and the amount of NanoZap particles in each fraction was analysed by agarose gel electrophoresis of heat- and SDS-disassembled particles. The fractions corresponding to the peak of the NanoZap amount were pooled and dialysed against 4000 volumes of 1 × TBS (10 mM Tris, 150 mM NaCl, pH 8.0) using 10 kDa cut-off Slide-a-Lyzer® dialysis cassettes (ThermoFisher).

2.2.8.2. Concentration of Phage-Derived Particles by Spin-Filtration

NanoZap particles in the collected CsCl fractions were concentrated by filtration through a 50 kDa-cut-off filter using centrifugal force in the Vivaspin system (GE Healthcare). Particles to be concentrated (~300 μL) were loaded onto filtration tubes, and the volume was increased to 500 μL by addition of 1 x TBS (10 mM Tris, 150 mM NaCl, pH 7.6). Filtration tubes were placed into collection tubes, and samples were centrifuged at 5000 x g for 10 minutes. Flow-through was removed and 1 x TBS was added to filtration tube up to final volume of 500 μL again,

and samples spun again at 5000 x g for 10 min. Filtration was carried out this way a total of six times. Elution of samples was carried out by adding the required volume of 1 x TBS for resuspension to the filter tubes and incubated overnight at 4^{o}C. The following day, the solution was gently pipetted up and down over the filter, before being removed. Concentration of phage particles was then determined by densitometry of the DNA content using agarose gel electrophoresis of disassembled particles.

2.2.9. Quantification of Bacteriophage Nanoparticles

2.2.9.1. Densitometry

For phage-derived nanoparticles that do not carry any markers and cannot be quantified by traditional titration methods (such as NanoZap), a densitometry-based quantification was employed (Rakonjac and Model, 1998). Phage samples to be quantified were diluted to various degrees and boiled in SDS-containing buffer (1 x TAE, 5% Glycerol, 1% SDS, 0.25% bromophenol blue) for 15 minutes to disassemble the virions and release the encapsulated DNA, then analysed by gel electrophoresis (0.8% agarose, 100 minutes at 70 V) along with serial dilutions of an ssDNA standard of known ssDNA amounts. DNA was visualised by staining in ethidium bromide at 1 µg/mL, and an image taken using a Molecular Imager® GelDocTM (Bio-Rad).

This image was then analysed using software ImageJ (National Institute of Health), where the pixels from the ssDNA standard bands were counted and plotted against the amount of DNA loaded, generating a standard curve. A second-order polynomial equation was fitted to this curve, and the counted pixels from the denatured phage sample bands used to determine the approximate amount of ssDNA present. By calculating the molecular weight of the encapsulated ssDNA, the

approximate number of phage particles was determined using the measured ssDNA amount.

2.2.10. Agarose Gel Electrophoresis

Native virions were analysed by agarose gel electrophoresis in 1 × TAE buffer (0.04 M Tris-acetate, 1 mM EDTA, pH 9.0, 0.8% agarose, 60 V, 120 min). Any residual plasmid or *E. coli* genomic DNA that could have been released from dead cells and precipitated with PEG (15%) was first visualised by staining in ethidium bromide. Next, the gel was soaked for 45 minutes in 0.2 M NaOH to disassemble the particles, followed by 10 minutes in MQ water to remove excess NaOH from the agarose gel before 15 minutes in 0.45 M Tris buffer (pH 7.1) to bring the gel back to a neutral pH. DNA released from the virions was visualised by staining again in 1 µg/mL ethidium bromide for 30 minutes.

2.2.11. TEM Visualisation of Bacteriophage Nanoparticles

The nanoparticles were visualised using a transmission electron microscope (TEM). Nanoparticles were diluted in autoclaved MQ water and taken to a TEM technician and prepared as outlined below:

In a glass petri dish lined with Parafilm place a small droplet (approximately 80 µL) of the sample onto the film. Place a carbon coated 200 mesh copper grid (Agar Scientific, coated in the lab) film side down onto the sample droplet and let sit for 4 minutes. Carefully lift the grid from the droplet, turn film side up and press the edge very gently to the cut side of Whatman No 1 filter paper to drain off all excess. Place film side down onto a drop of 2% Uranyl Acetate in MQ water and let sit for 4 minutes to stain. Drain off excess liquid as before, making sure all excess is gone before placing the grid onto Whatman No. 1 filter paper to dry. Image carefully in TEM at 100 kV (FEI Tecnai G2 Spirit BioTWIN, Czech Republic).

2.2.12. Production of Nanoparticles from pNanoZap NadC

2.2.12.1. Purification using PEG Precipitation

To check whether the newly created pNanoZap NadC vector can produce NanoZap particles, we transformed host cells K2515 with helper plasmid pRNano3 and then with the newly created vector, pNanoZap NadC. Nanoparticle production was then carried out as outlined above, however upon the addition of 15% PEG800 to the minimal media solution, crystallization occurred, and the nanoparticles became irretrievably trapped in the crystalline structures.

2.2.12.2. Concentration of Phage-Derived Particles by Pressure-Filtration

Nanoparticles from the culture supernatant obtained as described in Section 2.2.7 were concentrated by ultrafiltration, using an Amicon Stirred Cell 400 mL pressure system as per the method outlined in Rakonjac and Model (1998). The filtrate was collected and stored at 4^{o}C. The filter paper was also collected and placed into a sterile Petri dish followed by pipetting 2 mL of 1 × TBS (pH 7.6) onto the filter to extract the particles and left to slowly agitate on a rotatory platform overnight at 4^{o}C. The 2 mL of 1 × TBS (pH 7.6) were then collected and analysed by disassembled phage agarose gel electrophoresis, as outlined above to check for the presence of NanoZap particles.

Chapter III

3. Building a Double-Display Particle System for Diagnostic Application

The aim of this work was to test the hypothesis that a diagnostic setup can be developed, based on f1d3-filament-decorated, colour-tagged *E. coli* cells as detector particles. This system with a working name "double display" would be based on particles that are comprised of two components: *E. coli* that has been tagged (visualised) by the expression of a chromogenic protein, and that have been infected with *gIII* deleted (f1d3) bacteriophage that can be functionalised with a detector molecule. This current work focuses on the tagging of *E. coli* with a chromogenic protein and the subsequent infection of the *E. coli* with (non-functionalised) f1d3 bacteriophage.

3.1. Construction of *E. coli* Red-Fluorescent Strain to Enable Detection

To begin this work, a visible means of detecting the display particles was required. As such, colour-tagged *E. coli* were created using the pTinselPurple plasmid (**Figure 9**). The plasmid pTinselPurple was transformed successfully into the *E. coli* lab strain K2245, creating K2379 (K2245/pTinselPurple).

3.2. Gauging TinselPurple Expression to Balance Toxicity to *E. coli* with the Strength of the Signal

The pTinselPurple plasmid promoter (T5/*lac*) is IPTG induced, therefore an experiment was required to discover the optimum amount of IPTG for inducing protein expression without over-loading of the cell, which would cause cell death (Miroux and Walker, 1996). The cells transformed with pTinselPurple produced the pink-purple colouring in the liquid culture and on the plates even in the absence of IPTG, indicating that the T5/*lac* promoter is "leaky" or

somewhat active in the absence of induction (**Figure 10A; B**). The expression trials were done at two concentrations of IPTG, 0.1 mM and 1 mM. The former concentration (0.1 mM) demonstrated high protein expression (strong purple colour) yet maintained the same titre as on the plates without IPTG, hence were able to express increased amount of TinselPurple protein without killing the cells (**Figure 10C**). In contrast, IPTG concentration of 1 mM caused ~10-fold drop in plating efficiency, indicating a growth-inhibiting effect of the TinselPurple protein overexpression (**Figure 10D**). From this experiment it was concluded that optimal IPTG concentration, allowing strong colouration without interference with *E. coli* growth, was 0.1 mM.

3.3. Feasibility study for the double-display particles: making filamentous-phage-decorated *E. coli*

To display proteins/peptides on the filamentous phage (f1) that themselves were display on the surface of *E. coli*, it was planned that the cells containing pTinselPurple be infected with an f1 mutant (f1d3) that cannot be released from bacterial surface, thereby resulting in "hairy" *E. coli* cells (Rakonjac and Model, 1998). This phage carries a complete deletion of gene III (*gIII*), required for the release of the phage filament from the surface of *E. coli*. A stock f1d3 bacteriophage was first grown on a complementing strain, K1976 (Table 1) that expressed pIII under the control of a phage-infection-induced promoter (psp; (Rakonjac *et al.*, 1997)). This stock was used to infect the cells transformed with the pTinselPurple to observe whether the infection with f1d3 was compatible with the colouration of the *E. coli* cells.

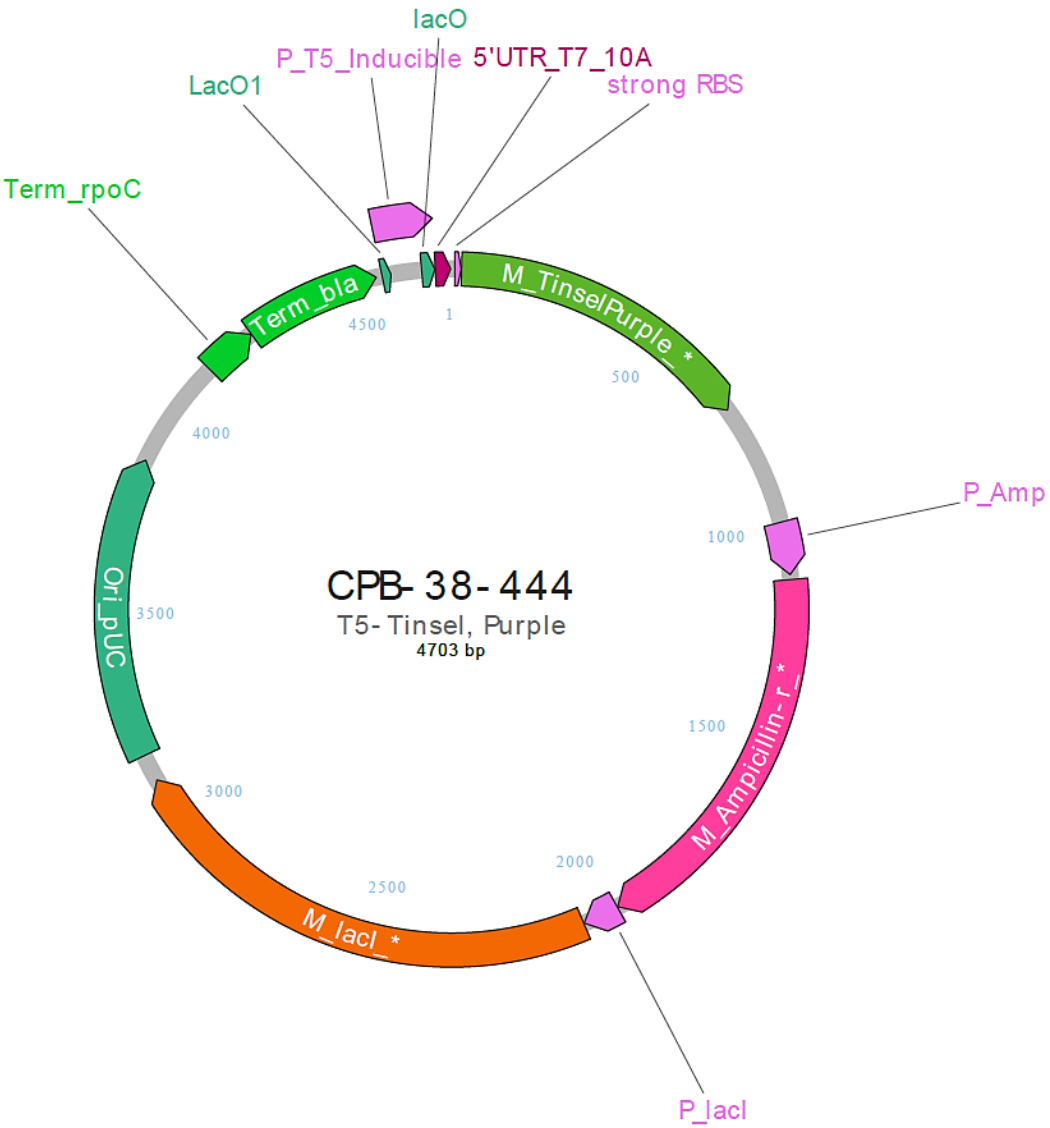

Figure 9: Tinsel Purple Plasmid Map.

Plasmid *ori* is shown in dark blue-green, ampicillin resistance marker dark pink, genes encoding promoters, light pink, and gene encoding the chromogenic protein, green. Plasmid was purchased from DNA 2.0.

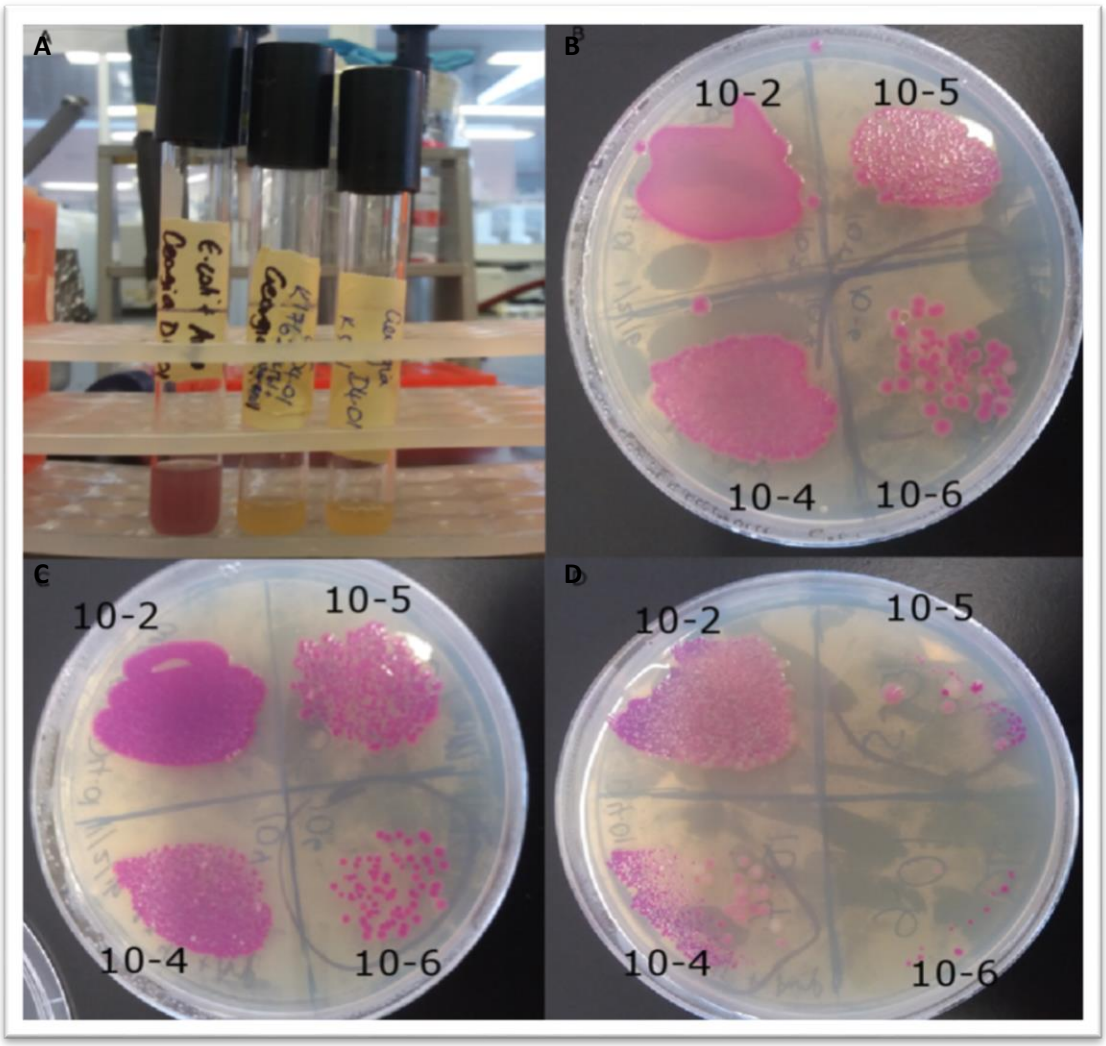

Figure 10: Causing Tinsel Purple protein expression.

pTinselPurple protein expression and culture colour. **A**) Overnight culture of K2379 (K2245/pTinselPurple), compared with overnight cultures of strains K2245 and K561 that do not contain pTinselPurple plasmid. No IPTG was present in the overnight culture. **B**) Overnight IPTG free control of K2379. **C**) Same as **B**), apart from addition of 0.1 mM IPTG to the plate. **D**) Same as **B**), apart from addition of 1 mM IPTG to the plate. The plates contained 100 mg/mL ampicillin.

3.4. f1d3 infection is Incompatible with TinselPurple Protein Expression in *E. coli*

The bacteriophage-infected K2379 (K2245/pTinselPurple) were observed for the colony and culture colour and viability, to assess compatibility of f1d3 infection with the TinselPurple protein expression. Exponentially growing log culture containing ampicillin was infected with f1d3 and incubated over 4 hours, along with an uninfected control. It was observed that 2 hours after infection the culture became colourless, showing that the purple protein expression was no longer expressed. In contrast, the uninfected K2379 culture maintained the purple colour, showing that they maintained the purple protein expression (**Figure 11**). Titration of the cultures on 2×YT media containing ampicillin showed sharp decline in the cell number. The viable titre of the infected cells was 2×10^5 in contrast to 8×10^9 of the uninfected cells.

Furthermore, most colonies derived from uninfected cells were coloured, whereas most of the colonies from the infected culture were colourless. These two observations show that most of the TinselPurple that were infected with f1d3 have not been able to form colonies, showing that the combination of f1d3 infection and TinselPurple expression is incompatible with f1d3 infection (**Figure 12**). Colonies of f1d3-infected *E. coli* are small and transparent; whereas uninfected cells are large and opaque. Most of the colonies derived from the infected culture are small and transparent; this colony morphology is characteristic of the f1d3 infected cells. These colonies were also colourless; hence they did not express TinselPurple. On the other hand, a few purple colonies that were observed were large and opaque, hence they were not infected by f1d3. These observations clearly show that TinselPurple and f1d3 infection are incompatible with each other.

3.5. Colouring *E. coli* cells using Chromogenic Substrate X-gal

Given that the loss of purple colouring from *E. coli* transformed with pTinselPurple plasmid makes it impossible to use *E. coli* as detection particles, a

different method of colouring the cell was explored. *E. coli* laboratory strain K91 (which is *lac*$^{+}$, in contrast to TG1 which is *lac*$^{-}$) was used in conjunction with IPTG and X-gal to colour the cells blue. LacZ (beta lactamase) induced by IPTG hydrolyses X-gal to galactose and 5-bromo-4-chloro-3-hydroxyindole. The latter product further dimerizes and is oxidized into 5,5'-dibromo-4,4'-dichloro-indigo, an intensely blue product which is insoluble. During this experiment the *E. coli* cells scraped from the plates that contained X-gal and IPTG and were intensely blue were scraped and re-suspended to determine whether they would maintain the blue colour. The suspended cells remained blue (**Figure 13**), however, over time the colour steadily faded. Furthermore, the colour faded in a proof-of-principle experiment where *E. coli* infected with f1d3 were incubated with a nitrocellulose filter containing spots of immobilised anti-Ff antibodies (**Figure 14**) (**Table 5**).

3.6. Discussion and Summary

To start building the double-display system, the plasmid pTinselPurple (Table 2) was transformed successfully into *E. coli* lab strain K2245. Since the pTinselPurple plasmid promoter (T5/*lac*) is IPTG induced, an experiment was conducted to discover the optimum amount of IPTG for inducing protein expression without over-loading of the cell. Between the two concentrations of IPTG tested (0.1 mM and 1 mM), 0.1 mM was shown to be the optimum concentration, with protein expression without cells becoming toxic (**Figure 10C**); while IPTG concentration of 1 mM had caused cell death due to the over-expression of the pTinselPurple protein (**Figure 10D**). The IPTG free control plate also showed purple protein expressing colonies (**Figure 10B**); which strongly indicates that the T5/*lac* promoter was leaky in the 2xYT medium. The next stage was to make stocks of f1d3 bacteriophage for ease of use. The f1d3 bacteriophage was grown on both TG1 and K1976 (Table 1) along with f1 wild-type bacteriophage (Table 3), for both comparison and purity. Bacteriophage titrations were carried out as explained in Materials and Methods. The next step was to infect *E. coli* with the f1d3 bacteriophage stock to allow the permanent display of bacteriophage on the surface of *E. coli*.

However, when the f1d3 stock of bacteriophage was added to the functionalised *E. coli*, the chromogenic protein was lost (**Figure 11-12**). This could have occurred for several reasons, with the most likely being that the chromogenic protein was degraded by cell machinery activated by the infection of the f1d3 bacteriophage. Since the chromogenic protein was lost, there was no visual way to detect *E. coli* cells. This presents a unique problem: how to visualise bacteriophage binding to the antibodies if the infected strain will not produce visible colour. Since our transformed strain K2379 lost the chromogenic protein in f1d3-infected cells, these particles will be of no use for visible colourimetric detection assays.

As such, another method of creating coloured *E. coli* was attempted. K91 was used in conjunction with IPTG and X-gal. LacZ (beta lactamase) induced by IPTG hydrolyses X-gal galactose and 5-bromo-4-chloro-3-hydroxyindole. This product further dimerizes and is oxidized into 5,5'-dibromo-4,4'-dichloro-indigo, an intensely blue product which is insoluble. During this experiment the *E. coli* cells scraped from the plates remained blue, however, over time the colour steadily faded (**Figure 12**). This is likely due to the cells releasing 5,5'-dibromo-4,4'-dichloro-indigo. No blue colour was detected on the nitrocellulose membrane containing anti-Ff antibodies (**Figure 13**).

We know that the cells remained blue in solution (through both re-suspension and centrifugation) (**Figure 12-13**), and that they were infected with the f1d3 bacteriophage (due to plating and looking at the infected cells), and as such, there are several potential reasons as to why there appeared to be a negative result: the test was actually positive, but the blue colour was simply too weak to be noticeable; the test was actually positive, but due to the bulk of the infected *E. coli* cells (detector particles) not enough were able to bind to such a small area of antibody to create a visible blue effect; or the test was negative due to the antibody drops having lost sensitivity. The antibody drops theory can currently be dismissed however, as further testing of their sensitivity has shown that the antibody drops used in these experiments work as expected, and that they have not expired.

In conclusion, the production of chromogenic cells that are also infected with f1d3 bacteriophage is an interesting challenge. Currently, infection of *E coli* cells seems to be the causative agent for the loss of pTinselPurple chromogenic protein expression. Hydrolysis of X-gal is not affected by f1d3 infection; however, the coloured hydrolysis product of X-gal is released from the cells, resulting in fading. This will need to be circumvented to allow future use of this colouration methodology.

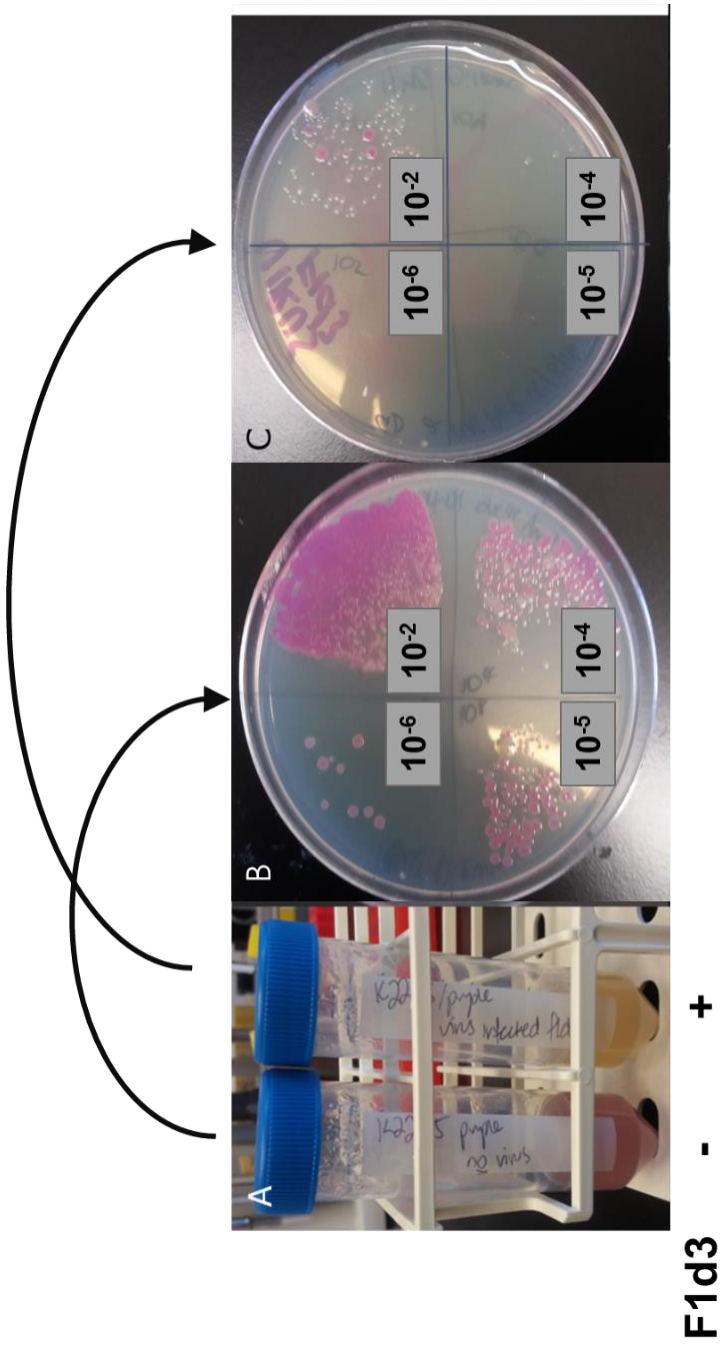

Figure 11: Bacteriophage infected *E. coli* cells lose their purple colouring.

A) Tubes containing the log phase cultures with the optimal amount of IPTG (0.1 mM). f1d3 (+) indicates infection, while f1d3 (-) indicates uninfected cells. The uninfected cells retained the purple colour, while the infected cells are clear. **B**) and **C**) show the titration of the cultures from **A**) on plates lacking Amp and containing 0.1 mM IPTG.

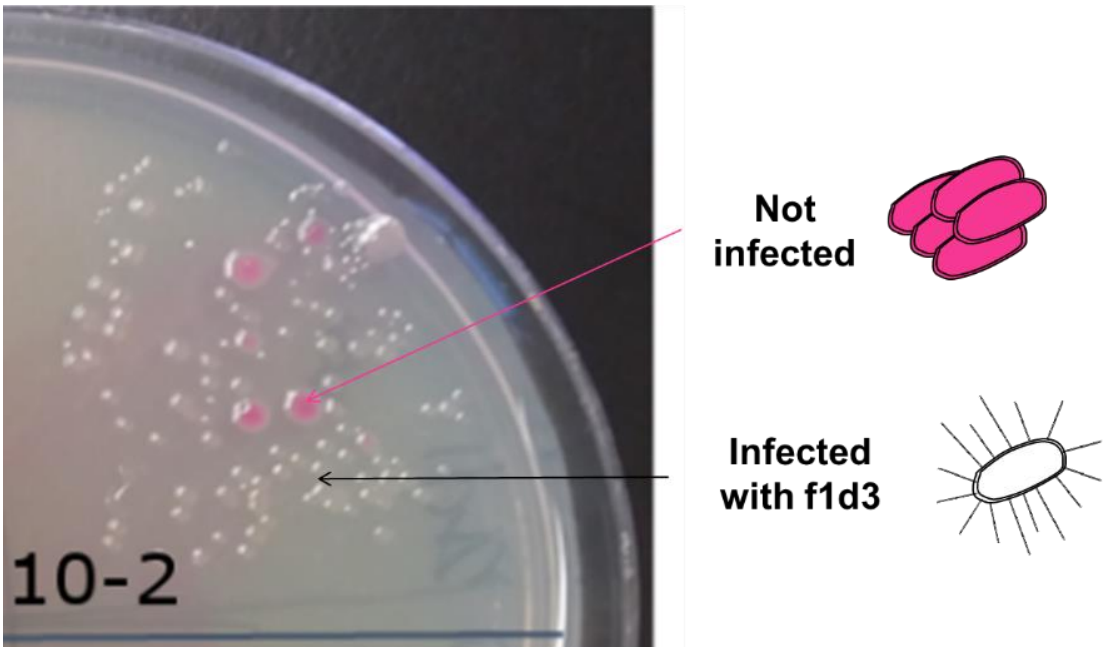

Figure 12: Colony morphologies from the f1d3-infected and uninfected cultures of pTinselPurple-containing plasmids

A close-up of the 10^2 dilution from the infected plate in **Figure 11C**. Colonies derived from uninfected and infected cells are indicated.

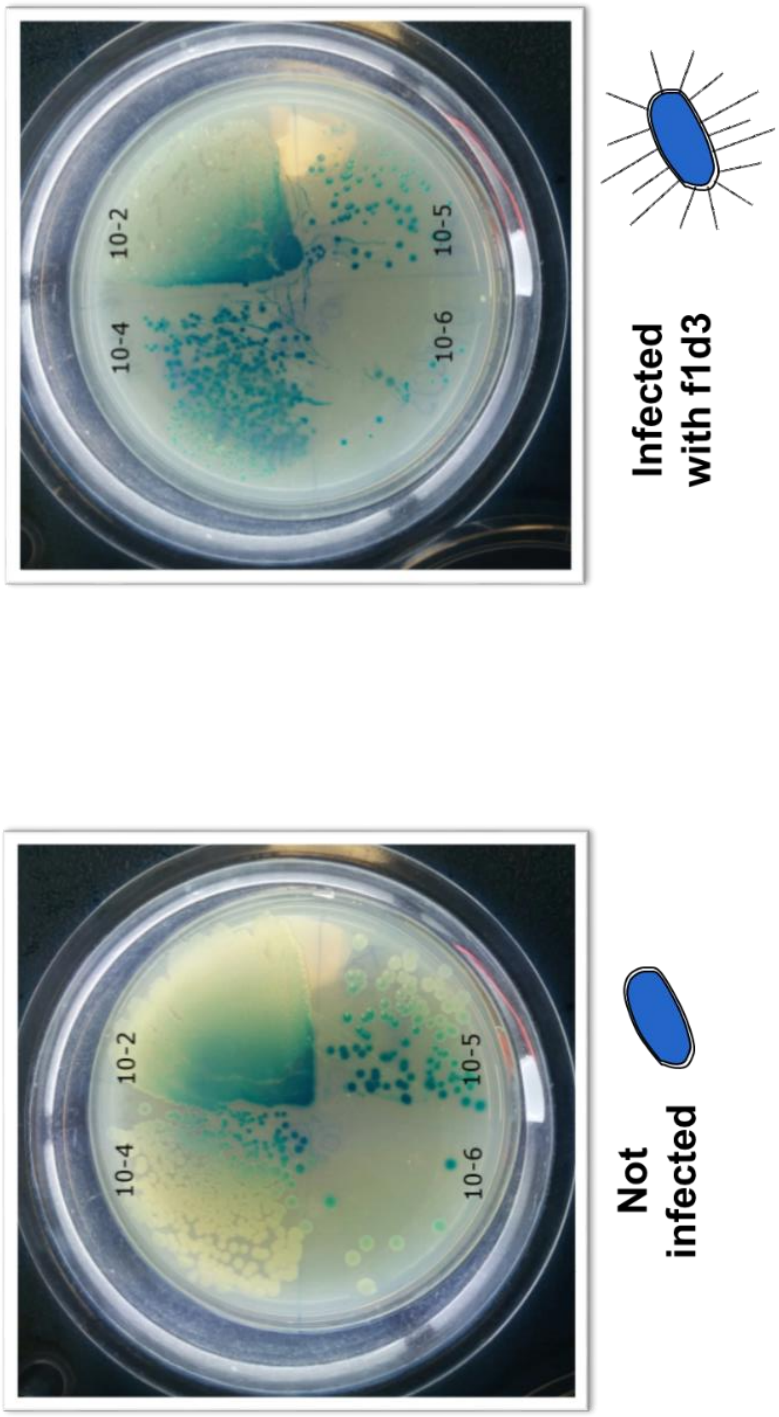

Figure 13: X-gal blue colouring of *E. coli* and f1d3 infection are compatible.

Exponentially growing culture (K91) was infected with f1d3 phage in the absence of IPTG and X-gal (and incubated in parallel with uninfected cells for 2 hours). The serial dilutions of uninfected **A**) and infected **B**) cultures were each spread on a plate containing IPTG and X-gal.

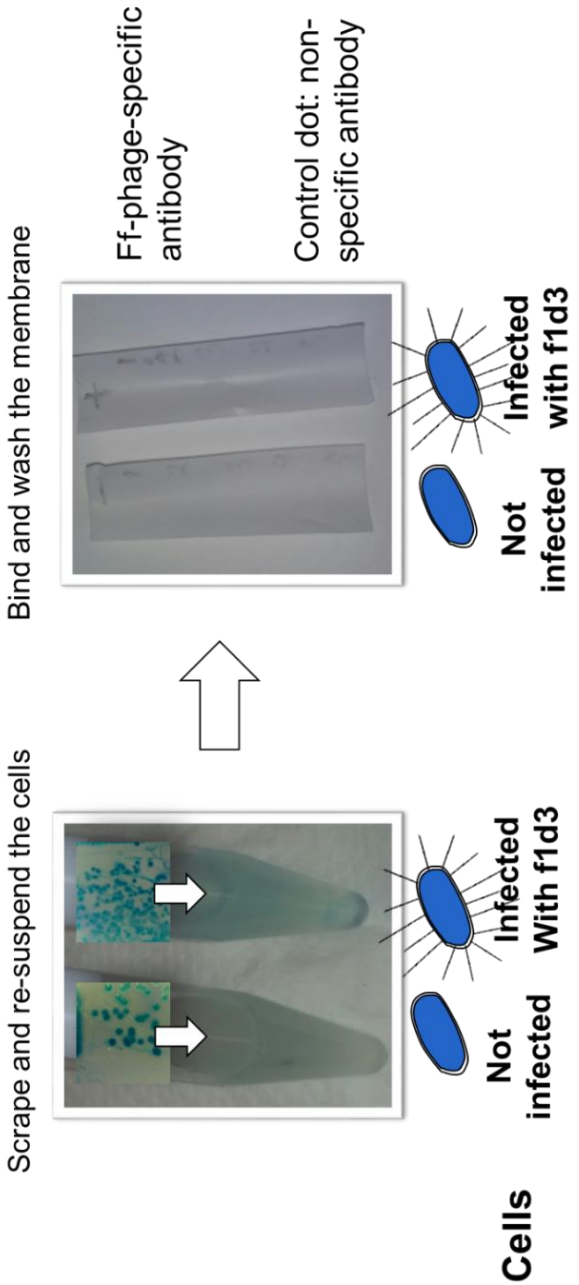

Figure 14: "Blue" K91/f1d3 trial

A) Resuspended blue colonies from **Figure 13**. **B)** Blot assay using the resuspended cells from **A**). Blots contained two spots of immobilised f1-specific and a spot of control antibodies, as indicated (also see Section 3.7.2).

Chapter IV

4. Biological Nanorods Derived from the f1 Phage: Remediation of the Particle Length Heterogeneity

Within the effort to convert Ff filamentous phage into non-infectious diagnostic/vaccine nanoparticles, a very different strategy of producing ultra-small (nano) f1-derived particles was explored. Work undertaken in the J. Rakonjac lab (Massey University) constructed a system for production of a series of short (~110 nm) nanorods derived from filamentous bacteriophage. The aim of this system is to produce biological nanoparticles that contain no coding sequences and no antibiotic resistance markers, thereby eliminating concerns linked to the use of full-length filamentous phage vectors as functionalised particles. These particles would have other uses, e.g. in microfluidic research or nanostructure assembly.

Preliminary results with the nanorod-production system demonstrated that the nanoparticles produced do not exist as monodisperse unit-length nanorods but are a mix of single-, double- and triple-length particles. The longer particles are a consequence of packing two or three ssDNA molecules sequentially before terminating assembly and releasing the particle from *E. coli*. This has been observed only in certain f1 mutants that have a lowered ratio of minor proteins (pIII, pVI, VIII, or pIX,) to the major coat protein (pVIII) (Lopez and Webster, 1983, Rakonjac *et al.*, 1999, Rakonjac and Model, 1998). The explanation for these reported observations was in that the minor proteins are responsible for termination and initiation of assembly, whereas pVIII is responsible for elongation. A lower amount of the minor proteins would therefore decrease the rate of termination (or initiation) favouring elongation by adding additional genomes into an assembling filament.

It was unclear as to what the cause of this phenomenon might have been in the nanorod production system, and how to overcome it to obtain uniform distribution of particle lengths. Although the short genome de facto underutilises pVIII by a factor of 10, creating excess of pVIII in the cell, prior work on even shorter particles (Ff nano; (Sattar *et al.*, 2015)) has demonstrated that unit-length particles were

produced. Furthermore, preliminary observations of multiple-length nanorods when low-efficiency assembly pVIII mutants were used has argued against this simple hypothesis (Bisset and Rakonjac, unpublished). To address these issues, several approaches have been taken, as described below.

4.1. Strategy of Stabilising pIII Minor Protein

One possible reason for lowered initiator/terminator proteins to pVIII could be the increased instability of the minor proteins. The only minor protein that is different from the wild-type is pIII, which contains an N-terminal insert of 15 amino acids between the signal sequence and the mature portion of the protein that correspond to multiple cloning site for display of proteins using pIII as a platform. This pIII variant was named pIIImcs.

A hypothesis has been put together that pIIImcs, due to the 15 unstructured amino acids at its terminus, is targeted and degraded by the main periplasmic chaperone DegP, degrading pIII and lowering the ratio of pIII to pVIII, ultimately causing lowered frequency of assembly termination and multiple-length particles.

To test the hypothesis that DegP is involved in pIII turnover, a delta degP mutant of *E. coli* was planned to be used as the producer strain of the nanorods. Previous work with the f1-encoded outer membrane secretion channel, pIV, showed that DegP mediates turnover of that protein (Spagnuolo *et al.*, 2010).

The periplasmic serine endoprotease DegP is required for the survival of *E. coli* at high temperatures. It acts as a general molecular chaperone at low temperatures but also functions as a peptidase at higher temperatures (Spiess *et al.*, 1999). DegP degrades transiently denatured, unfolded and/or misfolded proteins which accumulate in the periplasm following heat shock or other stress conditions (Isaac *et al.*, 2005). Kolmar *et al.* (1996) showed using model proteins that DegP is particularly efficient with Val-Xaa and Ile-Xaa peptide bonds; suggesting a preference for beta-branched side chain amino acids. These beta-branched side chain amino acids are typically buried in the hydrophobic core of proteins – thus normally

being inaccessible in correctly folded proteins - and were shown to be important determinants of cleavage specificity (Kolmar *et al.*, 1996). Only unfolded proteins, which are devoid of disulphide bonds appear capable of being cleaved, thereby preventing the non-specific proteolysis of folded proteins (Strauch *et al.*, 1989). Null mutations of DegP result in temperature sensitive growth (Strauch *et al.*, 1989).

A strain containing a complete deletion of the degP gene was constructed by P1 transduction, using the strain K1466 as donor and K2091 as the recipient. The Kn^R marker was further removed from this strain using transient expression of the FLP recombinase, as described in Methods (section 2.2.6). The resulting strain, K2442 (Table 1) was further analysed to examine whether it can support f1 phage replication. This was achieved by plating dilutions of wild-type f1 phage on this strain. It is expected that plaques are observed on the lawn of a host that is susceptible to f1 infection. However, no plaques were observed at any dilution of the wild-type f1 stock. This experiment has shown that degP is required for the Ff growth and henceforth cannot be eliminated from bacterial cell for the purpose of increasing stability of pIII. A different (partial) deletion mutant was shown to support f1 replication (Rakonjac, unpublished); however, that mutant contained a Kn^R marker inserted into the genome that could not be removed and was therefore incompatible with the pRNano3 (Kn^R) helper plasmid.

4.2. Increasing the Amount of Minor Proteins pVII and pIX

4.2.1. pNanoZap

To produce short non-self-replicating phage-derived particles, a novel template was constructed by Bisset and Rakonjac (unpublished). This template was designed based on the “zap” principle used previously in the lambda Zap vectors to excise phagemid from lambda phage genome in the presence of an Ff-derived helper phage (Short *et al.*, 1988). The aim was to construct a plasmid from which it would be possible to excise the shortest possible segment that has both (-) and (+) origin of f1 replication, and packaging signal (PS), to efficiently make very short particles. This plasmid is used in

conjunction with the helper plasmid pRNano3 to produce the short particles (see Introduction).

The pNanoZap vector **(Figure 15)** was derived from phagemid vector pUC118 and it contains a complete (+) origin of replication (*ori*1), followed by the intervening sequence that contains the multiple cloning site (MCS) and second origin sequence (*ori*2). This second origin contains both the (-) *ori*, packaging signal, and a truncated (+) *ori* (Δ29) that can only serve as (+) strand replication terminator, altogether completing the f1 *ori*, apart from 29 nucleotides deleted from the distal end.

The purpose of the MCS between the two origins is to allow insertion of DNA sequences of desired length, allowing fine-tuning of the size of the zapped ssDNA and consequently the length of the particles. In the presence of replication protein pII, the sequence between the two origins is expected to undergo (+) strand replication and produce circular (+) strand of 736 nt, starting the replication cycle. This DNA now contains the complete f1 *ori* and MCS. There are no antibiotic resistance markers or any other coding sequences in the 736-nt fragment.

The presence of (-) origin and PS in this circle allows replication from the (-) strand to form double-stranded replicative form (RF), permitting the complete cycle of the rolling circle one-strand-at-a-time replication of the 736-nt zapped circle to produce more (+) strands that can be packaged into the short "NanoZap" particles in comparison to the published Ff nano template whose replication results in 221-nt ssDNA with no (-) *ori*, which cannot serve as a template for replication of (-) strand (Bisset and Rakonjac, unpublished, Sattar, 2013).

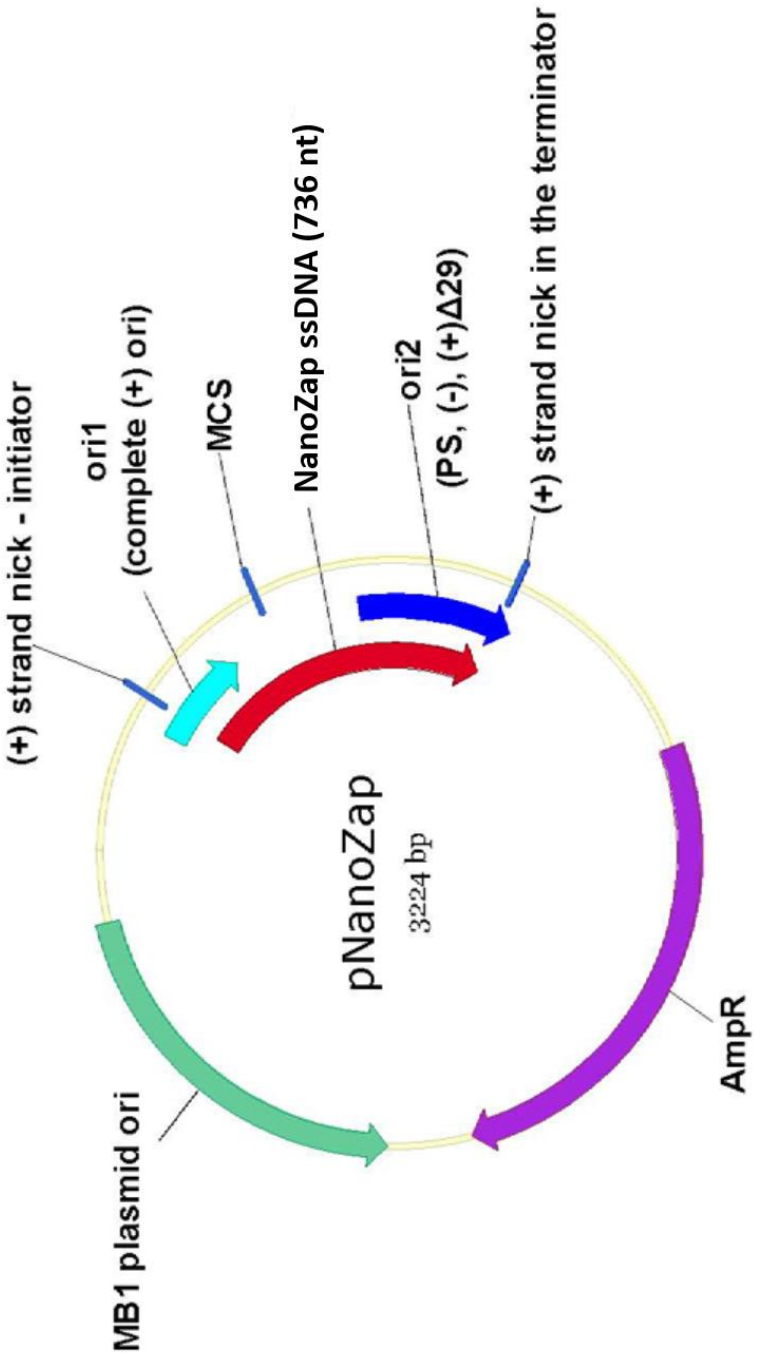

Figure 15: pNanoZap Plasmid Map.

Contains a plasmid *ori* (green) and ampicillin resistance marker (purple). Ori1 (light blue) is a complete (+) *ori*, which acts as an initiator of circular ssDNA synthesis, while ori2 (dark blue) contains a packaging signal (PS), (-) *ori*, and (+) Δ29, a mutant (+) *ori* containing a 29-nucleotide deletion and acts as a terminator of ssDNA synthesis. The region of DNA synthesized as circular ssDNA is shown in red. The presence of a multiple cloning site (MCS) between the two origins allows insertion of sequences to increase size of NanoZap ssDNA. Conversely, the ssDNA product can be shortened by deleting the intervening sequences between ori1 and ori2. Figure taken with permission from Bisset and Rakonjac (unpublished).

4.2.2. pNanoZap 719

It was hypothesised that if the palindromic sequences (restriction sites) found in the multiple cloning site of the pUC118 vector that is part of the zapped replicon could mediate annealing two or more circular ssDNA complexes derived from the NanoZap replicon via recA or pV and can be co-packaged to form multiple-length particles. Annealing of ssDNA from phage ϕX174 by a RecA homologue has been reported (Takaku *et al.*, 2010). To decrease the number of palindromic sequences in the MCS, approximately 18 nucleotides containing restriction sites were deleted from the multiple cloning site (MCS) of the pUC118. This new plasmid was constructed by Jasna Rakonjac and Sofia Khanum and was named pNanoZap 719 **(Figure 16)**. Outside this deletion the plasmid sequence is the same as the template plasmid pNanoZap 736.

4.2.3. pNanoZap SNgII

Another hypothesis was that multiple length particles were being produced due to the insufficient pVII and pIX relative to pVIII in the cell, and in particular in the vicinity of packaging signal derived from the zapped replicon, preventing effective re-initiation of filament assembly. As noted in Rakonjac and Model (1998), mutations in the coding sequences of pVII and pIX that lead to reduced expression of the minor coat proteins caused the phage produced to lengthen. pVII and pIX are found in pairs at the leading end of the bacteriophage, normally in 3 to 5 copies each, and are required to begin assembly of the bacteriophage, in conjunction with the packing signal and *gI* (Rakonjac and Model, 1998). As such, it was thought that if the *gVII* and *gIX* coding sequences were moved in the pNanoZap vector to between the ori1 and ori2 of the vector and were then directly hooked up to the *gII* promoter from which they are normally expressed, then this would decrease the proportion of longer particles produced by increasing the efficacy of initiation of assembly. This pNanoZap was constructed by Jasna Rakonjac and Sofia Khanum and was named pNanoZap SNgII (**Figure 18**).

4.2.4. pNanoZap SN*lac*

A third hypothesis was to test whether overexpression of pVII and pIX by attachment to an inducible promoter would help to further increase the efficiency of initiation of particle assembly. The coding sequences for *gVII, gIX,* were inserted downstream of the existing *lac* promoter within the pUC118 vector, between ori1 and ori2. The inducible *lac* promoter is one of the most commonly used promoters for heterologous protein expression in *E. coli*. Isopropyl-β-D-thiogalactoside (IPTG) is currently the most efficient molecular inducer for regulating this promoter's transcriptional activity (Briand *et al.*, 2016). Plasmid was constructed by Jasna Rakonjac and Sofia Khanum and was named pNanoZap SN*lac* (**Figure 19**).

When this pNanoZap plasmid was tested in this work, two separate batches were produced – induced and uninduced with IPTG. Expression from the pUC *lac* promoter has been shown to give good protein production in the absence of induction (Rakonjac *et al.*, 1995).

4.3. Production and Purification of the NanoZap Particles

After the pNanoZap plasmids were constructed, they were transformed into the K1030 strain containing the helper plasmid pRnano3. pNanoZap-derived nanorods were then produced and purified by PEG precipitation and CsCl gradient centrifugation as described in Materials and Methods (section 3.17 and 3.18). An example of analysing the fractions from a CsCl gradient is shown in **Figure 17**.

The NanoZap particles were quantified by densitometry (see Section 4.3) using ssDNA isolated from the NanoZap 736 nanorods as a standard **(Figure 20**; lanes labelled "Standard" and "ssDNA"**)**.

Native agarose gel electrophoresis was used to estimate the distribution of the nanoparticles between single-, double- and triple-length particles in each of the samples (**Figure 20**, lanes labelled "Native").

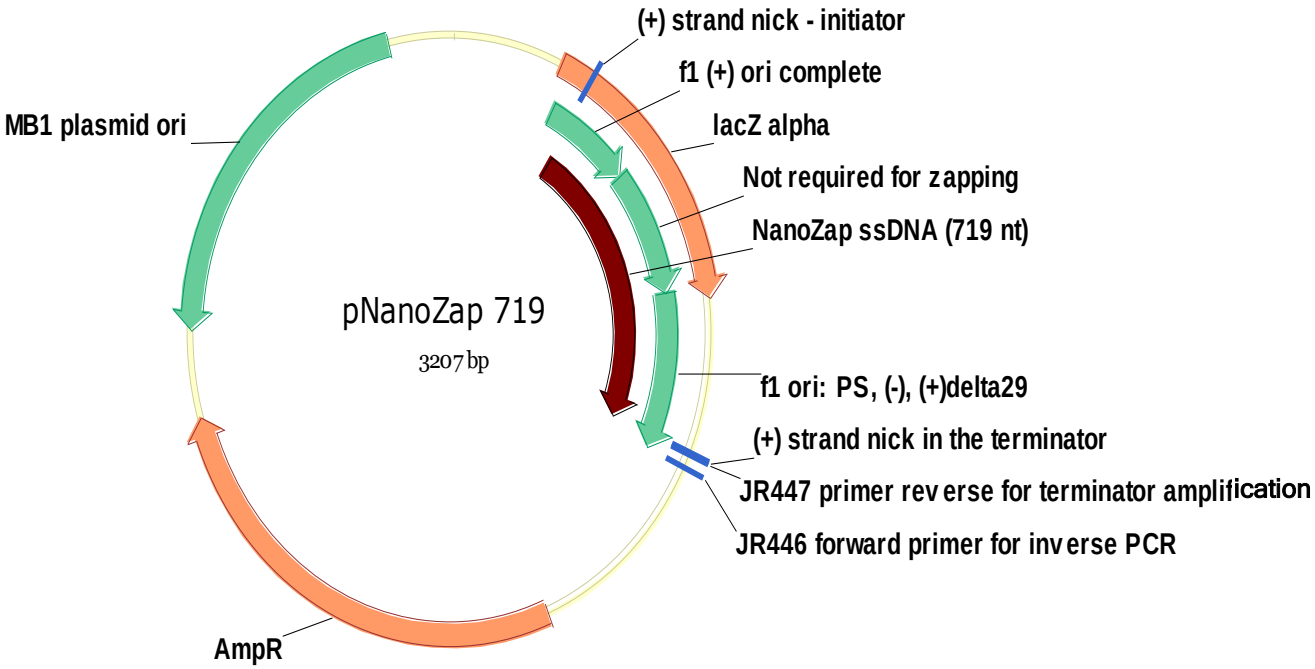

Figure 16: pNanoZap 719 Plasmid Map.

Plasmid *ori* (green) and ampicillin resistance marker (orange). Ori1 (light blue) is a complete (+) *ori*, which acts as an initiator of circular ssDNA synthesis, while ori2 (dark blue) contains a packaging signal (PS), (-) *ori*, and (+) Δ29, a mutant (+) *ori* containing a 29-nucleotide deletion and acts as a terminator of ssDNA synthesis. The presence of a multiple cloning site (MCS) between the two origins allowed the deletion of palindromic sequences encoding restriction sites to decrease the size of NanoZap ssDNA, and potentially also the nanoparticles produced. The region synthesised as circular ssDNA is indicated in red.

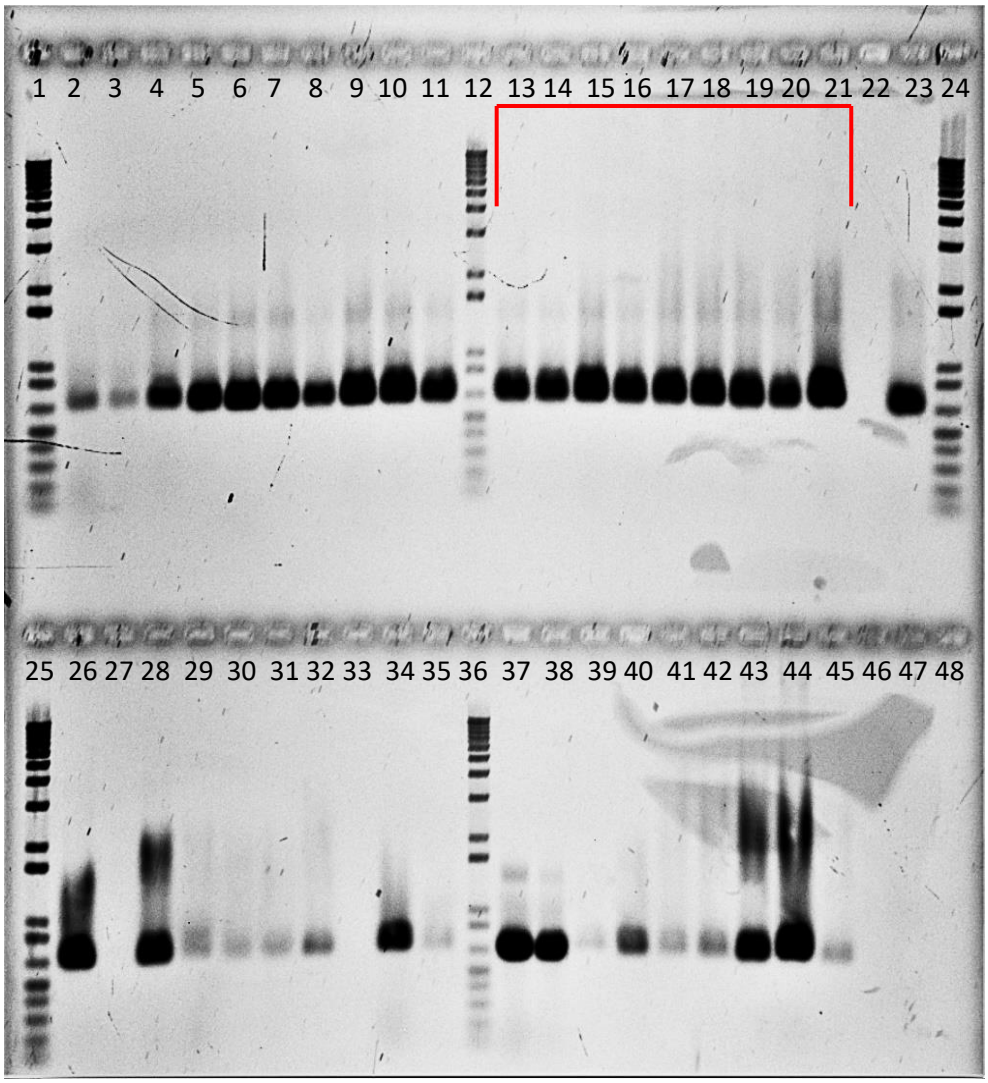

Figure 17: Analysis of Fractions from CsCl Gradient.

Particles were disassembled by heating in an SDS-containing buffer and the released DNA was analysed by agarose gel electrophoresis. Lanes: 1, 12, 24, 25 and 36 are 1 kb^+ ladder (Life Technologies). Lanes: 2 – 11, 13 – 23, 26 – 35, and 37 – 45 contain DNA from the disassembled particles. Lanes: 46, 47, and 48 are empty. The CsCl fraction samples corresponding to lanes 13 – 21, as indicated by the red bracket, were chosen, combined and purified.

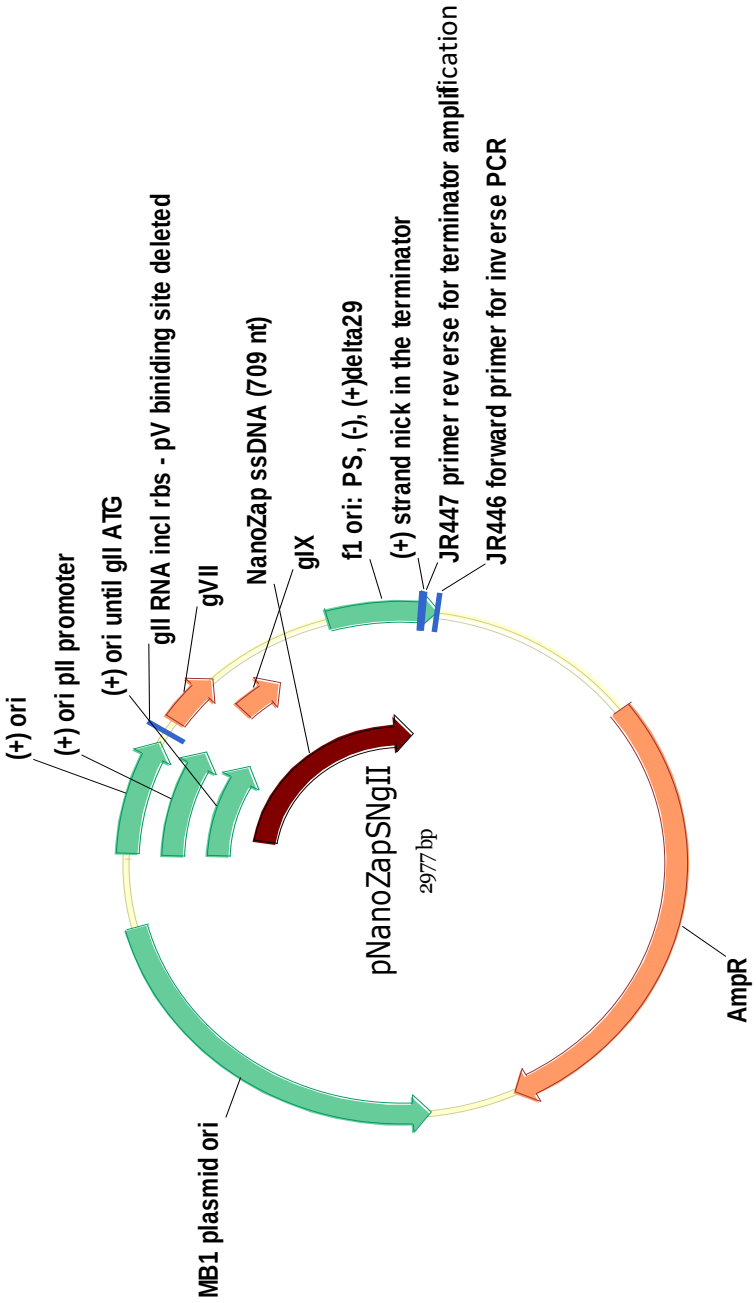

Figure 18: pNanoZap SNgII Plasmid Map.

Contains a plasmid *ori* (green) and ampicillin resistance marker (orange). Ori1 (green) is a complete (+) *ori*, which acts as an initiator of circular ssDNA synthesis, while ori2 (dark blue) contains a packaging signal (PS), (-) *ori*, and (+) Δ29, a mutant (+) *ori* containing a 29-nucleotide deletion and acts as a terminator of ssDNA synthesis. Ori1 also contains a coding sequence for pII promoter. The region of DNA synthesized as NanoZap ssDNA is shown in red. The presence of a multiple cloning site (MCS) between the two origins allowed the insertion of the *gVII* and *gIX* coding sequences encoding pVII and pIX to potentially decrease size of NanoZap particles produced.

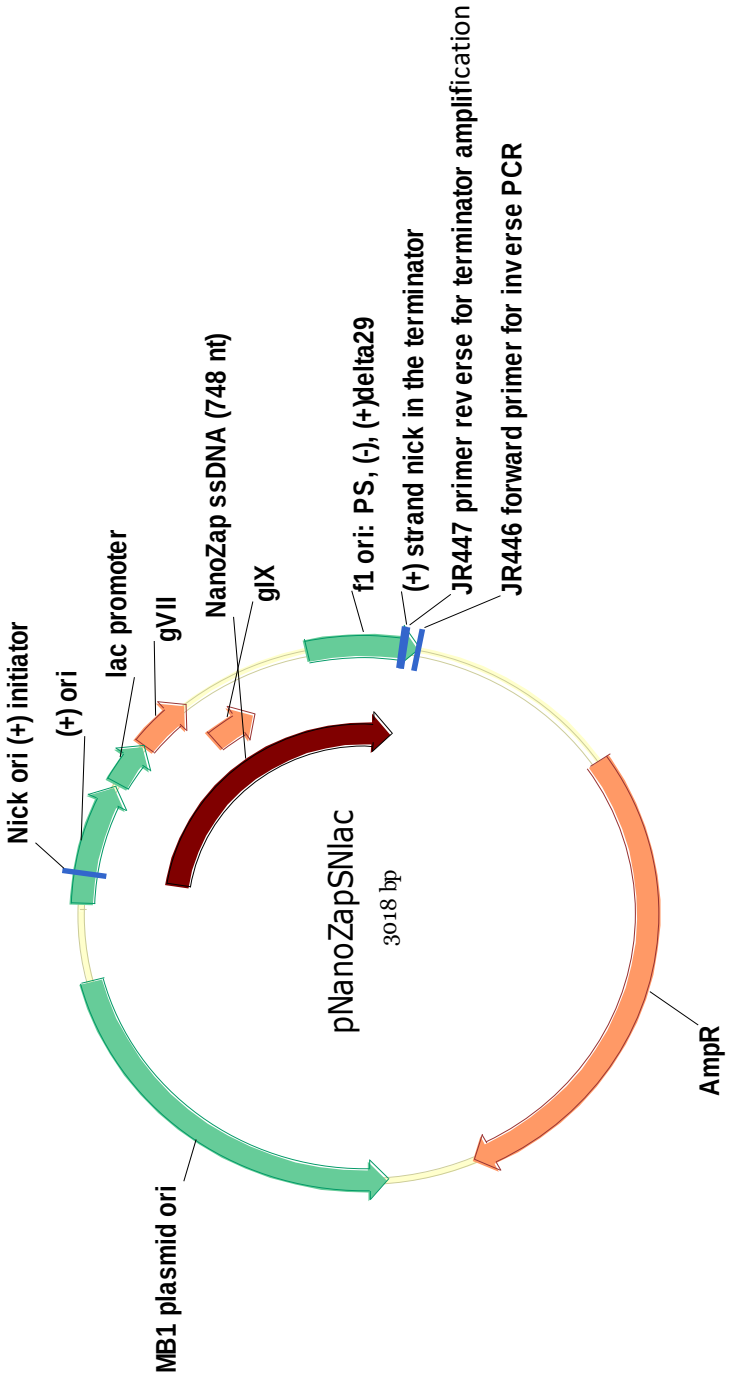

Figure 19: pNanoZap SN*lac* Plasmid Map.

Contains a plasmid *ori* (green) and ampicillin resistance marker (orange). Ori1 (green) is a complete (+) *ori*, which acts as an initiator of circular ssDNA synthesis, while ori2 (dark blue) contains a packaging signal (PS), (-) *ori*, and (+) Δ29, a mutant (+) *ori* containing a 29-nucleotide deletion and acts as a terminator of ssDNA synthesis. Ori1 also contains a coding sequence for *lac* promoter from M13. The presence of a multiple cloning site (MCS) between the two origins allowed the insertion of the *gVII* and *gIX* coding sequences encoding pVII and pIX to potentially decrease size of NanoZap particles produced.

4.4. Comparison of the Amount of Produced Nanorods From the Newly constructed pNanoZap variants

A densitometry-based quantification was employed to quantify the purified nanorods (Bisset and Rakonjac, unpublished, Rakonjac and Model, 1998). This was carried out as specified in Materials and Methods (section 2.1.9.1). First the ssDNA known standards were made by purifying and spectroscopically quantifying ssDNA from the NanoZap 736, and a standard curve was plotted. The standard was run on the same agarose gel with DNA from SDS-disassembled nanorods derived from the new NanoZap template variants: pNanoZap 719, pNanoZap SNgII, and both IPTG-induced and uninduced pNanoZap SN*lac*; the standard curve was used to quantify the ssDNA (and thereby the nanorod) amount. The particle concentration was expressed as the number of ssDNA genomes per mL. The final concentration of pNanoZap 719 was 2.6×10^{14} per mL, while the final concentration of pNanoZap SNgII was 4.3×10^{14} per mL. The concentration of pNanoZap SN*lac* nanoparticles produced by the uninduced batch was 6.8×10^{14} per mL, whereas the IPTG induced pNanoZap SN*lac* was 1.5×10^{15} per mL.

The results showed that pNanoZap 719, pNanoZap SNgII and the uninduced and induced batch of pNanoZap SN*lac* resulted in increasing concentration (and total amount) of purified particles, A two-fold increase in production of phage in the IPTG induced batch of the pNanoZap SN*lac*, compared to the IPTG uninduced batch, suggests that pVII and pIX are the limiting factor in the nanorod production.

.

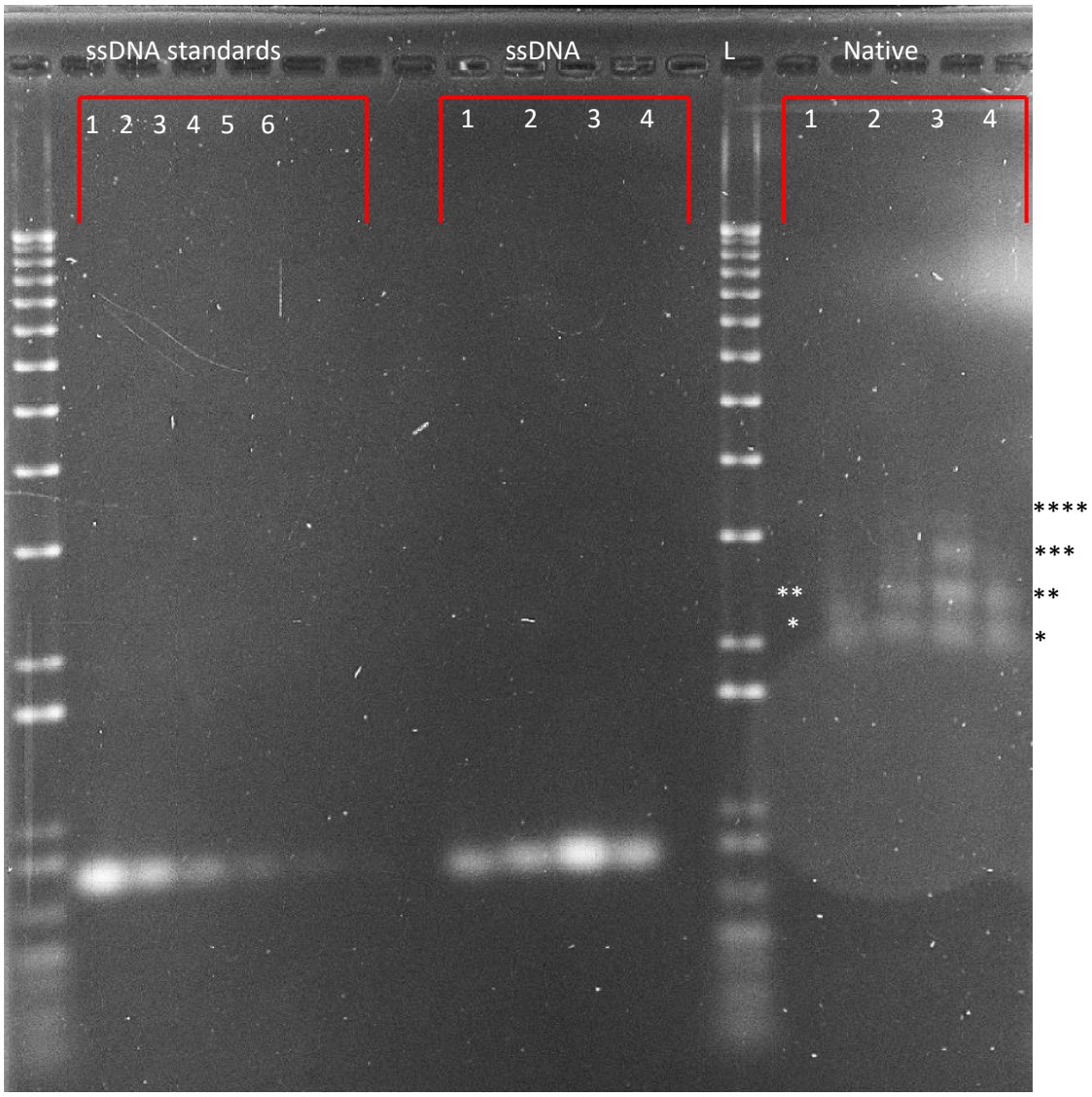

Figure 20: Agarose gel electrophoresis of disassembled and native nanorods made using the newly constructed pNanoZap variants.

1) pNanoZap 719, **2)** pNanoZap SNgII, and **3)** pNanoZap SN*lac*, IPTG induced; **4)** pNanoZap SNlac, IPTG uninduced. Lanes labelled "ssDNA Standards" contain the NanoZap 736 purified ssDNA of known amounts (2-fold serial dilutions, starting with 40 ng/µL (Lane 1) per lane); Lanes labelled "SDS-denatured lanes" are, heat- and in SDS-disassembled particles; Lanes labelled "Native", contain intact particles loaded onto the gel with 1× loading dye. They were visualised after soaking of the gel in a NaOH solution to strip the virion proteins in situ, followed by EtBr staining of exposed DNA. Asterisks denote nanorods of different lengths. Single and double white asterisks, NanoZap 719 nanorods, single- and double- length, respectively; Single, double, triple and quadruple black asterisks, NanoZap SNgII and SN*lac* nanorods, single-, double-, triple- and quadruple-length. **L)** 1 kb^{+} ladder (Life Technologies); used as a migration signpost (it cannot be used as a size standard for the nanorod circular ssDNA or for the native particles).

4.5. Length of the Novel Nanorod Variants

Native agarose electrophoresis (**Figure 20**; lanes labelled "Native") demonstrated that all four samples contained double-length particles (and longer). Among the four analysed samples the NanoZap 719 variant showed the relatively weakest band representing double-length nanorods (double white asterisk) relative to the single-length nanorods (single white asterisk) and no visible triple-length band. To corroborate the native agarose gel electrophoresis observation, purified particles were analysed by TEM at the Manawatu Microscopy and Imaging Centre (MMIC) at Massey University. Representative micrographs are shown in **Figures 21 - 24**. These and additional micrographs containing clearly separated nanorods were used to measure the length of 100 - 200 individual nanorods and plot the size distributions (**Figures 25A - E**).

Measurement of the length of 200 particles obtained using the original NanoZap 736 found that there are two major peaks in the number of at the lengths of 110 nm (presumably single-length particles) and 190 nm (presumably double-length particles) and the native agarose electrophoresis showed strong double- and triple-length particle bands (Bisset and Rakonjac, unpublished).

The micrographs (**Figure 21 - 24**) showed some aggregation of the NanoZap particles that in turn resulted in a number of filaments in the image appearing over a range of lengths. The NanoZap particles appear to have unequal termini, with one end appearing pointy, likely due to the formation of the pIII/pVI cap and the other appearing oval (Bennett and Rakonjac, 2006, Gray *et al.*, 1981).

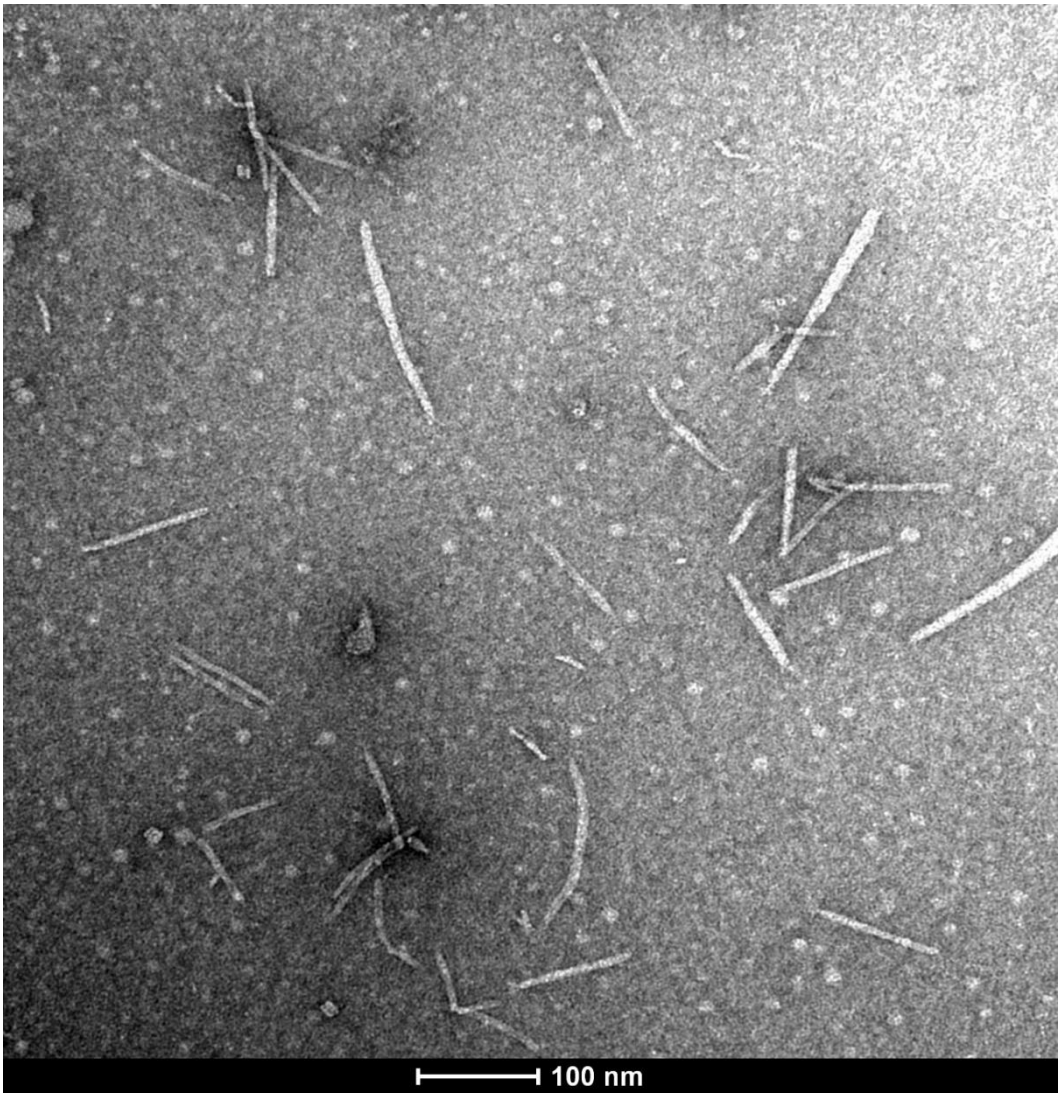

Figure 21: TEM of NanoZap 719 NanoZap Particles.

TEM of nanoparticles produced from pRNano3 + pNanoZap 719. The pointy and smooth caps are visible, along with the vesicles. It is also clear that the NanoZap particles produced are of differing lengths.

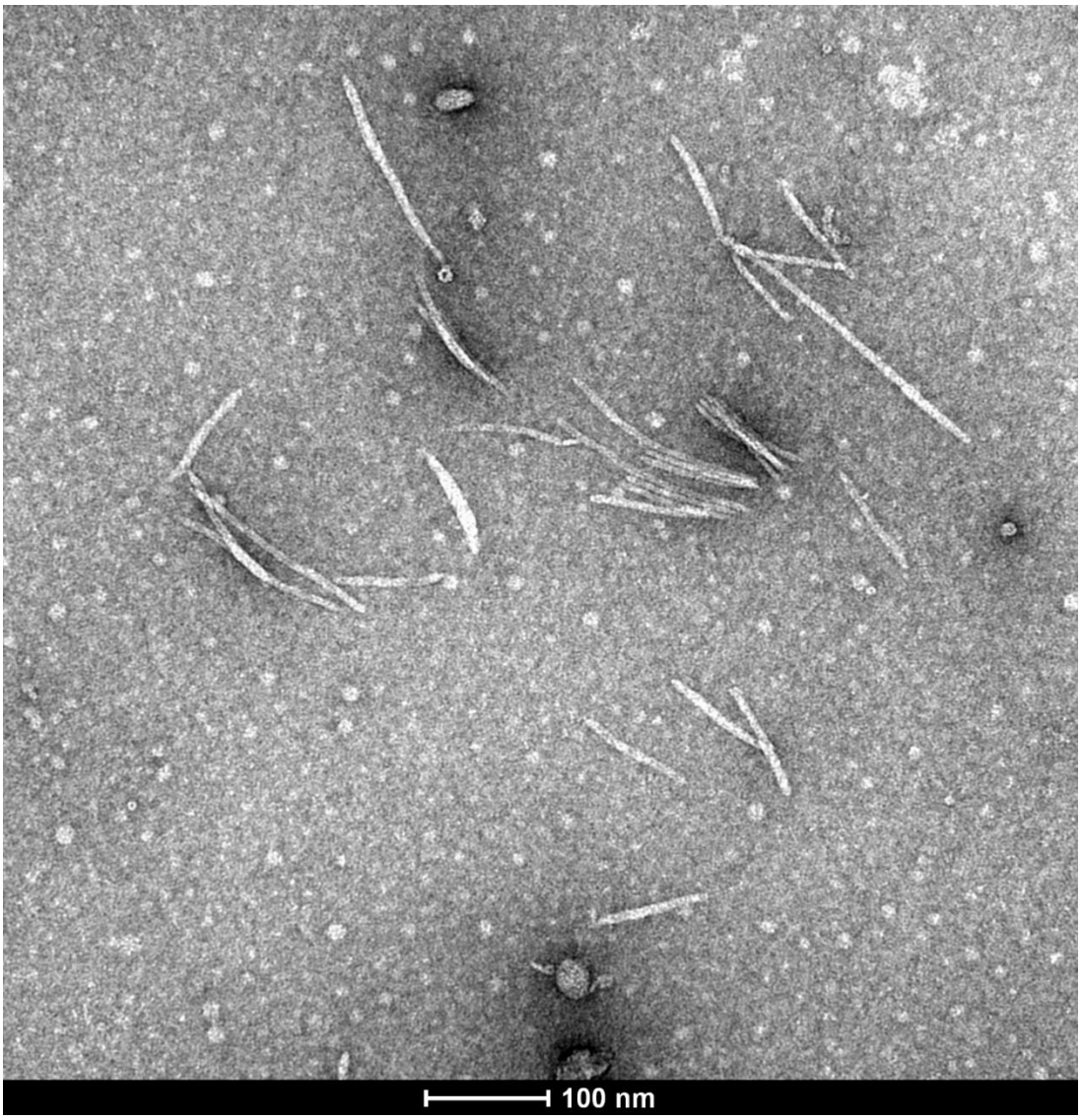

Figure 22: TEM of NanoZap SNgII NanoZap Particles.

TEM of nanoparticles produced from pRNano3 + pNanoZap SNgII. There is a high amount of NanoZap particles visible. It can clearly be seen in the electron micrograph that the NanoZap particles are sticking to one another, and that they appear to be of differing lengths.

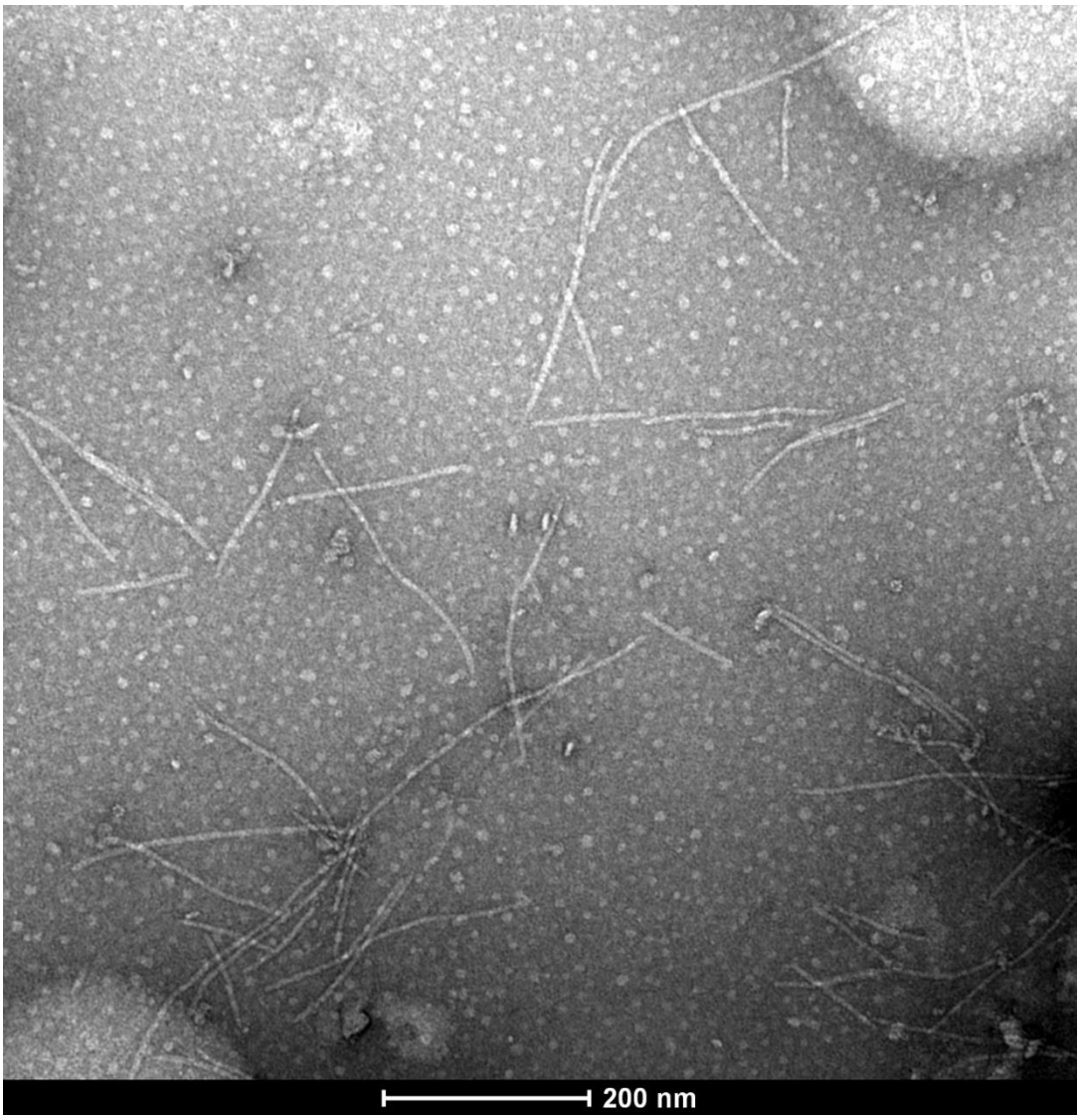

Figure 23: TEM of NanoZap SN*lac* IPTG induced NanoZap Particles

TEM of nanoparticles produced from pRNano3 + pNanoZap SN*lac*, IPTG induced. There is a high amount of NanoZap particles visible. It can clearly be seen in the electron micrograph that the NanoZap particles are sticking to one another, and that they appear to be of differing lengths.

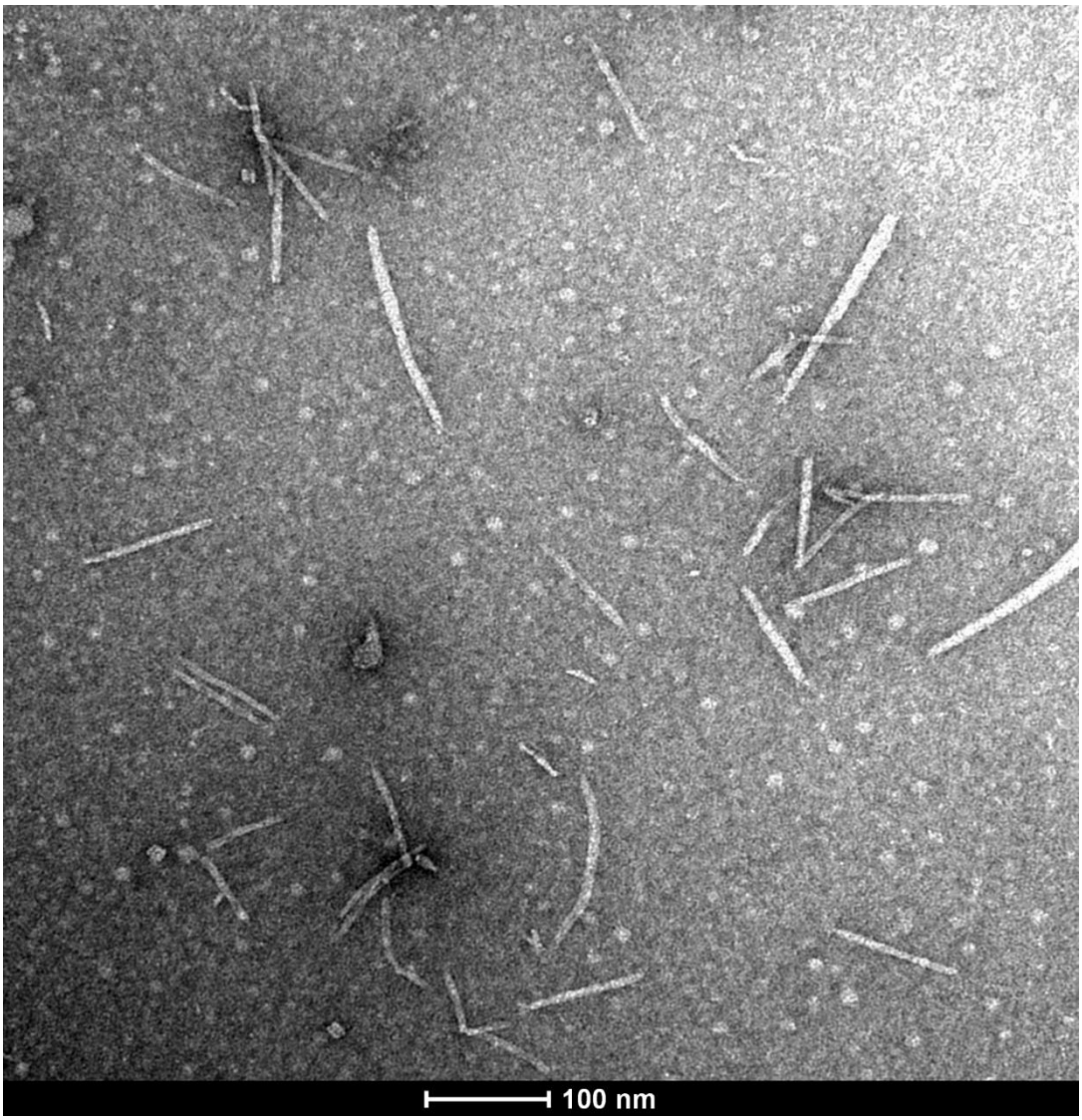

Figure 24: TEM of NanoZap SN*lac* IPTG uninduced NanoZap Particles

TEM of nanoparticles produced from pRNano3 + pNanoZap SN*lac*, IPTG uninduced. There is a high amount of NanoZap particles visible. It can clearly be seen in the electron micrograph that the NanoZap particles are sticking to one another, and that they appear to be of differing lengths. The unequal termini are also clearly visible in this micrograph.

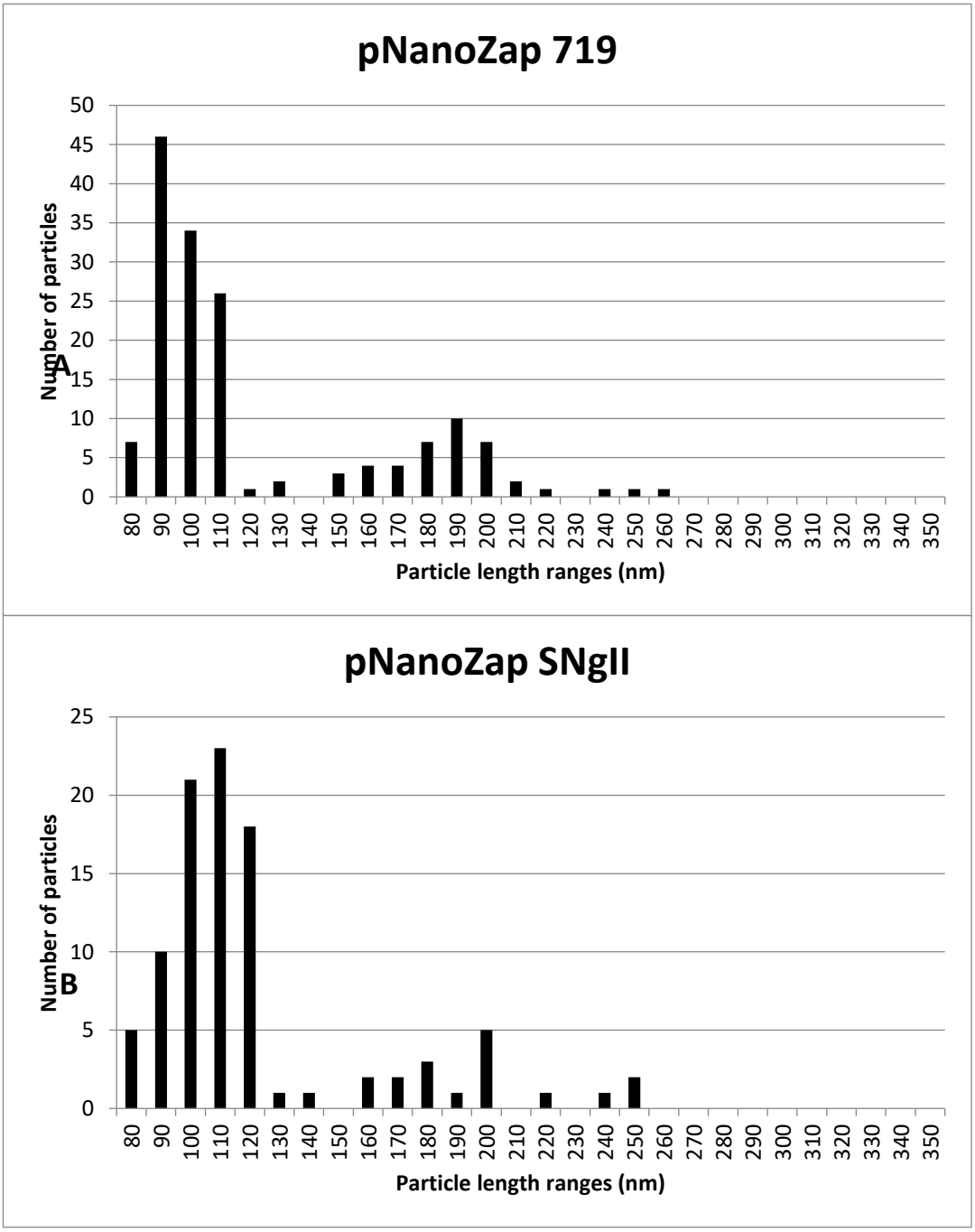

Figure 25A – B: Histograms of the Lengths of Produced NanoZap Particles.

Size distributions of nanorods produced by both pNanoZap 719 **A**) and pNanoZap SN*gII* **B**) are presented as histograms. Histograms were generated by measuring the length of approximately 100 - 200 individual particles in each sample using the ImageJ measurement function.

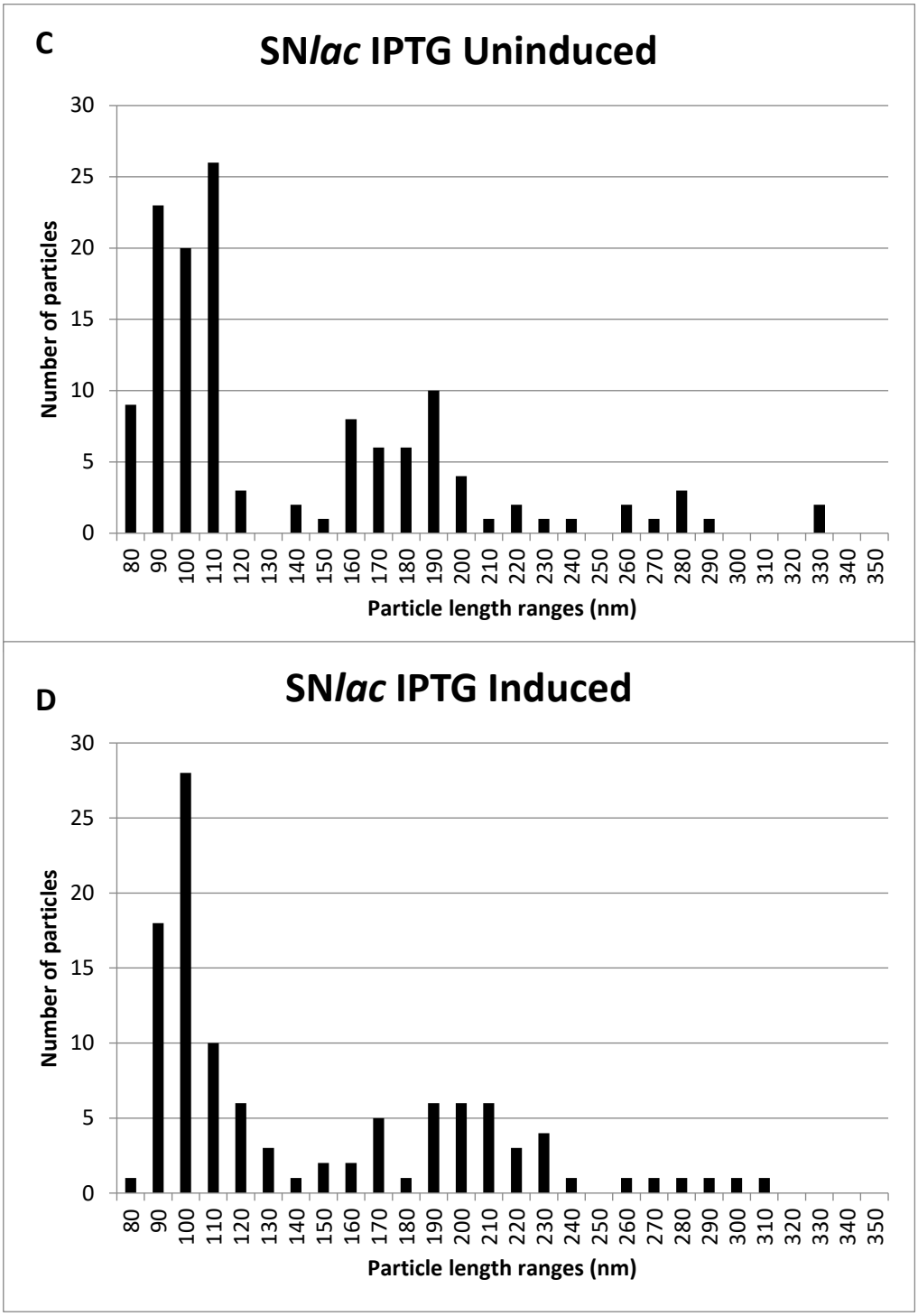

Figure 25C - D: Histograms of Produced NanoZap Particles.

Size distributions of nanorods produced by both pNanoZap SN*lac* uninduced **C**) and pNanoZap SN*lac* induced **D**) are presented as histograms. Histograms were generated by measuring the length of approximately 100 - 200 individual particles in each sample using the ImageJ measurement function.

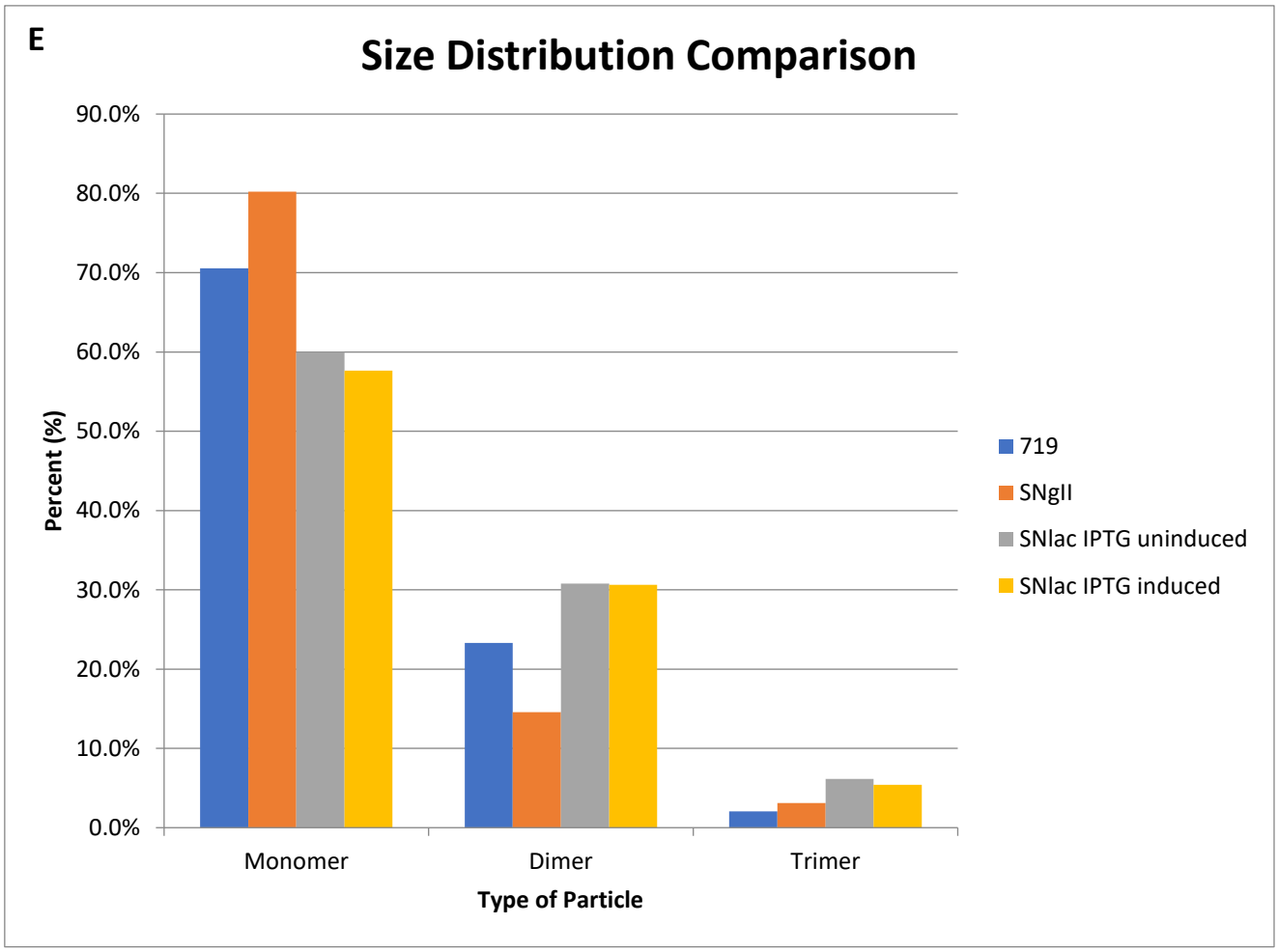

Figure 25E: Size Distribution Comparison.

Size distributions of nanorods produced by all four of the varying pNanoZap plasmids are presented as a histogram. The blue bar represents pNanoZap 719 nanorods, orange corresponds to SNgII nanorods, grey corresponds to SN*lac* IPTG uninduced nanorods, and yellow represents the SN*lac* IPTG induced nanorods. The size distributions have been organised into several sub-categories: monomers; dimers; and trimers. These have then been presented to show the percentages of each type of nanorod (monomer, dimer or trimer) counted in the micrographs for each sample.

Monomers fall within the length range of 80 – 129 nm; dimers fall within the length range of 160 – 229 nm; and trimers fall within the length range of 240 – 329 nm.

Furthermore, as the images produced using TEM are two dimensional and cannot give an accurate representation of possible three-dimensional arrangements of particles or the angle of the nanorods relative to the vision field plane (surface), another source of apparent length variability would be particles that do not lie parallel to the carbon coated grid plane. To assess the length of particles statistically, the lengths of discernible filaments in the micrographs were determined (between approximately 100 - 200 for each pNanoZap plasmid; 146 particles for pNanoZap 719; 96 particles for pNanoZap SNgII; 130 particles for pNanoZap SN*lac* IPTG uninduced; and 111 particles for pNanoZap SN*lac* IPTG induced) and the length distributions were presented using histograms **(Figure 25A - E)**.

Based on the histograms generated for each helper plasmid-produced NanoZap population, each different kind of NanoZap particle produced had different lengths (**Figure 25A - E**). NanoZap particles produced by pNanoZap 719 produced two different peaks, 90 nm and 190 nm, while NanoZap particles produced by pNanoZap SNgII also produced two different peaks, 110 nm and 200 nm. NanoZap particles produced by IPTG uninduced pNanoZap SN*lac* produced two different peaks, 110 nm and 190 nm, while NanoZap particles produced by IPTG induced pNanoZap SN*lac* also produced two different peaks of 100 nm and approximately 200 nm (the peak ranges from 190 nm – 210 nm).

There appeared to be no visible structural difference between the IPTG uninduced and induced batches of pNanoZap SN*lac*, and only minor peak differences of about 10 nm, which can be attributed to several factors affecting the accuracy of measurements taken from TEM images. The longer length of the SN*lac* particles was expected, given that the ssDNA zapped from this plasmid is the longest (748-nt) of the three variants; the NanoZap 719 giving a 719-nt ssDNA and the SNgII only 709-nt ssDNA. Calculation of the particle length has been derived from measuring Ff nano and NanoZap 736 particles to be Nnt/7.6nt nm^{-1} + 17 nm (Bisset and Rakonjac, unpublished). With this formula, the length of single-length particles in all analysed samples should be between 110 and 115 nm, a difference too small to observe by TEM, considering the numerous factors that can influence the length appearance.

Analysis of the NanoZap particles by agarose gel electrophoresis gave a somewhat different distribution of the different length nanorod population to the TEM (**Figure 20; lanes labelled "Native"**). All native virions gave a ladder of bands, with the NanoZap 719 particles having the relatively most dominant single-length particle band. The other three samples have had prominent double-length particles (equal or stronger than single-length, while the NanoZap SN*lac* (induced) sample demonstrated a strong triple-length and detectable quadruple-length particle band.

The size distribution comparison histogram (**Figure 25E**) clearly shows the percentages of each length of nanorod (e.g. monomer, dimer, trimer) produced by each of the four pNanoZap plasmids. Monomers fall within the length range of 80 – 129 nm; dimers fall within the length range of 160 – 229 nm; and trimers fall within the length range of 240 – 329 nm. It is important to note that it is difficult to establish multi-length particles from clusters of nanorods seen in the electron micrographs, and as such, the amount of trimers and potentially quadruple-length nanorods for each sample may have been underestimated. It is clear from the size comparison histogram that the pNanoZap SNgII particles had the most dominant single-length particles (80.2%), with the pNanoZap 719 monomer particles being the second most dominant (70.5%). The pNanoZap SN*lac* particles (both IPTG induced and uninduced) produced the most dimers (30.8% uninduced; 30.6% induced) and trimers (6.2% uninduced; 5.4% induced) of all four samples. This is interesting, as the analysis of the NanoZap particles by agarose gel electrophoresis indicated that pNanoZap 719 particles had produced the highest amount of single-length particles; however, the agarose gel electrophoresis allows for a better overall view of the lengths of the nanorods produced, as the histogram analysis is restricted to the nanorods that were photographed.

4.6. Discussion and Summary

The aim of these experiments was to see whether the alterations made to the NanoZap system would result in single-length NanoZap particles. pNanoZap 719 had approximately 18 nucleotides deleted from the multiple cloning site (MCS). These 18 nucleotides were palindromic sequences corresponding to restriction sites in the MCS. According to the native agarose gel electrophoresis this plasmid permitted assembly of

mostly single-length particles. In contrast, electron microscopy indicated a higher proportion of the double-length particles, with the peaks of the histogram at 90 nm and 190 nm (**Figure 25A**).

pNanoZap SNgII was altered from the original pNanoZap 736 design to include coding sequences for the minor proteins pVII and pIX and the *gII* promoter (from which they are normally transcribed). It was possible to do this and retain the short size of the zapped replicon because the two proteins are very small (32 and 33 amino acids, respectively) and they are located next to each other and in the same operon in the f1 phage genome (Endemann and Model, 1995, Rakonjac *et al.*, 2011, Rakonjac and Model, 1998, Sattar, 2013). Agarose gel electrophoresis of the native particles showed a strong double-length band. This agreed with the length measurements based on the TEMs, where most particles seen were 110 nm or 200 nm in length (**Figure 25B**).

pNanoZap SN*lac* is similar to pNanoZap SNgII, apart from having the *lac* promoter controlling the expression of *gVII* and *gIX*. Two different batches of NanoZap SN*lac* particles were produced and purified, one with induction of the *gVII* and *gIX* expression by IPTG, and the other that was uninduced. Both batches samples contained high proportion of double-length particles according to the native virion agarose gel electrophoresis. The induced NanoZap SN*lac* also contained a population of triple-length particles and a faint band of quadruple-length particles. TEM analysis and particle length measurements showed that the NanoZap SN*lac* particles produced from uninduced and induced cultures both fell into two peaks, of approximately 110 - 190 nm and 100 – approximately 200 nm (as the peak ranges from 190 – 210 nm) (**Figure 25C - D**).

The size distribution comparison histogram (**Figure 25E**) showed the percentages of each type of nanorod produced by the differing pNanoZap plasmids. 70.5% of the nanorods produced by pNanoZap 719 were single-length particles (monomers), with 23.3% of the nanorods produced being dimers, and only 2.1% of the nanorods being trimers. This is a significant result, with 70.5% of nanorods produced being monomers, however, the nanorods produced by SNgII were 80.2% monomers, which is a significant increase (10%) in the amount of monomers produced. pNanoZap SNgII also produced 14.6% dimers and 3.1% trimers, thus making it the most effective pNanoZap

plasmid out of the four tested at producing single-length nanorods; however, in this analysis, a monomer is a particle that falls within a length range of 80 nm to 129 nm. As a result, while producing single-length particles, these single-length particles still range in length, rather than being uniform in length.

pNanoZap SN*lac* (both IPTG uninduced and induced) produced lower amounts of single-length particles, and higher amounts of dimers and trimers were seen in both samples. IPTG uninduced SN*lac* produced nanorods were 60% monomers, 30.8% dimers and 6.2% trimers, while IPTG induced SN*lac* produced nanorods were 57.7% monomers, 30.6% dimers and 5.4% trimers; making the pNanoZap SN*lac* plasmid the most effective at producing multiple-length particles, regardless of induction with IPTG (**Figure 25E**).

In contrast to electron micrographs, the native agarose electrophoresis showed notable differences in the amount of longer-than-single-length particles among the four analysed samples. The NanoZap 719 particles were mostly single-length, with a minor portion of double-length particles, whereas the samples expressing pVII and pIX from the zapped replicon had equal or larger proportion of double-length particles. These bands were not quantified due to difference in the total loading. This electrophoresis should be repeated by loading exact same amount of particles and the amount of particles in each band should be quantified and their ratios compared. This analysis would quantify the amounts of each type of particles in each of the samples.

In summary, the pNanoZap 719 plasmid appears to have produced the largest proportion of the single-length particles among the four tested constructs, according to the agarose gel electrophoresis, whereas SNgII produced the most monomers, according to the size distribution histogram; induction of pVII and pIX production from the zapped replicon NanoZap SN*lac* increased production of nanorods by a factor of 5.6, relative to the pNanoZap 719 that does not express pVII and pIX.

In parallel to the work carried out as described above, another pNanoZap phage vector was constructed by J. Rakonjac and S. Khanum with the aim to decrease the length of the NanoZap particles produced. It was proposed that deleting the complete multiple cloning site (MCS) from the pNanoZap vectors to decrease the size and to remove

palindromic sequences, rather than adding the encoding sequences for pVII and pIX along with an associated promoter, would decrease the fraction of double-length NanoZap particles. This new plasmid (pNanoZap 537) contains a 537-nt ssDNA zapped replicon and has produced largely single-length 80-nm particles (S. Khanum, unpublished) (**Figure 26)**. This finding supports the hypothesis that palindromic sequences in the NanoZap replicon promote packaging of the NanoZap ssDNA into multiple-length particles.

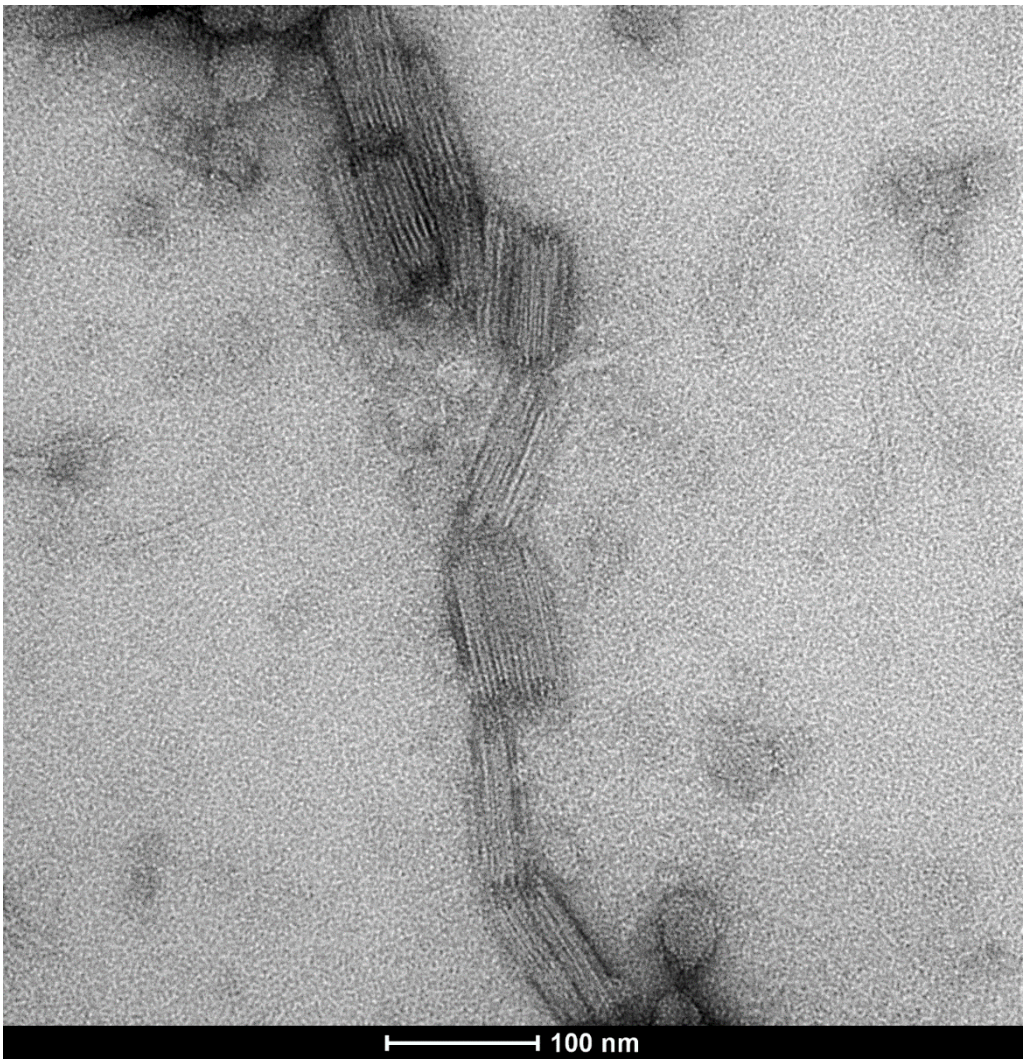

Figure 26: TEM of the NanoZap 537 nanorods

(Designed by J. Rakonjac; constructed, produced and purified by S. Khanum.) TEM by Jordan Taylor at the MMIC (Massey University, Palmerston North).

Chapter V

5. Removing Antibiotic Resistance Marker from the pNanoZap Plasmids

When the NanoZap or Ff nano particles are being assembled, one particle in a million packages the entire plasmid due to recombination that removes the terminator copy of the (+) ori. Given that these plasmids include antibiotic resistant genes, the produced phagemid particles could and likely would easily spread antibiotic resistance genes to other *E. coli* strains outside of the laboratory environment. One way to resolve this issue is to construct a new pNanoZap vector containing no antibiotic resistances. This was designed to be achieved using auxotrophic markers. An auxotrophic strain unable to synthesize a metabolite required for the bacterial growth (amino acid, vitamin, nucleotide, cofactor etc.) due to a mutation in one of the enzymes of the cognate biosynthetic pathway.

Auxotrophy for cofactor NAD was chosen, given that it does not require preparation of complex mixtures of amino acids, as is the case with auxotrophic markers involved in amino acid synthesis. The host strain for production of the NanoZap particles in this case was chosen to be a mutant lacking one of the enzymes of the NAD biosynthetic pathway, Δ*nadC*; encoding for the quinolinate phosphoribosyl transferase (Bhatia and Calvo, 1996); see Appendix I for the NAD biosynthesis pathway. The pNanoZap was modified by replacing the Amp^R marker (*bla* gene) with the *nadC* gene, to allow selection for the plasmid by complementation of NAD auxotrophy of the host strain.

5.1. NAD Biosynthesis Pathway and the Role of NadC

Quinolinate phosphoribosyltransferase (which is encoded for by the gene *nadC*) catalyses the third step in the biosynthesis pathway of NAD in *E. coli* (Flachmann *et al.*, 1988). In *E. coli* quinolinate biosynthesis is catalysed by a quinolinate synthetase complex from L-aspartate and dihydroxyacetone

phosphate. The quinolinate synthetase complex consists of the two enzymes quinolinate synthetases A and B, encoded for by the genes *nadA* and *nadB* respectively. L-aspartate is oxidised to iminoaspartate by quinolinate synthetase B, which is condensed by quinolinate synthetase A with dihydroxyacetone phosphate to quinolinate. Quinolinate is further converted to nicotinic acid mononucleotide via decarboxylation and phosphoribosylation by the *nadC* gene product, quinolinate phosphoribosyltransferase. The *nadC* mutant strains are not able to carry out this reaction and thus excrete quinolinate into the medium (Baba *et al.*, 2006, Bhatia and Calvo, 1996, Flachmann *et al.*, 1988, Zhou *et al.*, 2011, Dong *et al.*, 2010).

5.2. Construction of the Host Strain

The *nadC* knock-out mutation from the Keio collection Baba *et al.* (2006) was introduced into a host strain used for NanoZap production. This host has a suppressor C mutation (*supC*) to allow lowered production of pVIII from the helper plasmid, which in turn has an amber mutation within *gVIII*. Suppressed amber mutation results in 50% or less of translated product relative to a wild-type. This host strain (K2449) also contains a Δ*metE* mutation that allows incorporation of azidohomoalanine (at ATG codons using met tRNA) into phage and thereby in vivo functionalisation of phage by azides (M. Rajic and J. Rakonjac, unpublished). The *nadC* deletion was introduced into K2449 by P1 transduction, using *E. coli* strain JW0105 (the Keio collection Δ*nadC727::kan* mutant) as a donor, to obtain strain K2485. The complete *nadC* coding sequence in JW0105 (Baba *et al.*, 2006) is replaced by the Kn^R marker flanked by FRT sequences, the recognition site for FLP recombinase. The FRT sites have permitted removal of the Kn^R marker from the genome by transient expression of the FLP recombinase. The Kn^R marker was removed from the transductants after transformation of an FLP-expressing plasmid, followed by identification of Kn^S recombinants and removal of FLP-expressing plasmid, as described in Material and Methods section (2.2.6). The resulting strain was named K2487. Kanamycin marker was also removed from JW0105, to give strain K2515.

Once the required *E. coli* host strains were constructed, several experiments were carried out to establish whether the rich medium (2×YT) would allow growth of the Δ*nadC727* mutants. It was quickly established that the usual media 2×YT would not be suitable for use, as the *E. coli* K2515 cells were capable of growth on the media and are not suitable for auxotrophic selection required for transformation and maintenance of a NadC-expressing plasmid.

Minimal medium M9 containing Glucose and Casamino acids (M9 Glu Cas) was found to be the best candidate for use with the cell lines containing the *nadC* deletion, as they were not capable of growing on this medium without complementing mutation by episomal NadC expression (see below) or supplementation of nicotinic acid (NA) which serves as a substrate for alternative reaction from a scavenger pathway catalysed by nicotinic acid phosphoribosyltransferase (See Appendix I) (PncB; (Joyce *et al.*, 2006).

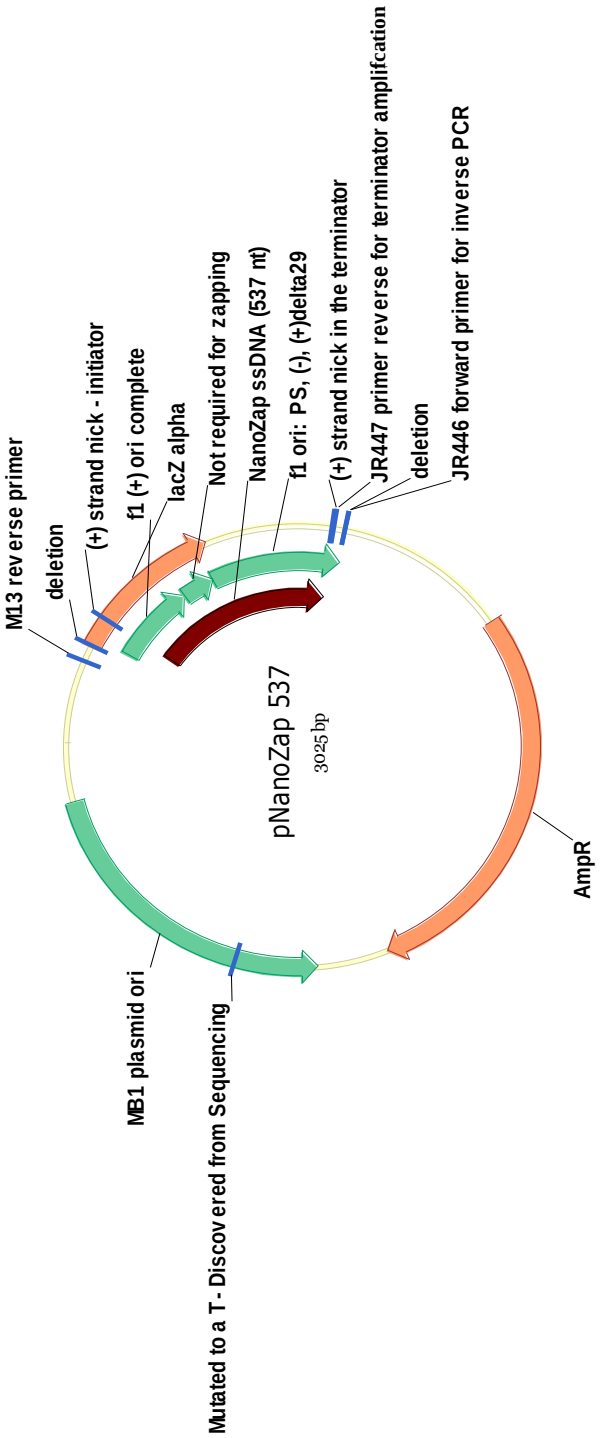

Figure 27: pNanoZap 537 Plasmid Map.

This NanoZap plasmid is a derivative of pNanoZap 719, that has had the complete multiple cloning site (MCS) deleted to decrease the size of the nanoparticles produced. The region of DNA synthesized as circular ssDNA is shown in red.

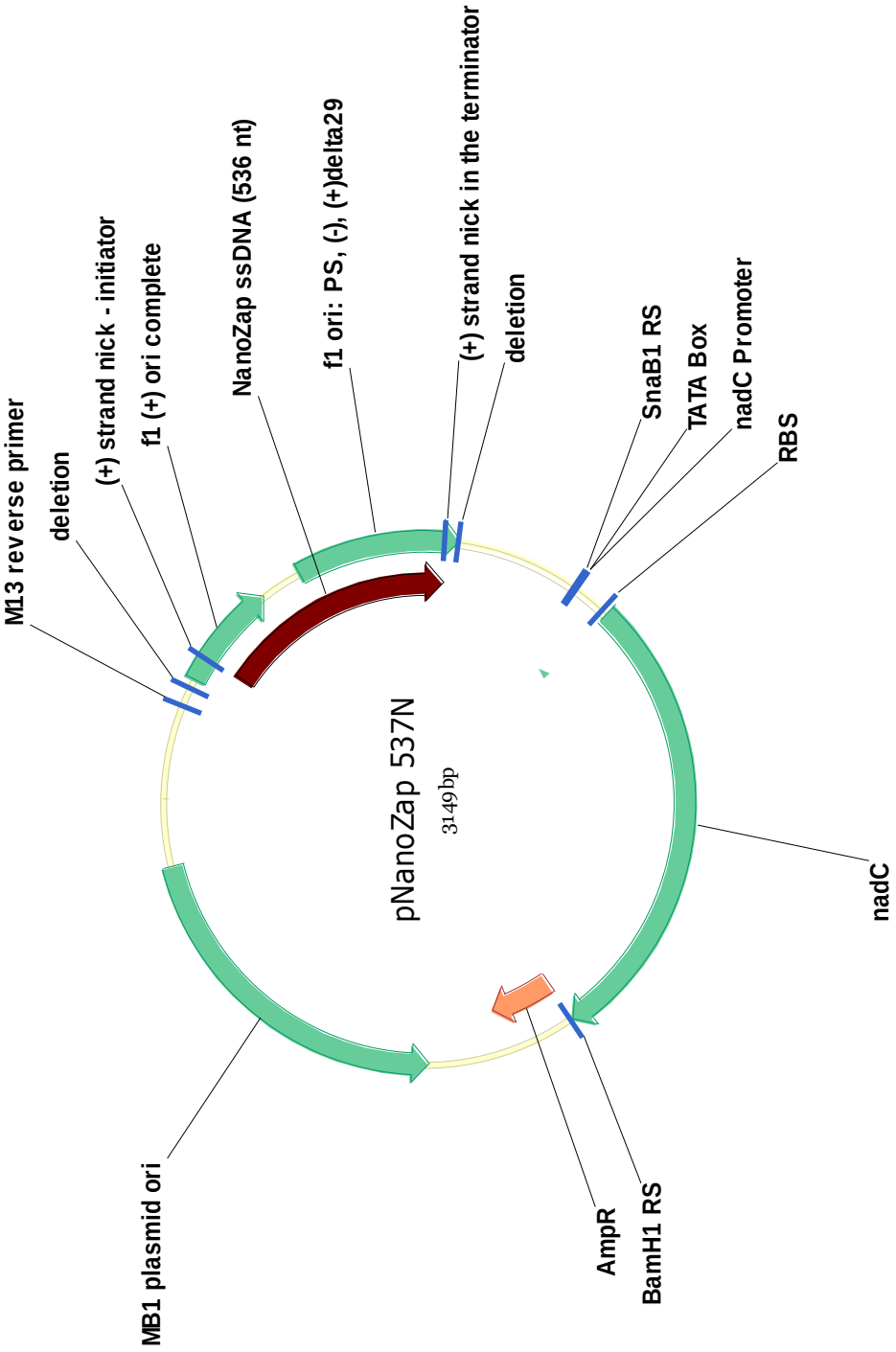

Figure 28: pNanoZap 537N Plasmid Map:

This plasmid map is a derivative of pNanoZap 537 from which the promoter and the coding sequence of the AmpR marker have been deleted (apart from 143 nt at the 5' end) and replaced with the *nadC* gene along with its cognate promoter. The region of DNA synthesized as circular ssDNA is shown in red. LacZalpha is disrupted by the (+) ori and is not expressed in this plasmid.

5.3. Construction of the Auxotrophic-Selection Plasmid pNanoZap - 537N

A modified pNanoZap 537 plasmid was designed, in which the *bla* gene encoding the Amp^R marker and its promoter (apart from a short 5' sequence, approx. 143 nt long) was replaced by the *nadC* gene (including the promoter). The portion of pNanoZap 537 (apart from the *bla* gene) was amplified using pNanoZap 537 (**Figure 27**) as the template and oligonucleotides GD01 and GD02 (Table 4), containing BamHI and SnaBI restriction endonuclease cut-sites, respectively. At the same time the chromosomal gene *nadC* encoding quinolinate phosphoribosyltransferase (Teramoto *et al.*, 2010) was amplified using *E. coli* (K1508) chromosomal DNA as a template and oligonucleotides GD03 and SnaBI restriction sites. After amplification, the PCR products were digested using SnaB1 and BamH1 restriction enzymes, and then ligated together to create a new vector, pNanoZap 537N **(Figure 28)**. The host strain used for cloning was one of the Δ*nadC727* mutants, K2515.

To first check whether the designed insert expresses NadC and can therefore be used for auxotrophic selection, the *nadC* insert was amplified as described above (but prior to the restriction digest) and was then ligated into pCR-Blunt vector (Life Technologies, USA). The ligation reactions were then analysed on an agarose gel (0.8%, pH 8.3, 70 V, 100 min) to confirm the successful ligation. The products of ligation reactions were transformed into the TOP10 cells and Kn^R colonies were selected. Plasmid preparations were done from several colonies to confirm the presence of insert. The confirmed correct recombinant plasmid pCR-Blunt::*nadC* was then transformed into K2515, and plated onto minimal media (BD agar 1.5%; M9 Salts 1×, $MgSO_4$ 2 mM; glucose 0.4%; $CaCl_2$ 0.1 mM) supplemented with casamino acids (2 g/L), after the cells were washed with minimal media (same recipe as above, *sans* BD agar 1.5%), to remove all nutrients from their hour-long incubation in SOC (tryptone 2%; yeast extract 0.5%; NaCl 10 mM; KCl 2.5 mM; $MgCl_2$ 10 mM; $MgSO_4$ 10 mM; glucose 20 mM).

Transformants were obtained on the selective medium at an efficiency of 2.5×10^9 cfu/µg; no colonies were obtained from a control in which no DNA was added to competent cells. To ascertain that the colonies on the M9 Glu Cas plate contained the pCR::*nadC* plasmid, a colony was selected, and plasmid DNA was purified. Due to the fact that the cells were transformed with already confirmed recombinant plasmid, it was reasonable to assume that all cells able to grow on the media contained the same recombinant plasmid. Restriction analysis and sequencing has confirmed the identity of the pNanoZap NadC plasmid.

Instead of using the PCR product, this plasmid (pCR Blunt::nadC) was used as a source of the *nadC* insert. After digestion of plasmid DNA overnight with BamH1 and SnaB1 at 37^{o}C, a preparative gel was run. The band corresponding to the *nadC* gene insert was cut out from the gel and then recovered. The recovered *nadC* gene was then ligated into the amplified pNanoZap vector cut with BamHI and SnaBI, and the ligation was transformed into strain K2515, washed in the M9 Glu Cas medium, and plated on the M9 Glu Cas plates. Multiple colonies were isolated and analysed by restriction digests and sequencing, thus confirming construction of the pNanoZap NadC plasmid.

5.4. Production and Purification of the Nanoparticles from pNanoZap 537N

The next step was to check whether the newly constructed pNanoZap 537N plasmid can produce NanoZap particles.

NanoZap particles were produced by transforming *nadC supD* strain (K2487) carrying the helper plasmid pRNano3 with the newly constructed pNanoZap NadC plasmid. The simplest method to concentrate NanoZap particles is precipitation with 15% PEG in 0.5 M NaCl, as outlined in Materials and Methods (Section 3.1.7). However, during the centrifugation step, an unexpected problem occurred. Massive crystals were forming in the solution during the centrifugation step, taking up about 1/3rd volume of the liquid. This

has prevented concentration of the NanoZap particles from the rest of the solution.

It was hypothesised that the reason for the crystalline structures formation was the phosphates found in M9 salts – a major part of the formula (200 g/L) for the minimal media that this work uses – were reacting in solution with either the PEG itself, or with the sodium chloride added directly afterwards. To test this hypothesis, a low (1/10) phosphate version of M9 salts and a no phosphate version of M9 salts were made and used as bases for two new batches of minimal media (M9 Glu Cas). In total, nine batches of minimal media were created and tested for crystallization. Each of the three different types of minimal media (full phosphate M9 salts, 1/10 phosphate M9 salts, and finally no phosphate M9 salts) were subjected to PEG (15%), sodium chloride (0.5 M), or both PEG (15%) and sodium chloride (0.5 M). These were dissolved at 4^{o}C, and then left for two hours before centrifugation.

The full phosphate minimal media (M9 Glu Cas) did not form crystals with the sodium chloride (0.5 M), but a small amount of crystallization was seen in the solution that contained 15% PEG. Crystals were also seen in the full minimal media (M9 Glu Cas) that contained both PEG (15%) and sodium chloride (0.5 M). The amount of crystals formed, however, was very small, in contrast to the major crystal formation observed during the nanorod production experiment. The 1/10 phosphate M9 salts and no phosphate M9 salts formed no crystals with the 15% PEG or the 0.5 M sodium chloride, separately or in conjunction. Given the low crystal amount in the M9 Glu Cas media to which PEG (15%) was added, the hypothesis that the phosphates in the M9 salts solution precipitate with PEG (15%) was discounted. Instead, it was concluded that the NanoZap particles or other soluble cellular material from the supernatant nucleate the crystals.

The next step taken was to see if using a lower phosphate version of M9 salts for the basis of the minimal media (M9 Glu Cas) was possible. This was undertaken by making overnight cultures of the K2515 strain (containing the *nadC* deletion, from which the KnR marker was removed) and checking the OD of the cells.

Both the 1/10 phosphate version of M9 salts and no phosphate version of M9 salts were tested in this manner, along with a negative control of each type of media. Due to the nature of the minimal media (i.e. that the K2487 cells containing the *nadC* deletion are not supposed to be able to grow on this minimal media), the media was supplemented with nicotinic acid (NA) (10 µg/mL). A control of K2487 cells with NA, in full phosphate minimal media was also set, along with a negative control for this tube.

No growth of K2515 cells was observed in either the minimal media supplemented with NA (10 µg/mL), based upon the no phosphate version of M9 salts, with an OD_{600} = 0.002, or in the 1/10 phosphate version of minimal media, with an OD_{600} = 0.004. These were compared to all three of the negative controls with no K2487 cells added, all of which had OD_{600} = 0.002 after incubation overnight, and the full phosphate version of M9 Glu Cas with NA (10 µg/mL) and K2515 cells, which had an OD_{600} = 2.6.

As it had now been established that using the full phosphate version of M9 salts based minimal media (M9 Glu Cas) would likely cause crystallization problems, thus not allowing access to any NanoZap particles produced, and using a lower phosphate version of M9 salts would result in no production of the NanoZap particles due to the host strain being unable to grow, it was decided that these particles should be concentrated using a method that does not involve PEG precipitation.

5.4.1. Ultrafiltration

Due to the reaction between the full phosphate M9 salts based minimal media (M9 Glu Cas) and the PEG (15%), it was decided to replace the PEG precipitation with an ultrafiltration step. Ultrafiltration using spin-filters was used to concentrate purified NanoZap particles after the CsCl gradient centrifugation (as described in Material and Methods), hence this method in its upscaled form should be successful in concentrating the NanoZap particles. Given the relatively large volume of the supernatant that needs to be subjected

to ultrafiltration (500 mL), a large-volume pressure chamber, rather than spin-filters, have been used in this experiment.

The ultrafiltration was first performed using K1030 cells, transformed with helper plasmid pRNano3 and pNanoZap 537 produced in the 2×YT media, as a control. This combination of plasmids and media have been used routinely to produce NanoZap particles in the laboratory, whereas the actual production of the NanoZap particles with the new pNanoZap 537N and in the M9 Glu Cas medium has never been tested for NanoZap particle production. The second experiment was performed using strain K2487, transformed with helper plasmid pRNano3 and pNanoZap 537N in the M9 Glu Cas medium.

Cells were transformed with their respective plasmids and incubated overnight as described in Material and Methods (Section 2.1.1). The Amicon 400 mL Stirred Cell apparatus was set up in the 4^{o}C cold room. Cells were pelleted by centrifugation (8000 × g, 45 mins, 4^{o}C), and the supernatant was then put through the pressurised filtration system to concentrate the NanoZap particles. Nitrogen gas was applied directly to the stirred cell apparatus, creating a pressure seal and forcing the supernatant through the filter membrane (300,000 MWCO/pore size). It was expected that the NanoZap particles, whose molecular weight is 1,720,000 Da, will be in the retentate and accumulated on the surface of membrane. Solutes larger than the membrane's molecular weight cut off (MWCO), also known as the membrane filters pore size, are expected to be retained, while any water and solutes smaller than the MWCO/pore size pass straight through the membrane into the filtrate. Filtrate was collected into a sterile beaker, to check whether the MWCO/pore size of the filter membrane was correct. If NanoZap particles were discovered in the filtrate, then it would be likely that the filter membrane chosen had too large of a pore size and a filter membrane with a smaller MWCO/pore size would be chosen for future experiments.

The filter membrane was removed from the Amicon 400 apparatus and the NanoZap particles were re-suspended in 2 mL of 1 × TBS (pH 7.1). This 2 mL of 1 × TBS (pH 7.1) also contained the retentate from the filtration step. After

treatment with DNAse and RNAse (10×), a second PEG (15%) precipitation was performed on the resuspension, to precipitate any NanoZap particles out of solution. The final resuspension was then run on a 0.8% native electrophoresis agarose gel (80 V/60 mins) to ascertain whether NanoZap particles were present in the resuspended membrane solution. Alongside this, the filtrate from the Amicon 400 mL Stirred Cell apparatus was run on the agarose gel (after it had also undergone a RNAse/DNAse (10×) and a 15% PEG precipitation step) to check that no NanoZap particles had passed through the 300,000 MWCO/pore size filter membrane (**Figure 29**).

Alongside this, culture supernatant that had not been filtered through the Amicon 400 mL Stirred Cell apparatus from the nutrient-rich 2×YT media was run on the agarose gel to check whether nanoparticles had been produced at all (**Figure 29**). The culture supernatant from the M9 Glu Cas media could not be PEG precipitated due to crystal formation, and therefore was not run on the agarose gel. This raises doubt about whether nanoparticles were produced by K2487, transformed with helper plasmid pRNano3 and pNanoZap 537N in the M9 Glu Cas medium.

Only one band was visible on the native agarose gel (0.8%/70 V/60 mins) after treatment with 0.2 M NaOH (45 mins), MQ water (10 mins), 0.45 M Tris (pH 7.1) (45 mins) and ethidium bromide (1 µg/mL) (20 mins) (**Figure 29**), in any of the lanes. The only band seen was from the culture supernatant of the positive control (K1030 strain transformed with helper plasmid pRNano3 and pNanoZap 537, a known NanoZap particle producing combination), thus allowing the conclusion that the nanoparticles are becoming physically stuck onto the filter membrane.

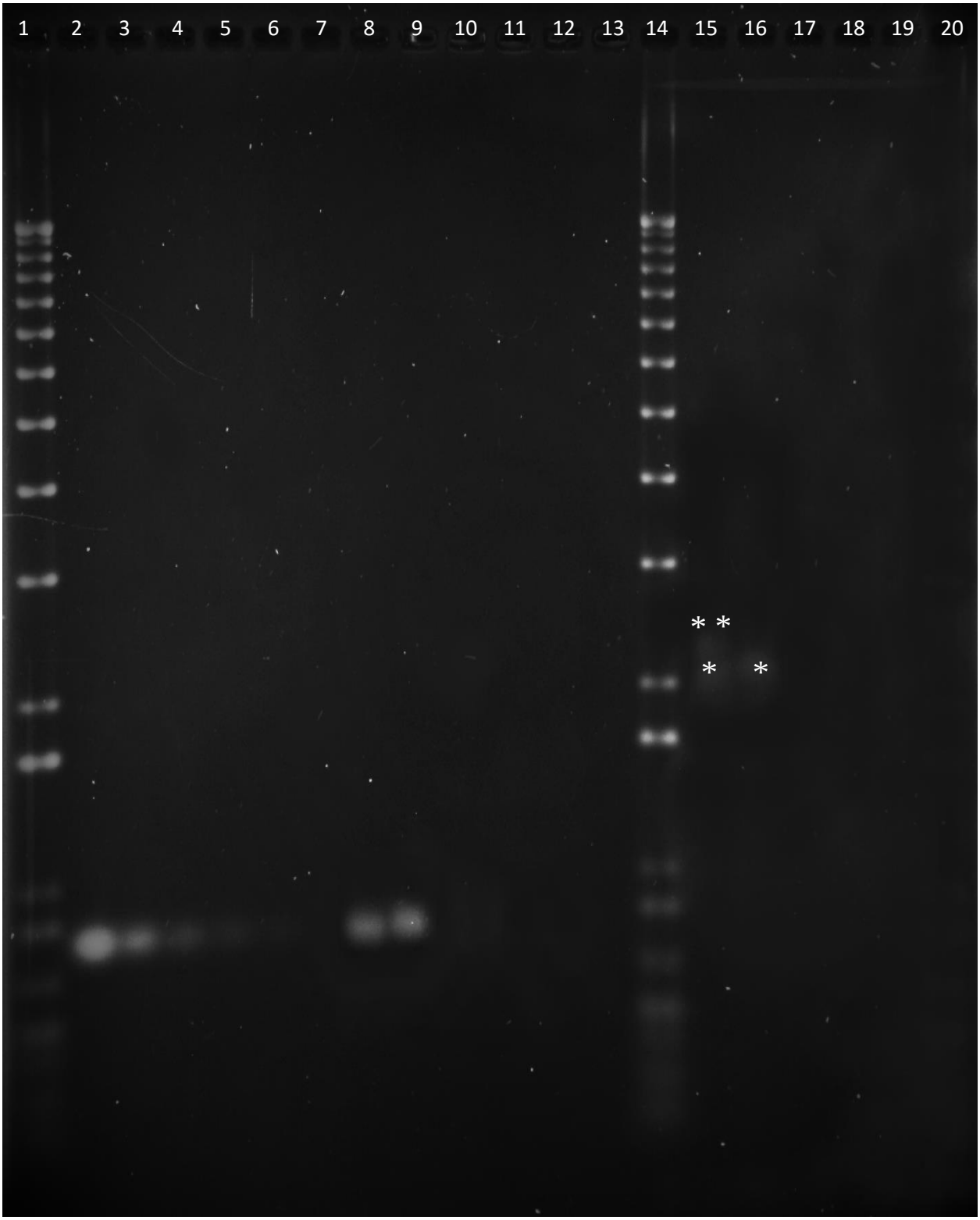
1 2 3 4 5 6 7 8 9 10 11 12 13 14 15 16 17 18 19 20
* *
* *

Figure 29: Native and disassembled agarose gel of NanoZap particles 719, 537 and 537N

1 kb+ ladder is shown in Lane 1 and 14. Lane 2, 3, 4, 5 and 6 contain the NanoZap 736 purified ssDNA of known amounts (2-fold serial dilutions, starting with 40 ng/µL (Lane 1) per lane); Lane 8 – 13 contain heat- and SDS-disassembled particles (Lane 8 contains NanoZap 719 particles, Lane 9 contains PEG precipitated NanoZap 537 particles from the culture supernatant, Lane 10 contains resuspended NanoZap 537 particles from the ultrafiltration membrane, Lane 11 contains the filtrate from the NanoZap 537 ultrafiltration experiment, and Lane 12 contains resuspended NanoZap 537N particles from the ultrafiltration membrane and 13 contains the filtrate from the NanoZap 537N ultrafiltration experiment); Lane 15 – 20 contains contain intact particles loaded onto the gel with 1× loading dye. They were visualised after soaking of the gel in a NaOH solution to strip the virion proteins in situ, followed by EtBr staining of exposed DNA. Lane 15 contains NanoZap 719 particles, Lane 16 contains PEG precipitated NanoZap 537 particles from the culture supernatant, Lane 17 contains resuspended NanoZap 537 particles from the ultrafiltration membrane, Lane 18 contains the filtrate from the NanoZap 537 ultrafiltration experiment, and Lane 19 contains resuspended NanoZap 537N particles from the ultrafiltration membrane and 20 contains the filtrate from the NanoZap 537N ultrafiltration experiment).

All the samples run on this gel were either purified with a PEG precipitation, or ultrafiltration, followed by treatment with DNase and RNase and a final PEG precipitation.

Asterisks denote the different particle lengths. One white asterisk denotes a single length particle, while two white asterisks denotes a double-length particle.

5.5. Discussion and Summary

In this thesis a novel vector for production of short Ff-derived nanorods has been constructed. This strategy was undertaken because the particles derived from the original pNanoZap series contained full plasmid (containing ampicillin resistance marker) at a frequency of $1/10^6$ (S. Khanum and J. Rakonjac, unpublished). To overcome this issue, a nanorod-producing vector in which the ampicillin-resistance marker was replaced with an auxotrophic marker was constructed in this thesis to eliminate antibiotic resistant particles. The constructed vector pNanoZap 537N contains the chromosomal gene *nadC*, encoding an enzyme in the NAD biosynthesis. It is used in combination with a Δ*nadC* host strain, which is auxotrophic for NAD.

Once the auxotrophic marker set had been proven to work through multiple replica plating experiments, this work proceeded to start a set of experiments to prove that the newly created pNanoZap 537N phage producing vector in conjunction with the helper phage pRNano3 plasmid can produce NanoZap particles. However, when the usual method of purifying the NanoZap particles was used, a problem was encountered. As the new plasmid pNanoZap 537N uses the auxotrophic marker *nadC*, the M9 minimal medium was required. The problem that was encountered during the normal PEG (15%) precipitation to purify the NanoZap particles was that the phosphates in the M9 salts based minimal media were reacting with the high concentration of PEG (15%) used to purify the NanoZap particles, forming crystals and thus trapping the NanoZap particles in crystalline structures. As such, a different method was required to purify the NanoZap particles.

The method chosen was one performed by Rakonjac and Model (1998), with an ultrafiltration step replacing the first high PEG (15%) concentration. The "standard" NanoZap production plasmid (pNanoZap537) was used, to be able to work out the concentration method on a system that has been tested for particle production. An Amicon 400 mL Stirred Cell apparatus was used for the ultrafiltration step, in conjunction with a 300,000 MWCO/pore size membrane

filter. In the control experiment with the routinely used NanoZap 537 vector in 2xYT medium, the particles were isolated only in the half of the sample that was concentrated by PEG precipitation; but not in the samples extracted from the membrane **(Figure 29)**. No particles were detected in the flow-through nor in the sample extracted from the ultrafiltration membrane by overnight incubation with the 1 × TBS buffer.

Chapter VI

6. Discussion

6.1. Introduction

The research presented in this thesis was carried out with several specific aims in mind: to construct and investigate the double-display *Escherichia coli*-filamentous bacteriophage particles for use in diagnostic assays; to create a reliable method of creating NanoZap particles of a single-unit length; to create a new template plasmid, pNanoZap NadC, where the antibiotic marker is replaced by an auxotrophic marker, to avoid the low –frequency packaging of antibiotic resistant gene into the particle, thus avoiding the horizontal transfer of antibiotic resistance among *E. coli* in the human GIT or outside of the laboratory containment. This project will discuss each of these aims in separate sections: double-display particle system for diagnostic applications; the remediation of the particle length heterogenicity of the biological nanorods derived from the f1 phage; and removing antibiotic resistance marker from the pNanoZap plasmids.

6.2. Building a Double-Display Particle System

To start building the double-display system, the plasmid pTinselPurple (Table 2) was transformed successfully into *E. coli* lab strain K2245. Since the pTinselPurple plasmid promoter (T5/*lac*) is IPTG induced, an experiment was conducted to discover the optimum amount of IPTG for inducing protein expression without over-loading of the cell. Between the two concentrations of IPTG tested (0.1 mM and 1 mM), 0.1 mM was shown to be the optimum concentration, with protein expression without cells becoming toxic (**Figure 10C**); while IPTG concentration of 1 mM had caused cell death due to the over-expression of the pTinselPurple protein (**Figure 10D**). The IPTG free control plate also showed purple protein expressing colonies (**Figure 10B**); which strongly indicates that the T5/*lac* promoter was leaky in the 2xYT medium. The next stage was to make stocks of f1d3 bacteriophage for ease of use. The f1d3 bacteriophage was grown on

both TG1 and K1976 (Table 1) along with f1 wild-type bacteriophage (Table 3), for both comparison and purity. Bacteriophage titrations were carried out as explained in Materials and Methods. The next step was to infect *E. coli* with the f1d3 bacteriophage stock to allow the permanent display of bacteriophage on the surface of *E. coli*.

However, when the f1d3 stock of bacteriophage was added to the functionalised *E. coli*, the chromogenic protein was lost (**Figure 11-12**). This could have occurred for several reasons, with the most likely being that the chromogenic protein was degraded by cell machinery activated by the infection of the f1d3 bacteriophage. Since the chromogenic protein was lost, there was no visual way to detect *E. coli* cells. This presents a unique problem: how to visualise bacteriophage binding to the antibodies if the infected strain will not produce visible colour. Since our transformed strain K2379 lost the chromogenic protein in f1d3-infected cells, these particles will be of no use for visible colourimetric detection assays.

As such, another method of creating coloured *E. coli* was attempted. K91 was used in conjunction with IPTG and X-gal. LacZ (beta lactamase) induced by IPTG hydrolyses X-gal galactose and 5-bromo-4-chloro-3-hydroxyindole. This product further dimerizes and is oxidized into 5,5'-dibromo-4,4'-dichloro-indigo, an intensely blue product which is insoluble. During this experiment the *E. coli* cells scraped from the plates remained blue, however, over time the colour steadily faded (**Figure 12**). This is likely due to the cells releasing 5,5'-dibromo-4,4'-dichloro-indigo. No blue colour was detected on the nitrocellulose membrane containing anti-Ff antibodies (**Figure 13**).

We know that the cells remained blue in solution (through both re-suspension and centrifugation) (**Figure 12-13**), and that they were infected with the f1d3 bacteriophage (due to plating and looking at the infected cells), and as such, there are several potential reasons as to why there appeared to be a negative result: the test was actually positive, but the blue colour was simply too weak to be noticeable; the test was actually positive, but due to the bulk of the infected *E. coli* cells (detector particles) not enough were able to bind to such a small area of antibody to create a visible blue effect; or the test was negative due to the antibody drops having lost sensitivity. The antibody drops theory can currently be dismissed however, as further testing of their sensitivity has shown that

the antibody drops used in these experiments work as expected, and that they have not expired.

In conclusion, the production of chromogenic cells that are also infected with f1d3 bacteriophage is an interesting challenge. Currently, infection of *E coli* cells seem to be the causative agent for the loss of pTinselPurple chromogenic protein expression. This however, could be further investigated through qPCR and Western blot, to see if there truly is a complete loss of mRNA and protein expression, or a mutation that renders the protein colourless. Hydrolysis of X-gal is not affected by f1d3 infection; however, the coloured hydrolysis product of X-gal is released from the cells, resulting in fading. This will need to be circumvented to allow future use of this colouration methodology.

6.3. Remediation of the Particle Length Heterogeneity of Biological Nanorods Produced by f1 Phage

The aim of these experiments was to see whether the alterations made to the NanoZap system would result in single-length NanoZap particles. pNanoZap 719 had approximately 18 nucleotides deleted from the multiple cloning site (MCS) that is located between the initiator and terminator of the Ff replicon. These 18 nucleotides were palindromic sequences corresponding to restriction sites in the MCS. According to the native agarose gel electrophoresis this plasmid permitted assembly of mostly single-length particles. In contrast, electron microscopy indicated a higher proportion of the double-length particles, with the peaks of the histogram at 90 nm and 190 nm (**Figure 25A**).

pNanoZap SNgII was altered from the original pNanoZap 736 design to include coding sequences for the minor proteins pVII and pIX and the *gII* promoter (from which they are normally transcribed). It was possible to do this and retain the short size of the zapped replicon because the two proteins are very small (32 and 33 amino acids, respectively) and they are located next to each other and in the same operon in the f1 phage genome (Endemann and Model, 1995, Rakonjac *et al.*, 2011, Rakonjac and Model, 1998, Sattar, 2013). Agarose gel electrophoresis of the native particles showed a

strong double-length band. This agreed with the length measurements based on the TEMs, where most particles were 110 nm or 200 nm in length (**Figure 25B**).

pNanoZap SN*lac* was similar to pNanoZap SNgII, apart from having the *lac* promoter controlling the expression of *gVII* and *gIX*. Two different batches of NanoZap SN*lac* particles were produced and purified, one with induction of the *gVII* and *gIX* expression by IPTG, and the other that was uninduced. Both batches samples contained high proportion of double-length particles according to the native virion agarose gel electrophoresis. The induced NanoZap SN*lac* also contained a population of triple-length particles and a faint band of quadruple-length particles. TEM analysis and particle length measurements showed that the NanoZap SN*lac* particles produced from uninduced and induced cultures both fell into two lengths, of approximately 110 - 190 nm and 100 – approximately 200 nm (as the peak ranges from 190 – 210 nm) (**Figure 25C - D**).

The size distribution comparison histogram (**Figure 25E**) showed the percentages of each type of nanorod produced by the differing pNanoZap plasmids. 70.5% of the nanorods produced by pNanoZap 719 were single-length particles (monomers), with 23.3% of the nanorods produced being dimers, and only 2.1% of the nanorods being trimers. This is a significant result, with 70.5% of nanorods produced being monomers, however, the nanorods produced by SNgII were 80.2% monomers, which is a significant increase in monomers produced, and a step towards achieving the end goal of monomers being more than 90% of nanorods produced. pNanoZap SNgII also produced 14.6% dimers and 3.1% trimers, thus making it the most effective pNanoZap plasmid at producing single-length nanorods; however, in this analysis, a monomer is a particle that falls within a length range of 80 nm to 129 nm. As a result, while producing single-length particles, these single-length particles still range in length, rather than being uniform in length.

pNanoZap SN*lac* (both IPTG uninduced and induced) produced lower amounts of single-length particles, and higher amounts of dimers and trimers were seen in both samples. IPTG uninduced SN*lac* produced nanorods were 60% monomers, 30.8% dimers and 6.2% trimers, while IPTG induced SN*lac* produced nanorods were 57.7%

monomers, 30.6% dimers and 5.4% trimers; making the pNanoZap SN*lac* plasmid the most effective at producing multiple-length particles (**Figure 25E**).

In contrast to electron micrographs, the native agarose electrophoresis showed notable differences in the amount of longer-than-single-length particles among the four analysed samples (**Figure 20;** lanes labelled "Native"). The NanoZap 719 particles were mostly single-length, with a minor portion of double-length particles, whereas the samples expressing pVII and pIX from the zapped replicon had equal or larger proportion of double-length particles. These bands were not quantified due to difference in the total loading. This electrophoresis should be repeated by loading exact same amount of particles and the amount of particles in each band should be quantified and their ratios compared. This analysis would quantify the amounts of each type of particles in each of the samples.

Discrepancy between the native particle agarose gel electrophoresis and microscopy probably stems from the fact that the f1 phage tend to adhere to each other along the length of the particle in the presence of salts, including the negative stain, Uranyl acetate. Strings of two or more particles are not easy to distinguish from single particle that is longer than unit-length by simple observation, giving rise to a range of measured lengths in TEM. Furthermore, if a particle is at an angle relative to the microscopic grid plane, the observed length will be shorter than the actual length.

The high proportion of double-length particles obtained from the *gVII*- and *gIX*-expressing templates (pNanoZap SNgII and pNanoZap SN*lac*) rule out that the increase in the ratio of pVII + pIX to pVIII and expression of these two minor proteins in the vicinity of the NanoZap replicon is responsible for the multiple-length particle production.

Interestingly, the total amount of particles is increased by expression of pVII and pIX from the zapped replicon. pNanoZap SNgII and the IPTG uninduced batch of pNanoZap SN*lac* contained progressively higher amounts of NanoZap particles in comparison to the NanoZap 719, which does not express the two minor proteins from the zapped replicon (NanoZap 719: 2.6×10^{14} particles per mL; NanoZap SNgII: 4.3×10^{14} particles per mL; NanoZap SN*lac* uninduced: 6.8×10^{14} particles per mL and $1.5 \times$

10^{15} particles per mL for the induced sample), A notable result is the a two-fold higher amount of particles by induction of pVII and pIX expression from the lac promoter.

In summary, the pNanoZap 719 plasmid produced the largest proportion of the single-length particles among the four tested constructs, according to the agarose gel electrophoresis, whereas SNgII produced the most monomers, according to the size distribution histogram; induction of pVII and pIX production from the zapped replicon NanoZap SN*lac* increased production of nanorods by a factor of 5.6, relative to the pNanoZap 719 that does not express pVII and pIX.

6.4. Removing Antibiotic Resistance Marker from the pNanoZap Plasmids

In this thesis a novel vector for production of short Ff-derived nanorods has been constructed. This strategy was undertaken because the particles derived from the original pNanoZap series contained full plasmid (containing ampicillin resistance marker) at a frequency of $1/10^6$ (S. Khanum and J. Rakonjac, unpublished). Projected medical and home diagnostic applications are incompatible with the presence of particles containing antibiotic resistance markers, because they will spread antibiotic resistance genes in both patients and the environment.

To overcome this issue, a nanorod-producing vector in which the ampicillin-resistance marker was replaced with an auxotrophic marker was constructed in this thesis to eliminate antibiotic resistant particles. The constructed vector pNanoZap 537N contains the chromosomal gene *nadC*, encoding an enzyme in the NAD biosynthesis pathway. It is used in combination with a Δ*nadC* host strain, which is auxotrophic for NAD.

Once the auxotrophic marker set had been proven to work through multiple replica plating experiments, this work proceeded to start a set of experiments to prove that the newly created pNanoZap 537N phage producing vector in conjunction with the helper phage pRNano3 plasmid can produce NanoZap particles. This was done in parallel with pNanoZap 537 vector, in conjunction with the helper phage pRNano3 plasmid, which is

a combination of plasmids that are known to produce the NanoZap particles (see Chapter IV).

However, when the usual method of purifying the NanoZap particles was used, a problem was encountered. As the new plasmid pNanoZap 537N uses the auxotrophic marker *nadC*, the M9 minimal medium was required. The *nadC* gene was deleted from the K2515 strain, and when the pNanoZap 537N plasmid containing the *nadC* gene was transformed into the strain, this allowed normal growth. As such, a medium was needed that did not allow the cells containing the deletion to grow without the plasmid. This medium was determined to be the M9 minimal medium; as the usual nutrient rich 2xYT medium did not allow the auxotrophic selection.

The problem that was encountered during the normal PEG (15%) precipitation step to purify the NanoZap particles was that the phosphates in the M9 salts based minimal media were reacting with the high concentration of PEG (15%) used to purify the NanoZap particles, forming crystals and thus trapping the NanoZap particles in crystalline structures. As such, a different method was required to purify the NanoZap particles.

The method chosen was one performed by Rakonjac and Model (1998), with an ultrafiltration step replacing the first high PEG (15%) concentration. The "standard" NanoZap production plasmid (pNanoZap 537) was used, to be able to work out the concentration method on a system that has been tested for particle production. An Amicon 400 mL Stirred Cell apparatus was used for the ultrafiltration step, in conjunction with a 300,000 MWCO/pore size membrane filter. In the control experiment with the routinely used NanoZap 537 vector in 2xYT medium, the particles were isolated only in the half of the sample that was concentrated by PEG precipitation; but not in the samples extracted from the membrane (**Figure 29**). No particles were detected in the flow-through nor in the sample extracted from the ultrafiltration membrane by overnight incubation with 1 × TBS buffer. It can therefore be concluded that all nanorods were tightly bound to the membrane and could not be extracted by incubation with the TBS buffer. For the novel vector, only the ultrafiltration samples were available. Because the "standard" particles were lost when ultrafiltration was used, it is not possible to deduce whether particles were produced from this new vector.

Chapter VII

7. Future Directions and Conclusions

7.1. Building a Double-Display Particle System

7.1.1. Colour-tagging *E. coli*

The next step for this series of experiments is to repeat the dot blot/visibility assay, once again using the IPTG and X-gal colouration methodology to obtain chromogenic proteins for the visual detection of the Ff bacteriophage infected cells binding to the antibody drops. However, for this experiment, the *E. coli* proteins will be crosslinked with the insoluble chromogenic substrate using a method that will form covalent links between the chromogenic substrate and *E. coli* proteins as soon as colour is produced, to prevent the chromogenic molecules from being lost from the cell. This should then allow their use as visible detection particles.

Another potential colour-tagging method that will be attempted is the colouration of the *E. coli* cells using crystal violet or other stains that colour *E. coli*, followed by fixing the cells to cross-link the dye to the cellular proteins and to kill and fix the *E. coli* cells, making them stable during storage and transport. It is likely that this attempt will allow the use of the double display particles as a visible detector.

7.1.2 Double-Display Particles Binding to Antibody Drops

Two possible reasons for the lack of positive results which was mentioned above was the possibility that the coloured molecules were exported out of the cells during the incubation, or that the cells were not binding to the antibody drops. This likelihood can be checked through performing another dot blot/visibility assay, where a second anti-bacteriophage specific antibody and alkaline

phosphatase were used to detect whether the double display particles were bound to the Ff filamentous bacteriophage specific capture antibody immobilised on the nitrocellulose filter.

7.1.3 Functionalising the Ff Bacteriophage

To display a detector molecule on *E. coli*-attached phage, the protein must be fused to either major capsid protein pVIII or minor capsid protein pIX. For pVIII, a test detector/analyte pair of known properties will be used to establish the system. A pVIII fusion of the detector molecule will be constructed in a plasmid phage display vector p8split. The test detector molecule will be FnB (fibronectin binding protein), which binds with high affinity to human fibronectin. A PCR-amplified coding sequence for FnB will be inserted into the multiple cloning site of the vector p8split, in frame with the upstream signal sequence and downstream mature portion of pVIII.

Once the recombinant plasmid is constructed and tested for correct sequence in an appropriate cloning host, it will be transformed into the *E. coli* cells that can be coloured by a method compatible with f1d3 infection. Display of the FnBP-pVIII fusion will first be tested by infecting the cells containing the recombinant plasmid with a wild-type Ff phage. The assembled particles will be analysed for FnB display by ELISA assay, to determine whether they bind to the cognate ligand, human fibronectin, which in turn will demonstrate display of FnB. Phage binding to immobilised Fn will be assessed using a phage-specific antibody that recognises the major phage protein pVIII encoded by the wild-type phage. Quantitative, direct and competitive assays will be carried out to determine the sensitivity of the particles.

Once display of FnBP on the phage is confirmed, *E. coli* cells will be transformed with the pFnB-8 plasmid. In order to display FnB in the double-display system, these cells will be infected with f1d3, resulting in cells decorated with hundreds of long phage filaments, otherwise known as “hairy *E. coli*” (**Figure 3**) (Rakonjac *et al.*, 2011).

Double-displaying *E. coli* is a non-pathogenic laboratory strain; however, it is also a genetically modified organism, and cannot be released into the environment. To use these *E. coli* cells as detection particles, they will have to be killed without modifying the contact residues on the detector molecule that interact with the analyte. It is expected that this step will require optimisation in the terms of the type of crosslinker and reaction conditions. For example, the fixative glutaraldehyde, which is a common sterilization tool could be used to allow the dipstick test to be used without releasing live organisms into the environment. It is also likely that the cells will need to be fixed as a part of the colour-tagging methodology, to allow the visibility of the double-display particles for detection.

The double-displaying *E. coli* will be examined by optical and transmission electron microscopy to establish whether the staining was successful and whether the fixing has changed the morphology of particles; the samples will also be plated to ascertain that no living cells remain. Binding of the particles to fibronectin will be examined initially by ELISA assays as described above, except that the detection will be carried out directly at the wavelength of maximal absorption of the chromogenic tinsel purple protein.

Display of pVIII fusion will result in multiple copies of the detector molecules (FnB) per phage; however, they will be displayed along the filaments, with displayed FnB emanating from the shaft of the filaments. Each Fn has two FnB binding sites, potentially causing cross-linking of filaments, which may obstruct access to the capturing reagent on the dipstick which is required for the formation of a coloured band to monitor the detection of fibronectin. If this kind of interference is observed, the detector molecules will need to be displayed on the distal end (tip) of the filament by fusing the FnB coding sequence to pIX instead. This protein has been used in the past to display single-chain antibodies (scFvs), proving that pIX is suitable for display (Loset and Sandlie, 2012).

A recombinant vector will be constructed which is similar to the p8split vector, apart from having pIX instead of pVIII coding sequence and used to insert the

FnB coding sequence. The experimental approach to produce phage displaying FnB-pIX and double-display *E. coli* will be the same as for pVIII display, except that the phages used in this case will be a double gene IX *gIX/gIII* deletion mutant for double-display on *E. coli*.

7.1.4 Dipstick Assay

Once produced and tested in the ELISA format, the *E. coli* double-display particles will be assayed in a dipstick assay (**Figure 30**; (Sattar *et al.*, 2015)). The test line of the dipstick contains a capture molecule, collagen, which binds to fibronectin with high affinity and also binds at a different epitope to the fibronectin binding protein (FnB) and is therefore suitable for capturing the human fibronectin bound to the detection particles (Sattar *et al.*, 2015).

The control line is printed with a pVIII-specific (anti-bacteriophage) antibody to ensure that the Ff bacteriophage infected colour-tagged *E. coli* cells that did not bind to any fibronectin will be captured by the control line. As bacteriophage will always be present in the diagnostic particles, this will make a good control line. To measure the sensitivity of the assay, the signal in the test line ratio will be quantified from a set of dipstick assays with a series of fibronectin concentrations. The lowest concentration of fibronectin that can be detected by the dipstick assay determines the assay sensitivity (**Figure 30**).

7.1.5 Botulism Toxin Assay

To develop assays to detect food contaminants, the above described methods are carried out, except that instead of fusing FnB as a detector to the major capsid protein pVIII or minor protein pIX, genes encoding linked variable domains of monoclonal antibody (or single-chain antibody, scFv) specific for the analyte will be fused to these phage proteins. The detection test for a potential food contaminant will be for botulinum toxin A (BoT A) of *Clostridium botulinum*. This allows positive detection of *C. botulinum*, as only *C. botulinum* produces toxin A. The test line for this assay will contain a second antibody against BoT

whose epitope does not overlap with the epitope of displayed detector scFv or recombinant receptor protein (SV2c; List Biological Labs, Inc.). The recombinant heavy chain of BoT A (List Biological Labs, Inc) will be used as the analyte for gauging sensitivity of the assay.

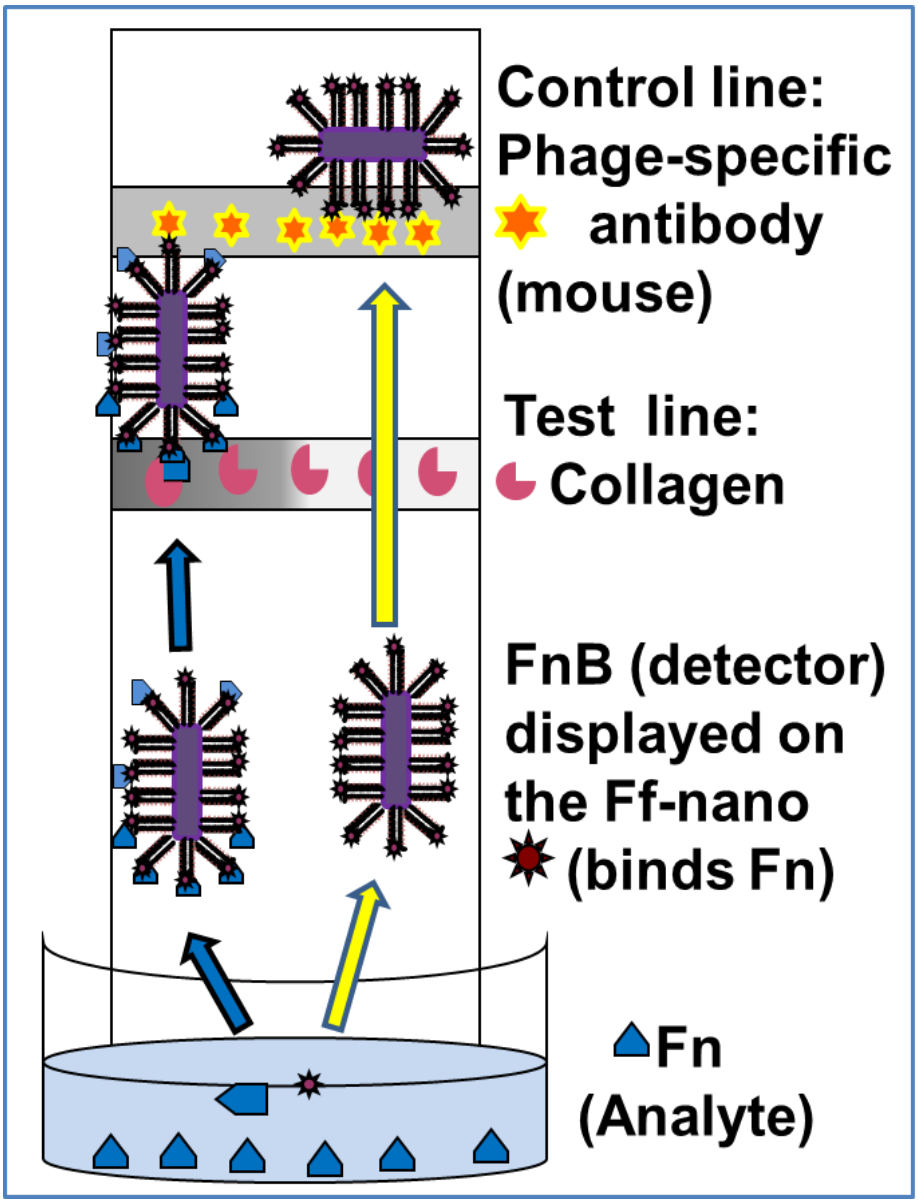

Figure 30: Schematic representation of a lateral-flow dipstick assay using phage.

The fibronectin analyte (Fn), is added to a liquid media, and the double display particles are exposed to it. The functionalised Ff bacteriophage are displaying fibronectin binding repeats (FnB), which act as the detector for the Fn. If the double display particle binds to Fn through FnB, then the double display particle will bind to the collagen test line (as fibronectin has a high affinity for binding to collagen). If the double-display particle does not bind to any fibronectin, then it will not bind to the test line printed with collagen, but will instead bind to the control line, which has been printed with anti-pVIII antibodies. The anti-phage antibodies will capture the Ff bacteriophage, thus causing the control line to be positive in all tests. The dipstick assay will then be read visibly, as the colour-tagged *E. coli* that the Ff bacteriophage are bound to will cause bright purple line/s to form. Adapted from (Sattar *et al.*, 2015).

7.2 Removing Antibiotic Resistance Marker from the pNanoZap Plasmids

7.2.1 Identifying production and purification conditions for antibiotic-resistance-free NanoZap production system

In future work, a range of media will be explored to find a selective medium that will nevertheless enable concentration of phage using PEG.

With respect to the ultrafiltration method of concentration, membranes with smaller molecular weight cut-off will be used, to prevent entry of the nanorods into the porous material. Ultrafiltration used to concentrate the NanoZap particles after CsCl purification and dialysis (Section 2.8.8 and Section 5.5) was carried out using a 50,000 Da cut-off membranes; this same cut-off will be used in the future for the pressure concentration of the nanorods.

In future work, the hypothesis that no NanoZap particles were seen on the native electrophoresis gel needs to be investigated further. 1 × TBS was used to resuspend the NanoZap particles off the filter membrane. The filter membrane was placed into a 50 ml falcon tube, and the TBS was pipetted over the filter membrane while at 4^{o}C. However, due to the amount of pressure used to concentrate the NanoZap particles, it is possible that simply pipetting the TBS solution over the filter membrane was not enough to lift the concentrated NanoZap particles off the membrane.

A more vigorous way of resuspending the NanoZap particles off the filter membrane is therefore required. One possibility is to place the 50 mL falcon tube in a rotating holder and leave it to spin the 1× TBS solution over the filter membrane. Another possibility is increasing the temperature, or pH at which the NanoZap particles are resuspended, as this may help dissociate the NanoZap particles from the filter membrane. Another possibility would be to leave the filter membrane suspended in the 1× TBS solution overnight. All these possibilities would need to be investigated in future work.

7.2.2 Investigation into NanoZap 537N Particles

After the problem of the NanoZap 537N nanoparticles purification from the filter membrane has been solved an investigation into the length of the NanoZap 537N particles will be required, given that the particle length is an important parameter when it comes to useful therapeutic properties, such as diffusion. .

The newly created pNanoZap 537N plasmid is hypothesised to produce the NanoZap 537N particles that are the same length as the NanoZap 537 particles, due to the pNanoZap 537N and pNanoZap 537 plasmids being an exact match in the segment corresponding to the Ff-dependent replicon that is zapped out of the plasmid in the presence of helper plasmid. Indeed, the only difference between the two NanoZap plasmids is that pNanoZap 537 contains an ampicillin resistance gene, while pNanoZap 537N contains the chromosomal gene *nadC* instead.

This difference in the plasmid construction should not cause any differences in structure or length of the produced and purified NanoZap particles, as the distance between the two cut sites (537 base pairs; **Figure 28**) within the two positive origins of replication determines the length of the NanoZap ssDNA genome and therefore the length of the produced particle (Bennett and Rakonjac, 2006, Bisset and Rakonjac, unpublished, Rakonjac *et al.*, 2011, Sattar, 2013); but without further investigation, this has not yet been confirmed experimentally.

The amount of NanoZap 537N particles produced will also need to be investigated. NanoZap 537 particles were produced at a concentration of 1.3×10^{14} particles from 500 ml of culture (S. Khanum, unpublished). This comparison will also give insight into how the use of auxotrophic markers, rather than the use of antibiotic markers affects the amount of the produced NanoZap particles. This will need to be investigated, likely in future work.

8. References

ANANY, H., BROVKO, L., EL DOUGDOUG, N. K., SOHAR, J., FENN, H., ALASIRI, N., JABRANE, T., MANGIN, P., MONSUR ALI, M., KANNAN, B., FILIPE, C. D. M. & GRIFFITHS, M. W. 2018. Print to detect: a rapid and ultrasensitive phage-based dipstick assay for foodborne pathogens. *Anal Bioanal Chem,* 410**,** 1217-1230. Available: DOI 10.1007/s00216-017-0597-y.

BABA, ARA, HASEGAWA, TAKAI, OKUMURA, BABA, DATSENKO, TOMITA, WANNER & MORI 2006. Construction of Escherichia coli K-12 in-frame, single-gene knockout mutants: the Keio collection. *Molecular Systems Biology,* 2**,** 2006.0008-2006.0008. Available: DOI 10.1038/msb4100050.

BALIAN, G., M CLICK, E., CROUCH, E., DAVIDSON, J. & BORNSTEIN, P. 1979. *Isolation of collagen-binding fragment from fibronectin and cold-insoluble globulin*.

BAR, H., YACOBY, I. & BENHAR, I. 2008. Killing cancer cells by targeted drug-carrying phage nanomedicines. *BMC Biotechnology,* 8**,** 1-14. Available: DOI 10.1186/1472-6750-8-37.

BARDHAN, N. M., GHOSH, D. & BELCHER, A. M. 2014. M13 virus based detection of bacterial infections in living hosts. *J Biophotonics,* 7**,** 617-23. Available: DOI 10.1002/jbio.201300010.

BENNETT, N. J. & RAKONJAC, J. 2006. Unlocking of the filamentous bacteriophage virion during infection is mediated by the C domain of pIII. *J Mol Biol,* 356**,** 266-73. Available: DOI 10.1016/j.jmb.2005.11.069.

BERNARD, J. M. L. & FRANCIS, M. B. 2014. Chemical strategies for the covalent modification of filamentous phage. *Frontiers in Microbiology,* 5**,** 7. Available: DOI 10.3389/fmicb.2014.00734.

BHATIA, R. & CALVO, K. C. 1996. The sequencing expression, purification, and steady-state kinetic analysis of quinolinate phosphoribosyl transferase from Escherichia coli. *Arch Biochem Biophys,* 325**,** 270-8. Available: DOI 10.1006/abbi.1996.0034.

BISSET, S. & RAKONJAC, J. unpublished. Producing tuneable nanorods derived from filamentous bacteriophage without helper phage. Palmerston North, New Zealand: Massey University.

BRADBURY, A. R. & MARKS, J. D. 2004. Antibodies from phage antibody libraries. *J Immunol Methods,* 290**,** 29-49. Available: DOI 10.1016/j.jim.2004.04.007.

BRANSTON, S. D., STANLEY, E. C., WARD, J. M. & KESHAVARZ-MOORE, E. 2013. Determination of the survival of bacteriophage M13 from chemical and physical challenges to assist in its sustainable bioprocessing. *Biotechnology and Bioprocess Engineering,* 18**,** 560-566. Available: DOI 10.1007/s12257-012-0776-9.

BRIAND, L., MARCION, G., KRIZNIK, A., HEYDEL, J. M., ARTUR, Y., GARRIDO, C., SEIGNEURIC, R. & NEIERS, F. 2016. A self-inducible heterologous protein expression system in Escherichia coli. *Scientific Reports,* 6**,** 33037. Available: DOI 10.1038/srep33037.

BUHRER, S. S., SMITS, H. L., GUSSENHOVEN, G. C., VAN INGEN, C. W. & KLATSER, P. R. 1998. A simple dipstick assay for the detection of antibodies to phenolic glycolipid-I of Mycobacterium leprae. *Am J Trop Med Hyg,* 58**,** 133-6.

CARRICO, Z. M., FARKAS, M. E., ZHOU, Y., HSIAO, S. C., MARKS, J. D., CHOKHAWALA, H., CLARK, D. S. & FRANCIS, M. B. 2012. N-Terminal labeling of filamentous phage to create cancer marker imaging agents. *ACS Nano,* 6**,** 6675-80. Available: DOI 10.1021/nn301134z.

CHASTEEN, L., AYRISS, J., PAVLIK, P. & BRADBURY, A. R. 2006. Eliminating helper phage from phage display. *Nucleic Acids Res,* 34**,** e145. Available: DOI 10.1093/nar/gkl772.

CHEREPANOV, P. P. & WACKERNAGEL, W. 1995. Gene disruption in Escherichia coli: TcR and KmR cassettes with the option of Flp-catalyzed excision of the antibiotic-resistance determinant. *Gene,* 158**,** 9-14.

CHUNG, W.-J., OH, J.-W., KWAK, K., LEE, B. Y., MEYER, J., WANG, E., HEXEMER, A. & LEE, S.-W. 2011. Biomimetic self-templating supramolecular structures. *Nature,* 478**,** 364. Available: DOI 10.1038/nature10513

https://www.nature.com/articles/nature10513#supplementary-information.

CLICK, E. M. & WEBSTER, R. E. 1998. The TolQRA proteins are required for membrane insertion of the major capsid protein of the filamentous phage f1 during infection. *J Bacteriol,* 180**,** 1723-8.

DANG, X., QI, J., KLUG, M. T., CHEN, P. Y., YUN, D. S., FANG, N. X., HAMMOND, P. T. & BELCHER, A. M. 2013. Tunable localized surface plasmon-enabled broadband light-harvesting enhancement for high-efficiency panchromatic dye-sensitized solar cells. *Nano Lett,* 13**,** 637-42. Available: DOI 10.1021/nl3043823.

DONG, W.-R., XIANG, L.-X. & SHAO, J.-Z. 2010. Novel Antibiotic-Free Plasmid Selection System Based on Complementation of Host Auxotrophy in the NAD De Novo Synthesis Pathway. *Applied and Environmental Microbiology,* 76**,** 2295-2303. Available: DOI 10.1128/AEM.02462-09.

DOTTO, G. P., HORIUCHI, K. & ZINDER, N. D. 1982. Initiation and termination of phage f1 plus-strand synthesis. *Proceedings of the National Academy of Sciences of the United States of America,* 79**,** 7122-7126.

ENDEMANN, H. & MODEL, P. 1995. Location of filamentous phage minor coat proteins in phage and in infected cells. *J Mol Biol,* 250**,** 496-506.

ENGVALL, E. 1978. Preparation of Enzyme-labelled Staphylococcal Protein A and its Use for Detection of Antibodies. *Scandinavian Journal of Immunology,* 8**,** 25-31. Available: DOI doi:10.1111/j.1365-3083.1978.tb03881.x.

FLACHMANN, R., KUNZ, N., SEIFERT, J., GUTLICH, M., WIENTJES, F. J., LAUFER, A. & GASSEN, H. G. 1988. Molecular biology of pyridine nucleotide biosynthesis in Escherichia coli. Cloning and characterization of quinolinate synthesis genes nadA and nadB. *Eur J Biochem,* 175**,** 221-8.

FORRER, P., JUNG, S. & PLUCKTHUN, A. 1999. Beyond binding: using phage display to select for structure, folding and enzymatic activity in proteins. *Curr Opin Struct Biol,* 9**,** 514-20. Available: DOI 10.1016/s0959-440x(99)80073-6.

GAO, C., MAO, S., LO, C. H., WIRSCHING, P., LERNER, R. A. & JANDA, K. D. 1999. Making artificial antibodies: a format for phage display of combinatorial heterodimeric arrays. *Proc Natl Acad Sci U S A,* 96**,** 6025-30.

GHOSH, D., LEE, Y., THOMAS, S., KOHLI, A. G., YUN, D. S., BELCHER, A. M. & KELLY, K. A. 2012. M13-templated magnetic nanoparticles for targeted in vivo imaging of prostate cancer. *Nat Nanotechnol,* 7**,** 677-82. Available: DOI 10.1038/nnano.2012.146

nnano.2012.146 [pii].

GRAY, C. W., BROWN, R. S. & MARVIN, D. A. 1981. Adsorption complex of filamentous fd virus. *Journal of Molecular Biology,* 146**,** 621-627. Available: DOI https://doi.org/10.1016/0022-2836(81)90050-4.

HAYMAN, E. G. & RUOSLAHTI, E. 1979. Distribution of fetal bovine serum fibronectin and endogenous rat cell fibronectin in extracellular matrix. *The Journal of Cell Biology,* 83**,** 255. Available: DOI 10.1083/jcb.83.1.255.

HEMMINGA, M. A., VOS, W. L., NAZAROV, P. V., KOEHORST, R. B. M., WOLFS, C. J. A. M., SPRUIJT, R. B. & STOPAR, D. 2010. Viruses: incredible nanomachines. New advances with filamentous phages. *European Biophysics Journal,* 39**,** 541-550. Available: DOI 10.1007/s00249-009-0523-0.

HERMANSON, G. T. 2013. Chapter 3 - The Reactions of Bioconjugation. *Bioconjugate Techniques (Third edition).* Boston: Academic Press. Available: DOI http://dx.doi.org/10.1016/B978-0-12-382239-0.00003-0.

HESS, G. T., CRAGNOLINI, J. J., POPP, M. W., ALLEN, M. A., DOUGAN, S. K., SPOONER, E., PLOEGH, H. L., BELCHER, A. M. & GUIMARAES, C. P. 2012. M13 bacteriophage display framework that allows sortase-mediated modification of surface-accessible phage proteins. *Bioconjug Chem,* 23**,** 1478-87. Available: DOI 10.1021/bc300130z.

HIGASHITANI, A., HIGASHITANI, N. & HORIUCHI, K. 1997. Minus-strand origin of filamentous phage versus transcriptional promoters in recognition of RNA polymerase. *Proceedings of the National Academy of Sciences of the United States of America,* 94**,** 2909-2914.

HOANG, T. T., KARKHOFF-SCHWEIZER, R. R., KUTCHMA, A. J. & SCHWEIZER, H. P. 1998. A broad-host-range Flp-FRT recombination system for site-specific excision of chromosomally-located DNA sequences: application for isolation of unmarked Pseudomonas aeruginosa mutants. *Gene,* 212**,** 77-86.

HORIUCHI, K. 1997. Initiation mechanisms in replication of filamentous phage DNA. *Genes to Cells,* 2**,** 425-432. Available: DOI 10.1046/j.1365-2443.1997.1360334.x.

ISAAC, D. D., PINKNER, J. S., HULTGREN, S. J. & SILHAVY, T. J. 2005. The extracytoplasmic adaptor protein CpxP is degraded with substrate by DegP. *Proc Natl Acad Sci U S A,* 102**,** 17775-9. Available: DOI 10.1073/pnas.0508936102.

JOYCE, A. R., REED, J. L., WHITE, A., EDWARDS, R., OSTERMAN, A., BABA, T., MORI, H., LESELY, S. A., PALSSON, B. O. & AGARWALLA, S. 2006. Experimental and computational assessment of conditionally essential genes in Escherichia coli. *J Bacteriol,* 188**,** 8259-71. Available: DOI 10.1128/jb.00740-06.

KOLMAR, H., WALLER, P. R. & SAUER, R. T. 1996. The DegP and DegQ periplasmic endoproteases of Escherichia coli: specificity for cleavage sites and substrate conformation. *J Bacteriol,* 178**,** 5925-9.

LEE, S. W., MAO, C., FLYNN, C. E. & BELCHER, A. M. 2002. Ordering of quantum dots using genetically engineered viruses. *Science,* 296**,** 892-5. Available: DOI 10.1126/science.1068054.

LEE, Y. J., YI, H., KIM, W. J., KANG, K., YUN, D. S., STRANO, M. S., CEDER, G. & BELCHER, A. M. 2009. Fabricating genetically engineered high-power lithium-ion batteries using multiple virus genes. *Science,* 324**,** 1051-5. Available: DOI 10.1126/science.1171541.

LI, K., CHEN, Y., LI, S., NGUYEN, H. G., NIU, Z., YOU, S., MELLO, C. M., LU, X. & WANG, Q. 2010. Chemical modification of M13 bacteriophage and its application in cancer cell imaging. *Bioconjug Chem,* 21**,** 1369-77. Available: DOI 10.1021/bc900405q.

LOPEZ, J. & WEBSTER, R. E. 1983. Morphogenesis of filamentous bacteriophage f1: orientation of extrusion and production of polyphage. *Virology,* 127**,** 177-93.

LOSET, G. A. & SANDLIE, I. 2012. Next generation phage display by use of pVII and pIX as display scaffolds. *Methods,* 58**,** 40-46. Available: DOI http://dx.doi.org/10.1016/j.ymeth.2012.07.005.

MARVIN, D. A., SYMMONS, M. F. & STRAUS, S. K. 2014. Review: Structure and assembly of filamentous bacteriophages. *Progress in Biophysics and Molecular Biology,* 114**,** 80-122. Available: DOI 10.1016/j.pbiomolbio.2014.02.003.

MARVIN, D. A., WELSH, L. C., SYMMONS, M. F., SCOTT, W. R. & STRAUS, S. K. 2006. Molecular structure of fd (f1, M13) filamentous bacteriophage refined with respect to X-ray fibre diffraction and solid-state NMR data supports specific models of phage assembly at the bacterial membrane. *J Mol Biol,* 355**,** 294-309. Available: DOI 10.1016/j.jmb.2005.10.048.

MARZARI, R., SBLATTERO, D., RIGHI, M. & BRADBURY, A. 1997. Extending filamentous phage host range by the grafting of a heterologous receptor binding domain. *Gene,* 185**,** 27-33.

MERZLYAK, A. & LEE, S.-W. 2009. Engineering Phage Materials with Desired Peptide Display: Rational Design

Sustained through Natural Selection. *Bioconjugate Chem***,** 2300-2310.

MIROUX, B. & WALKER, J. E. 1996. Over-production of proteins in Escherichia coli: mutant hosts that allow synthesis of some membrane proteins and globular proteins at high levels. *J Mol Biol,* 260**,** 289-98. Available: DOI 10.1006/jmbi.1996.0399.

MODEL, P. & RUSSEL, M. 1988. Filamentous Bacteriophages. *In:* CALENDAR, R. (ed.) *The Bacteriophages.* New York: Plenum Publishing.

NEWMAN, J., SWINNEY, H. L. & DAY, L. A. 1977. Hydrodynamic properties and structure of fd virus. *J Mol Biol,* 116**,** 593-603.

NGWENIFORM, P., ABBINENI, G., CAO, B. & MAO, C. 2009. Self-assembly of drug-loaded liposomes on genetically engineered target-recognizing M13 phage: a novel nanocarrier for targeted drug delivery. *Small,* 5**,** 1963-9. Available: DOI 10.1002/smll.200801902.

OH, D., QI, J., HAN, B., ZHANG, G., CARNEY, T. J., OHMURA, J., ZHANG, Y., SHAO-HORN, Y. & BELCHER, A. M. 2014. M13 Virus-Directed Synthesis of Nanostructured Metal Oxides for Lithium–Oxygen Batteries. *Nano Letters,* 14**,** 4837-4845. Available: DOI 10.1021/nl502078m.

OVERMAN, S. A., TSUBOI, M. & THOMAS, G. J. 1996. Subunit orientation in the filamentous virus Ff(fd, f1, M13). *JOURNAL OF MOLECULAR BIOLOGY,* 259**,** 331-336.

PETRENKO, V. A., SMITH, G. P., GONG, X. & QUINN, T. 1996. A library of organic landscapes on filamentous phage. *Protein Engineering,* 9**,** 797-801. Available: DOI 10.1093/protein/9.9.797.

RAKONJAC, J. unpublished.

RAKONJAC, J., BENNETT, N. J., SPAGNUOLO, J., GAGIC, D. & RUSSEL, M. 2011. Filamentous bacteriophage: biology, phage display and nanotechnology applications. *Curr Issues Mol Biol,* 13**,** 51-76.

RAKONJAC, J., FENG, J.-N. & MODEL, P. 1999. Filamentous phage are released from the bacterial membrane by a two-step mechanism involving a short C-terminal fragment of pIII. *JOURNAL OF MOLECULAR BIOLOGY,* 289**,** 1253 - 1265.

RAKONJAC, J., JOVANOVIC, G. & MODEL, P. 1997. Filamentous phage infection-mediated gene expression: construction and propagation of the gIII deletion mutant helper phage R408d3. *Gene,* 198**,** 99-103.

RAKONJAC, J. & MODEL, P. 1998. Roles of pIII in filamentous phage assembly. *JOURNAL OF MOLECULAR BIOLOGY,* 282**,** 25-41.

RAKONJAC, J., ROBBINS, J. & FISCHETTI, V. 1995. DNA sequence of the serum opacity factor of group A streptococci: identification of a fibronectin-binding repeat domain. *Infection and Immunity,* 63**,** 622-631.

REBAR, E. & PABO, C. 1994. Zinc finger phage: affinity selection of fingers with new DNA-binding specificities. *Science,* 263**,** 671-673. Available: DOI 10.1126/science.8303274.

RODIONOVA, I., M SCHUSTER, B., GUINN, M., SORCI, L., A SCOTT, D., LI, X., KHETERPAL, I., SHOEN, C., CYNAMON, M., LOCHER, C., J RUBIN, E. & OSTERMAN, A. 2014. *Metabolic and Bactericidal Effects of Targeted Suppression of NadD and NadE Enzymes in Mycobacteria*. Available: DOI 10.1128/mBio.00747-13.

RUOSLAHTI, E., VUENTO, M. & ENGVALL, E. 1978. Interaction of fibronectin with antibodies and collagen in radioimmunoassay. *Biochimica et Biophysica Acta (BBA) - Protein Structure,* 534**,** 210-218. Available: DOI https://doi.org/10.1016/0005-2795(78)90003-X.

RUSSEL, M. & MODEL, P. 1989. Genetic analysis of the filamentous bacteriophage packaging signal and of the proteins that interact with it. *Journal of Virology,* 63**,** 3284-3295.

SALMOND, G. P. C. & FINERAN, P. C. 2015. A century of the phage: past, present and future. *Nature Reviews Microbiology,* 13**,** 777. Available: DOI 10.1038/nrmicro3564.

SAMBROOK & RUSSELL 2001. *Molecular Cloning: A Laboratory Manual.,* Cold Spring Harbour, N.Y. , Cold Spring Harbour Laboratory.

SATTAR, S. 2013. *Filamentous phage-derived nano-rods for applications in diagnostics and vaccines : a thesis presented in partial fulfillment of the requirements for the degree of Doctor of Philosophy in Biochemistry at Massey University, Palmerston North, New Zealand*.

SATTAR, S., BENNETT, N. J., WEN, W. X., GUTHRIE, J. M., BLACKWELL, L. F., CONWAY, J. F. & RAKONJAC, J. 2015. Ff-nano, short functionalized nanorods derived from Ff (f1, fd, or M13) filamentous bacteriophage. *Front Microbiol,* 6**,** 316. Available: DOI 10.3389/fmicb.2015.00316.

SCHMELCHER, M. & LOESSNER, M. J. 2014. Application of bacteriophages for detection of foodborne pathogens. *Bacteriophage,* 4**,** e28137. Available: DOI 10.4161/bact.28137.

SCHWARTZ, F. M. & ZINDER, N. D. 1968. Morphological changes in Escherichia coli infected with the DNA bacteriophage f1. *Virology,* 34**,** 352-355. Available: DOI https://doi.org/10.1016/0042-6822(68)90246-8.

SHORT, J. M., FERNANDEZ, J. M., SORGE, J. A. & HUSE, W. D. 1988. Lambda ZAP: a bacteriophage lambda expression vector with in vivo excision properties. *Nucleic Acids Res,* 16**,** 7583-600.

SMARTT, A. E. & RIPP, S. 2011. Bacteriophage reporter technology for sensing and detecting microbial targets. *Anal Bioanal Chem,* 400**,** 991-1007. Available: DOI 10.1007/s00216-010-4561-3.

SMITH, G. P. 1985. Filamentous fusion phage: novel expression vectors that display cloned antigens on the virion surface. *Science,* 228**,** 1315-7.

SPAGNUOLO, J., OPALKA, N., WEN, W. X., GAGIC, D., CHABAUD, E., BELLINI, P., BENNETT, M. D., NORRIS, G. E., DARST, S. A., MARJORIE., R. & RAKONJAC, J. 2010. Identification of the gate regions in the primary structure of the secretin pIV. *Molecular Microbiology,* 76**,** 133-150. Available: DOI doi:10.1111/j.1365-2958.2010.07085.x.

SPECTHRIE, L., HORIUCHI, K., MODEL, P., RUSSEL, M., BULLITT, E. & MAKOWSKI, L. 1992. Construction of a microphage variant of filamentous bacteriophage. *Journal of Molecular Biology,* 228**,** 720-724.

SPIESS, C., BEIL, A. & EHRMANN, M. 1999. A temperature-dependent switch from chaperone to protease in a widely conserved heat shock protein. *Cell,* 97**,** 339-47.

STIEGLER, N., DALBEY, R. E. & KUHN, A. 2011. M13 procoat protein insertion into YidC and SecYEG proteoliposomes and liposomes. *J Mol Biol,* 406**,** 362-70. Available: DOI 10.1016/j.jmb.2010.12.036.

STRAUCH, K., POGLIANO, K. & BECKWITH, J. 1989. *Characterization of degP, a gene required for proteolysis in the cell envelope and essential for growth of Escherichia coli at high temperature*. Available: DOI 10.1128/jb.171.5.2689-2696.1989.

TAKAKU, M., TAKAHASHI, D., MACHIDA, S., UENO, H., HOSOYA, N., IKAWA, S., MIYAGAWA, K., SHIBATA, T. & KURUMIZAKA, H. 2010. Single-stranded DNA catenation mediated by human EVL and a type I topoisomerase. *Nucleic Acids Res,* 38**,** 7579-86. Available: DOI 10.1093/nar/gkq630.

TERAMOTO, H., SUDA, M., INUI, M. & YUKAWA, H. 2010. Regulation of the Expression of Genes Involved in NAD De Novo Biosynthesis in Corynebacterium glutamicum. *Applied and Environmental Microbiology,* 76**,** 5488-5495. Available: DOI 10.1128/AEM.00906-10.

TOMASINI-JOHANSSON, B. & MOSHER, D. F. 2009. Plasma fibronectin concentration in inbred mouse strains. *Thromb Haemost,* 102**,** 1278-80. Available: DOI 10.1160/th09-03-0141.

VELAPPAN, N., FISHER, H. E., PESAVENTO, E., CHASTEEN, L., D'ANGELO, S., KISS, C., LONGMIRE, M., PAVLIK, P. & BRADBURY, A. R. 2010. A comprehensive analysis of filamentous phage display vectors for cytoplasmic proteins: an analysis with different fluorescent proteins. *Nucleic Acids Res,* 38**,** e22. Available: DOI 10.1093/nar/gkp809.

WHALEY, S. R., ENGLISH, D. S., HU, E. L., BARBARA, P. F. & BELCHER, A. M. 2000. Selection of peptides with semiconductor binding specificity for directed nanocrystal assembly. *Nature,* 405**,** 665-668.

WU, C.-H., LIU, I. J., LU, R.-M. & WU, H.-C. 2016. Advancement and applications of peptide phage display technology in biomedical science. *Journal of Biomedical Science,* 23**,** 8. Available: DOI 10.1186/s12929-016-0223-x.

ZHOU, Y., WANG, L., YANG, F., LIN, X., ZHANG, S. & ZHAO, Z. 2011. *Determining the Extremes of the Cellular NAD(H) Level by Using an Escherichia coli NAD+-Auxotrophic Mutant*. Available: DOI 10.1128/AEM.00630-11.

9. Appendix I

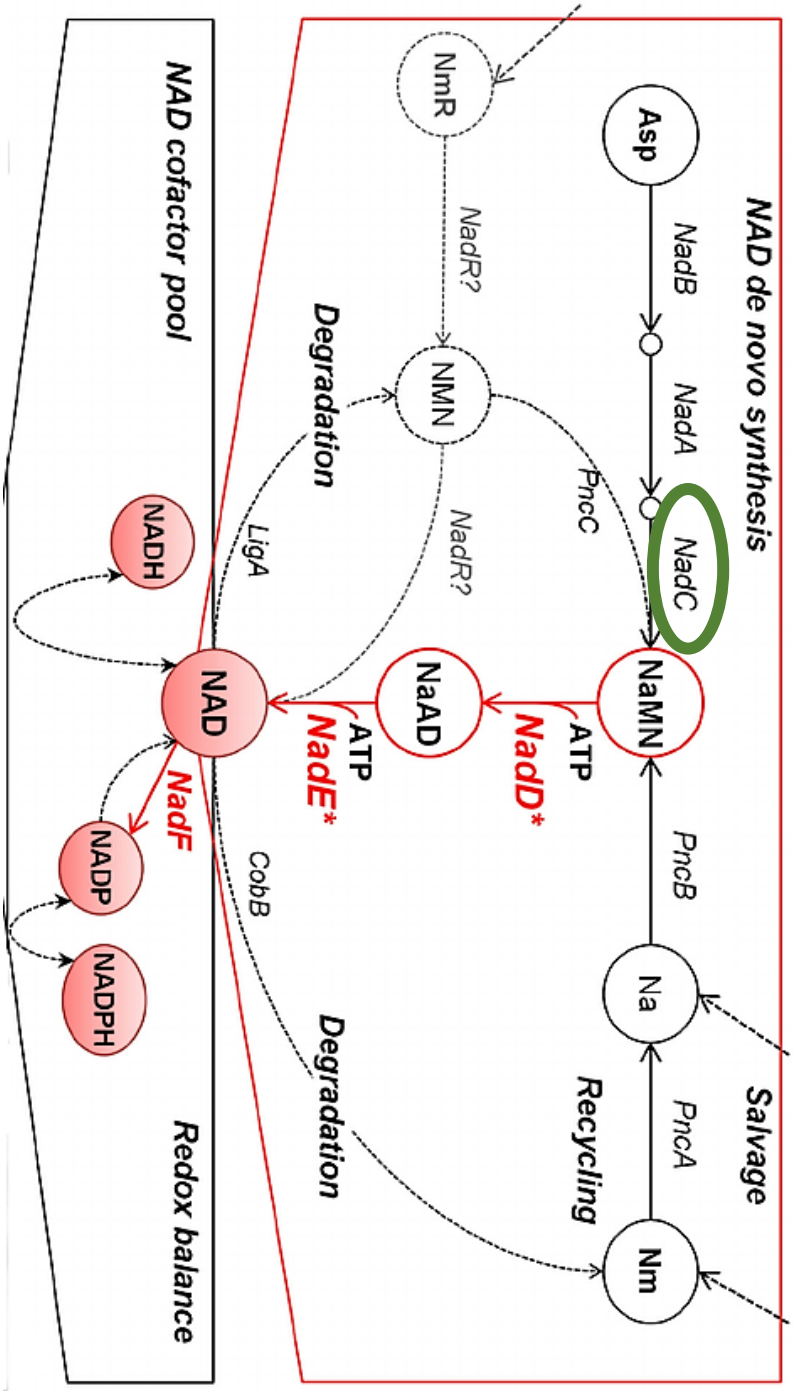
NAD de novo synthesis
Asp
NadB
NadA
NadC
NaMN
PncB
Na
PncA
Nm
Salvage
Recycling
NmR
NadR?
NMN
PncC
Degradation
LigA
NadR?
NaAD
ATP
NadD*
ATP
NadE*
NAD
CobB
Degradation
NADH
NADP
NADPH
NadF
NAD cofactor pool
Redox balance

Figure 31: Overview of the NAD Biosynthesis Pathway

In this simplified diagram of genomics-based reconstruction of NAD biogenesis and homeostasis the key intermediary metabolites are shown by abbreviations in circles as follows: Asp, aspartate; Na, nicotinic acid; Nm, nicotinamide; NmR, nicotinamide riboside; NaMN, nicotinic acid mononucleotide; NMN, nicotinamide mononucleotide; NaAD, nicotinic acid adenine dinucleotide.

Enzymes are indicated as products of the respective genes above corresponding biochemical transformations (arrows). The auxotrophic mutation used in this study encodes NadC (outlined in green). This enzyme is essential for *E. coli* survival in the absence of externally added NAD or precursors downstream of NadC-catalysed step in the pathway, NaMN or NaAD, and precursors from the salvage pathways (NMN, Na, Nm). These are all absent from the minimal medium containing casamino acids ((Dong *et al.*, 2010)., and two enzymes selected as targets in this study, nicotinate mononucleotide adenylyltransferase (NadD) and NAD synthetase (NadE), are marked by an asterisk (*).

Figure and legend adapted from Rodionova *et al.* (2014)